AZACROWN[18]-N_6 DERIVATIVES: SYNTHESIS, LIQUID CRYSTALLINE PROPERTIES, AND COMPLEXATION

By

MINGYANG ZHAO

Bachelor of Science
Qinghua University
Beijing, P. R. China
1978

Master of Engineering
Beijing Research Institute
of Chemical Industry
Beijing, P. R. China
1984

Submitted to the Faculty of the
Graduate College of the
Oklahoma State University
in partial fulfillment of
the requirements for
the degree of
DOCTOR OF PHILOSOPHY
May, 1993

AZACROWN[18]-N_6 DERIVATIVES: SYNTHESIS,
LIQUID CRYSTALLINE PROPERTIES,
AND COMPLEXATION

Thesis Approved:

Warren T. Ford
Thesis Adviser

K D Berlin

Wad El Rays

Dean of the Graduate College

ACKNOWLEDGMENTS

It is a pleasure and good fortune to study in the Department of Chemistry at Oklahoma State University. I wish to express my sincere gratitude to the faculty and staff members who assisted me in this project and during my coursework at Oklahoma State University. In particular, I wish to thank Dr. Warren T. Ford, my advisor, for his intelligent guidance and support; his instruction and patience are forever appreciated. I am also grateful to Dr. K. Darrell Berlin; Dr. Ziad El Rassi, and Dr. Gary L. Foutch for serving on my graduate committee.

I express my thanks to Dr. David Tatarsky and Dr. Krishna G. Banerjee for their early efforts and experience in this project. I also extend my thanks to fellow graduate students and postdoctorates of our research group for their help and friendship.

Special thanks go to my wife, Hui Yu, for her love, support, and encouragement, to my father and mother and my daughter for all they had to sacrifice during my graduate work.

TABLE OF CONTENTS

Chapter Page

LIST OF TABLES

Chapter I

Chapter II

Chapter III

Chapter IV

LIST OF FIGURES

Chapter I

Chapter II

CHAPTER I

INTRODUCTION

Liquid Crystals. Liquid crystals are highly anisotropic fluids that exist between the boundaries of the crystalline solid and isotropic liquid phases. Liquid crystalline phases are referred to as mesophases. Any substance which exists as a liquid crystal is also referred to as a mesogen. There are two kinds of liquid crystals. Thermotropic liquid crystals change phases with change of temperature. Lyotropic liquid crystals change phases with change in the amount of solvent.[1-3] Many organic compounds and some polymers exhibit thermotropic liquid crystallinity. Most liquid crystalline compounds are calamitic, composed of rod-like molecules. Two distinctive structural classes of liquid crystals have been identified for calamitic phases: nematic (N) and smectic (S). In nematic phases the long axes of molecules remain substantially parallel. Smectic phases are distinguished not only by parallel long axes of the molecules, but also by a layering of the molecules in two-dimensional planes. Based on the layer structure, ten smectic phases labeled by the alphabet letters A through K have been described. The order of the letters indicates the order of the discovery. The letter I has been excluded to avoid confusion with the isotropic phase. Besides the classical calamitic liquid crystals based on rod-like molecules, thermotropic discotic liquid crystals have been extensively studied since 1977.[4-18] Discotic liquid crystals are formed from disc-like molecules, which have more or less planar cores with usually six or more lateral substitutents. The structures are based on the tendency of the molecular discs to align with their short axes parallel. To date, two different classes of discotic phases have been described: nematic (N_D) and columnar (D). In the nematic phase, the discs tend to align parallel and the disc-normals tend to point

along a common direction. The columnar liquid crystal phases are characterized by stacked columns of molecules, the columns being packed together with two-dimensional order. Within the columns, the disc-like molecular positions may have short- or long-range order, but the columns are not in register along their axes. There are four known columnar phases, D_{ho}, D_{hd}, D_{rd} and D_{ob}.[1] The differences among these four phases are attributed to the order or disorder of the molecular stacking in the columns and the two-dimensional lattice symmetry of the columnar packing. The main classifications and the schematic structures of thermotropic liquid crystals are given in Figures 1 and 2.

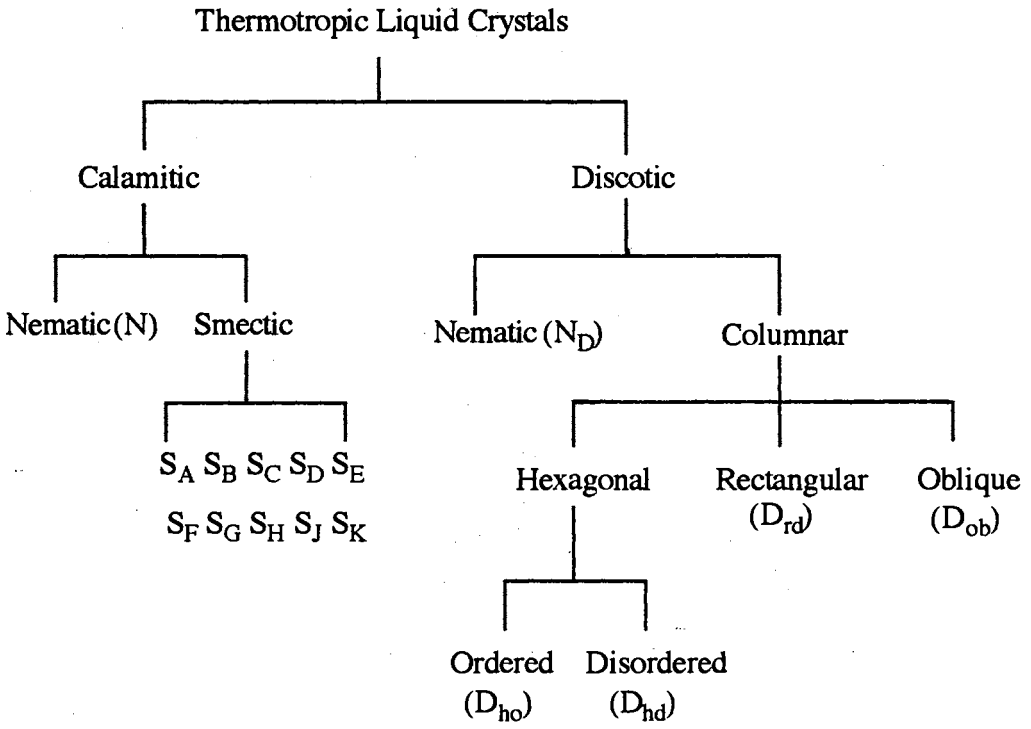

Figure 1. Classification of thermotropic liquid crystal structures.

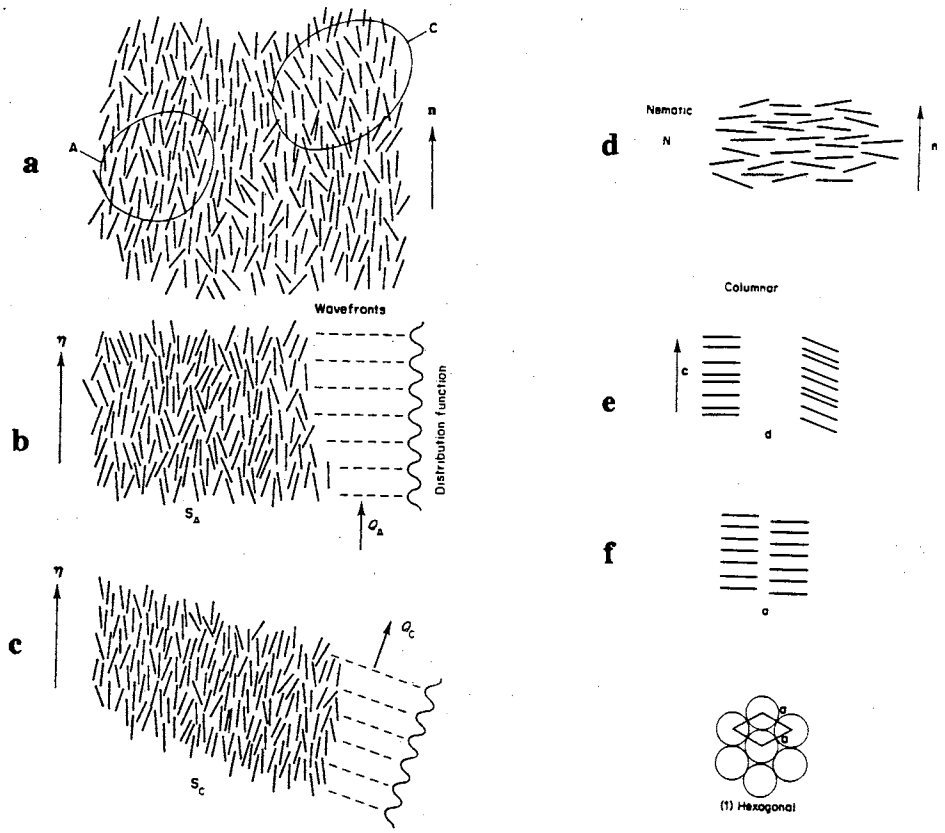

Figure 2. Schematic representation of typical mesophasic structures. (a) nematic; (b) smectic A; (c) smectic C; (d) discotic nematic; (e) discotic hexagonal disordered columnar; (f) discotic hexagonal ordered columnar. (The drawings are reproduced from reference 1).

Liquid crystals may have low or high molar mass. If the rod-like or disc-like mesogens are incorporated into the main chain or side chain of a polymer, usually a polymer liquid crystal is formed (Figure 3). In a side chain liquid crystal polymer the rigid mesogenic molecules are connected with the polymer backbone by flexible spacers, which are alkylene or alkyleneoxy chains. These spacers enable the mesogenic units to order anisotropically by decoupling of the motions between the mesogenic units and the polymer backbone.[1]

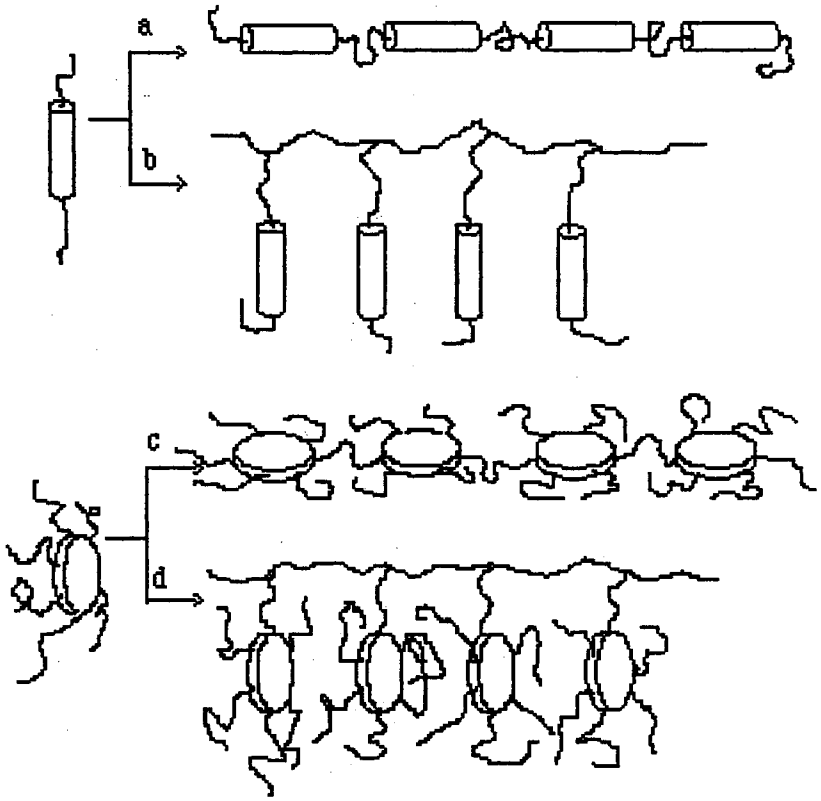

Figure 3. Schematic representation of liquid crystal polymers. (a) main chain liquid crystal polymer with rod-like mesogens; (b) side chain liquid crystal polymer with rod-like mesogens; (c) main chain liquid crystal polymer with disc-like mesogens; (d) side chain liquid crystal polymer with disc-like mesogens.

Polymer liquid crystals combine the anisotropic physical properties of the liquid crystals with the characteristic properties of the polymers. At elevated temperature the polymers can be ordered in the liquid crystal phases, and the order often can be retained in an anisotropic glass by cooling quickly to room temperature. These functional polymers also can be processed to films for technical applications. Drawbacks to polymer liquid crystals are the more difficult identification of the phases, the occurrence of phase transitions over broad ranges of temperature, and the higher viscosity, which makes them slow to change their supramolecular structures. So far the most common polymer liquid

crystals are based on the rod-like mesogens, and only a few disc-like mesogen based polymer liquid crystals have been reported.[18-26] One reason is that it is more difficult to synthesize a discotic mesogen with one or two of six or more side chains functionalized.

Azamacrocyclic Liquid Crystals. Azamacrocyclic compounds, which consist of cyclic carbon structures containing nitrogen, have been studied as macrocyclic ligands for a long time. The azamacrocycle having a ring of 12 carbons and 6 nitrogens is known as hexacyclen or 1,4,7,10,13,16-hexaazacyclooctadecane. It is similar in structure to the crown ether 18-crown-6 (**[18]-O_6**). So it also is known as azacrown **[18]-N_6**.

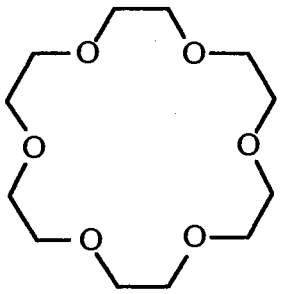

Crown Ether **[18]-O_6**

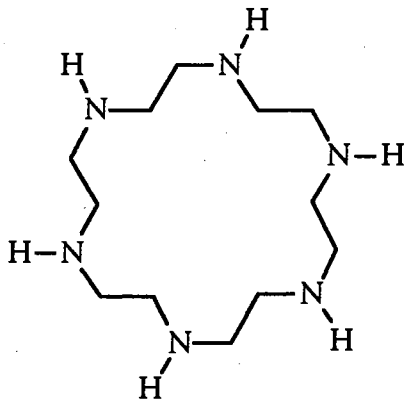

Azacrown **[18]-N_6**

In recent years some liquid crystalline macrocyclic ligands have been synthesized.[27-55] These new materials combine the complexing properties of ligands with the anisotropic properties provided by thermotropic liquid crystals. An effort has been made to investigate the structure-liquid crystal property relationships of macrocycles and metal cation transport in liquid crystalline phases. The first liquid crystalline macrocyclic ligand with a columnar mesophase was reported by Lehn, Malthete, and Levelut in 1985.[27] He, Wada, Kikukawa and Matsuda reported the first macrocyclic ligand with calamitic

mesophases in 1987.[41] The first liquid crystalline macrocyclic ligands bound to side chain polymers were prepared by Percec and Rodenhouse in 1989.[48]

In search of novel liquid crystals by using macrocycles fitted with suitable lateral chains as basic units, Lehn, Malthete, and Levelut found three hexa-acylated azamacrocyclic compounds that exhibited mesophases. Based on the measurements of X-ray diffraction using low resolution techniques as well as optical microscopy, they suggested the new mesophases to have a hexagonal-tubular structure. In this "tubular mesophase" the macrocyclic molecules stack into parallel columns placed at the vertices of a hexagonal lattice (Figure 4).

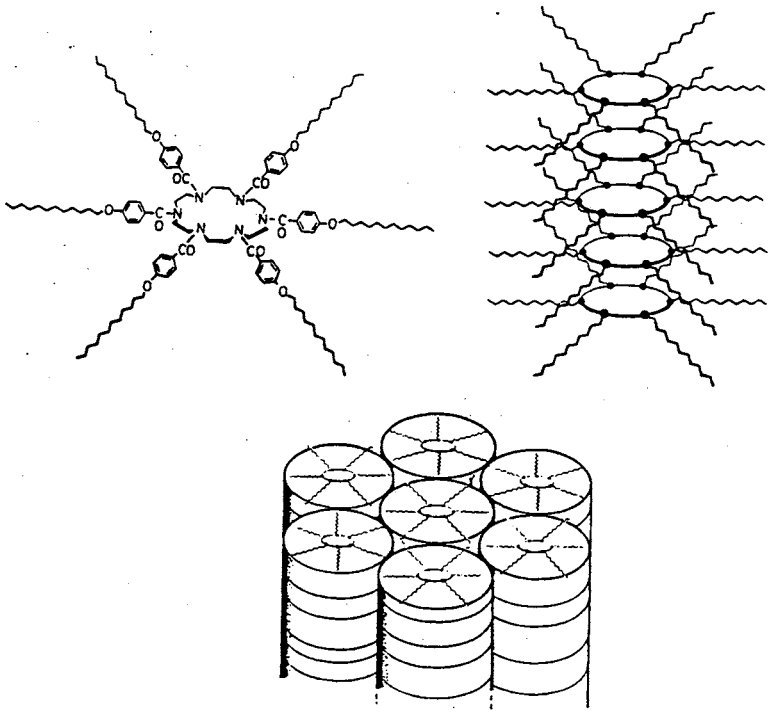

Figure 4. Schematic representation of the "tubular mesophase" formed by stacking of macrocycles. (The drawings are reproduced from reference 27).

If the stacked disc-like macrocycles really form hollow columns, this kind of supramolecular architecture would be very interesting. They might be used as molecular or ionic channels, such as phase-dependent ion-conducting channels for controllable cation-selective semipermeable membranes. Since the first report of Lehn, more effort has been made to synthesize and study liquid crystalline azacrown[18]-N_6 derivatives.[28-38] A summary of the reported structures and phases is given in Table I.

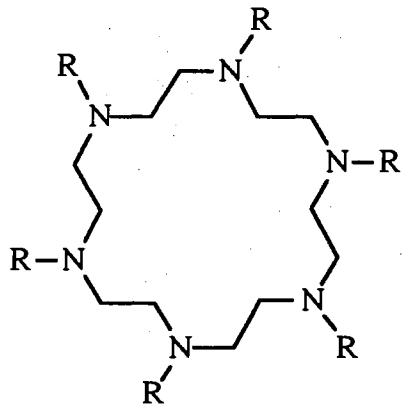

Azacrown[18]-N_6 Derivatives

Table I. Phase Transitions of Azacrown[18]-N_6 Derivatives

	R	Phases (°C)[a]	Reference
1	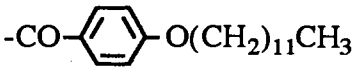	see Table III	27
2	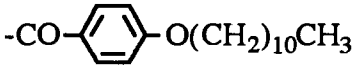	C 106 D 142 I	32
3	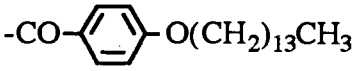	C 106 D 136 I	30
4	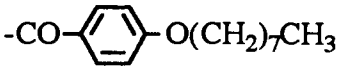	C 120 D 139 I	29
5	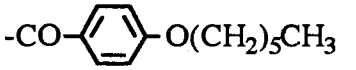	C 109 I	31
6	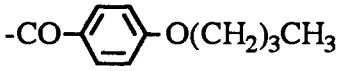	glassy	32
7	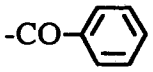	C 160 I	32
8	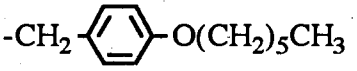	C 73 I	32
9	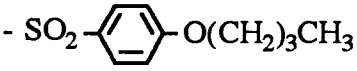	C 186 I	30
10	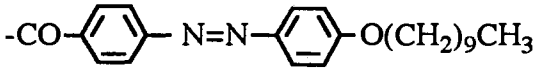	C 237 D 245 I	30
11	$-CO-(CH_2)_4CH_3$	C 96 I	32
12	$-CO-(CH_2)_{12}CH_3$	C 107 I	32
13	$-CO-(CH_2)_{14}CH_3$	C 107 I	32

Table I. (continued)

	R	Phases (°C)	Reference
14		C 217 D 233 I	30
15	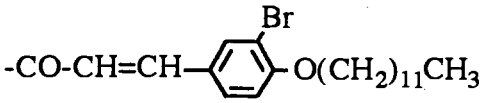	C 180 D_{ho} 326 I	35
16	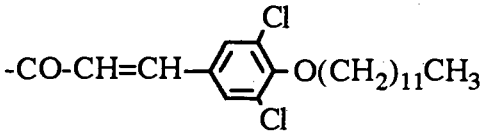	g 25 D_{ho} 344 I	35
17	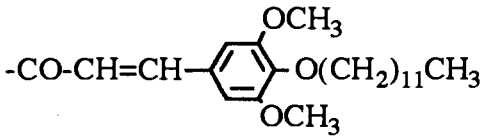	g 4 D_{ho} 356 I	35
18	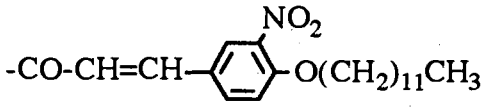	C 204 D_{ho} 325 I	35
19	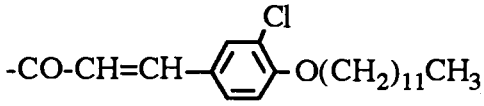	C 168 D_{ho} 325 I	35
20	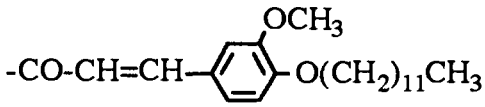	C 164 D_{ho} 348 I	35
21	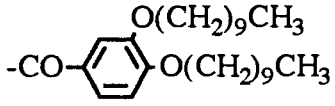	C 104 D 140 I	34
22	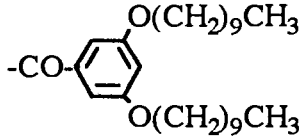	glassy	34

Table I. (continued)

	R	Phases (°C)	Reference
23	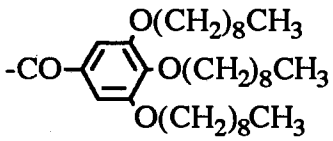	glassy	30

[a] C = crystal; D = discotic columnar; D_{ho} = discotic ordered hexagonal columnar; I = isotropic; g = glass

To be able to form a columnar mesophase usually the disc-like molecule contains a rigid, flat core with six or more flexible aliphatic tails. For azamacrocyclic liquid crystals the conformation of the disc depends on the planar rigid substitutents. Only aromatic carboxylic acid derivatives of **[18]-N_6** are known to be liquid crystalline. The optimized space filling of aliphatic hydrocarbon tails is also important. For example, a minor change of molecular structure from 3,5-bis(alkoxy)benzoyl substituents (**22**) to the 3,4-isomer (**21**) leads to different liquid crystalline properties (Table I). The important influence of substituent group on the liquid crystallinity of azacrowns is also confirmed by comparison of diaza-18-crown ether derivatives **24-26**.[56-59]

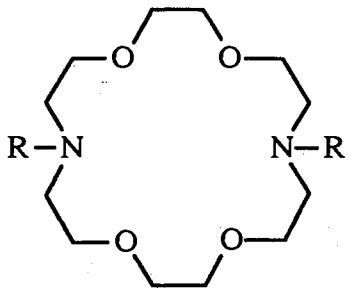

24: R = 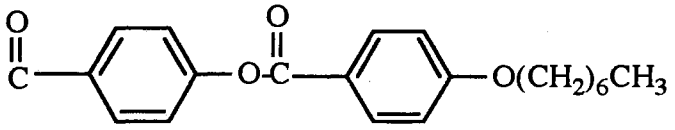 (liquid crystal)

25: R = 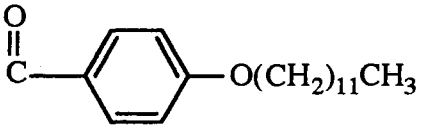 (non liquid crystal)

26: R = 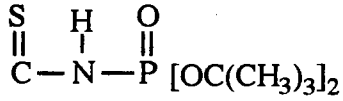 (liquid crystal)

The "tubular mesophase", i.e., the hexagonal columnar mesophase, can be identified by X-ray diffraction and polarizing microscopy, and differential scanning calorimetry (DSC) measurements can be used to identify phase transitions. For hexagonal order both 100 and 110 diffraction peaks should be visible in the high resolution X-ray diffractograms.[33] The typical polarizing microscopic texture of an ordered hexagonal phase is a mosaic with some linear birefringent defects. Most disordered hexagonal phases show focal conic or fan-shaped textures, which are similar to those observed with an S_A phase. On cooling from the isotropic liquid, the D_{hd} phase grows like a crystal with straight boundaries. The $D_{ho} \rightarrow I$ transition heats determined from DSC measurements are higher (typically 2 kcal/mol) than $D_{hd} \rightarrow I$ transition heats (typically 0.3 kcal/mol).[6]

The hexagonal order in the "tubular mesophase" of two hexcyclene derivatives (**14**, **15**, in Table I) has been confirmed by the existence of higher order diffraction peaks in high resolution powder X-ray diffraction.[33] So far the evidence of hexagonal order of compound **1** is still not clear, and there is argument about whether compound **1** forms a columnar mesophase.[32,37]

The strong interest in the liquid crystalline and complexation properties has led to increased concern for the synthesis of azamacrocycles. The multi-step synthesis of the unsubstituted **[18]-N_6** is tedious but not very difficult, and several methods have been reported.[60-64] The synthesis of hexsubstituted [18]-N_6 derivatives is also not difficult.[27,30,32,34,38] The mono N-functionalized polyaza macrocycles can be synthesized by two different strategies.[65-83] One method is first to prepare the mono N-functionalized or protected half macrocycle and then finish cyclization. The other method requires an initial cyclization followed by the mono N-functionalization with an excess amount of macrocycle. So far, there is no report about the synthesis of a liquid crystalline polymer containing [18]-N_6 derivatives.

Complexation of Azacrowns with Cations in Aqueous Solution. The coordination behavior of azacrown[18]-N_6 has been studied in recent years.[84-91] The stepwise protonation constants, which were determined by potentiometry, of azacrown[18]-N_6 are pK_1=10.15, pK_2=9.48, pK_3=8.89, pK_4=4.27, pK_5=2.21, and pK_6=1.0.[87] This macrocyclic amine behaves as a relatively strong base in the first half of its protonation steps and as a weaker base in the second half. This behavior was ascribed to the electrostatic repulsions among the positive charges on the protonated cyclic polyamines. The complexation equilibrium constants of azacrown[18]-N_6 with various metal ions in aqueous solutions were measured potentiometrically by Kodama as reported in Table II.[86] Unlike crown ether[18]-O_6, azacrown[18]-N_6 has appreciable affinity for transition metals.

Table II. Equilibrium Constants (log K_{ML}) for Azacrown[18]-N_6 Complexation.[a]

Metal ion:	Hg^{2+}	Ni^{2+}	Co^{2+}	Cd^{2+}	Zn^{2+}	Pb^{2+}	Sr^{2+}	Ca^{2+}	K^+
log K_{ML}:	29.1	19.6	18.9	17.9	17.8	14.1	3.2	2.5	0.8

[a] log $K_{ML} = [ML^{2+}]/[M^{2+}][L]$.

The coordination behavior of substituted azacrown[18]-N_6 hexamide **27** and hexamine **28** for organic cations was also reported.[92-95]

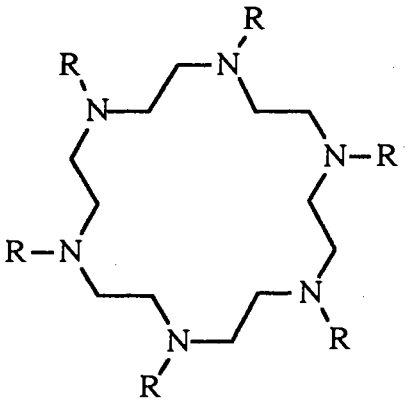

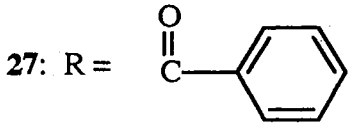

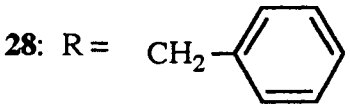

Hexamine **28** shows specific binding and cation-transport ability for the ammonium cations of amino acid ester salts, such as glycine ethyl ester (GlyOEt) and phenylalanine ethyl ester (PheOEt). By appropriate design of the donor sites, the ring size of the azacrown and the co-transported anions, it is possible to transport selectively amino acid derivatives and other biological organic cations.[92-94] Hexamide **27** did not show strong affinity for metal cations. It only showed weak complexing with amino acid salts.

A silica gel-bound [18]-N_6 hexamine (**29**) was prepared and bound with metal cations, and the acidity constants were measured. The results are cited in Table III.[96]

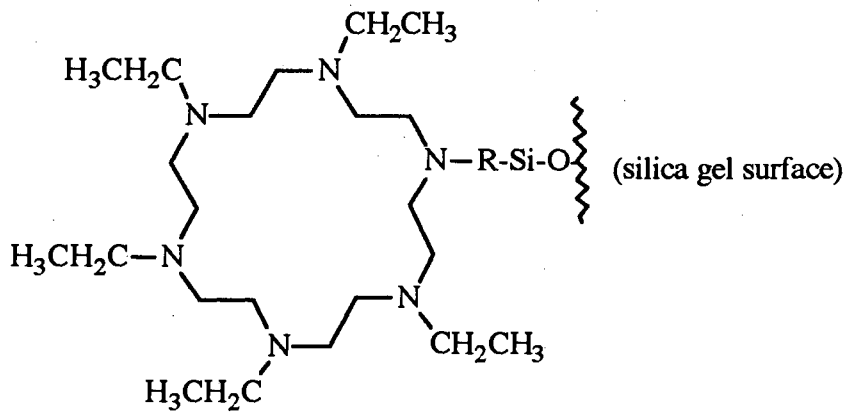

29

Table III (a). Binding Constants (log K) for Silica Gel-Bound **29** to Metal Cations

metal ion	Hg^{2+}	Cu^{2+}	Pb^{2+}	H^+	Cd^{2+}	Zn^{2+}	Ni^{2+}	Ag^+	Sr^{2+}	K^+
log K	28.8	16.3	14.0	11.4	11.2	10.0	9.8	9.3	<0.2	<0.2

Table III (b). Acidity Constants (log K) of Protonated Silica Gel-Bound **29**

H^+	HL/H·L	H_2L/H·HL	H_3L/H·H_2L	H_4L/H·H_3L	H_5L/H·H_4L	H_6L/H·H_5L
log K	11.4	8.3	5.6	3.2	1.5	1.3

To determine the log K values, small amounts of the silica gel-bound azamacrocycles were equilibrated with known concentrations of the cations in well defined matrices. After equilibrium was reached, the amount of bound cation was measured by stripping the gel with an acidic solution. The metal concentration in the eluent was then determined by atomic absorption spectroscopy.[96]

Not only cations but also anions can be bound to azacrowns.[97-101] The binding ability of a macrocyclic polyamine may be controlled by varying the pH of the solution, i.e., by controlling the number and the location of protonated amino groups on the receptor and the ionic substrate. For example the macrocyclic hexaamine [24]-N_6O_2, which was covalently attached to polystyrene beads, was able to bind nucleotide polyphosphate anions, such as adenosine di- and triphosphate, from a solution of pH 4. The uptake was due to the binding of the negatively charged polyphosphate chain of the nucleotide by the polyprotonated macrocycle. At pH 11, the unprotonated macrocyclic polyamine released the bound nucleotide.[97] Tsukube investigated anion-binding and transport properties of a series of lipophilic polyammonium macrocycles.[98] Liquid-liquid extraction experiments revealed that picrate and other guest anions were effectively extracted *via* interactions with protonated polyamine macrocycles, and that the extracted amounts of guest anions largely depended on the ring-size of the polyamine compounds and the pH value of the aqueous phase.

Other interesting properties of azamacrocycles include reversible binding of dioxygen in aqueous solution by Ni(II) and Co(II) complexes,[102-105] catalysis of the hydrolysis of adenosine triphosphate (ATP) by protonated macrocycles,[106-109] and the binding of carbon dioxide and its electrochemical reduction at Zn(II) and Ni(II) complexes.[64,65,110]

Usually the cation-binding properties were evaluated by a liquid-liquid extraction method. The metal salts, usually picrates, were extracted from water into an equal volume

of chloroform or other organic phase containing macrocyclic ligand.[84] The cation transport abilities of ligand were assessed by a liquid membrane method in a U-tube glass cell.[94] For membrane transport the ligand must possess a specific binding capability for the substrate. However, this binding capability should not be too high, for if the complex is too stable there will be insufficient free ligand available to diffuse back across the membrane and complete the transport cycle.

Liquid Crystalline Behavior of Complexed or Doped Azamacrocycles. One new research field of liquid crystalline macrocyclic ligands is how the liquid crystalline properties are affected by the complexation of metal ions. It has been found that the complexed metal has strong influence on the phase behavior.[54,95] The non-liquid crystalline [18]-N_6 hexamine **30** showed columnar mesophases after complexation with transition metal ions.[95] This phenomenon may be attributed to a conformational rigidification of the macrocycle and the interaction between the complexed metal ions.

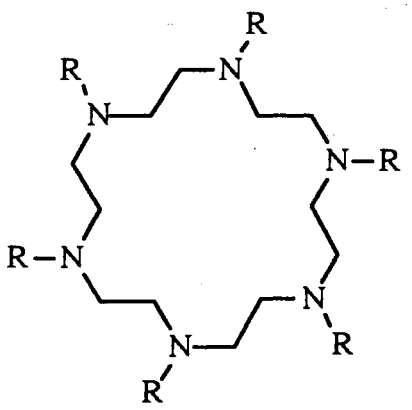

30: R = 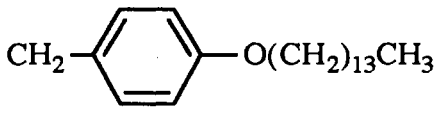

Charge transfer complexation is another useful tool for varying mesomorphic phase behavior. When certain non-liquid-crystalline disc-like electron donor molecules or polymers are doped with electron acceptor molecules, such as 2,4,7-trinitrofluorenone

(TNF), new liquid crystalline phases may be induced.[111,112] Doping also can be used to functionalize liquid crystals with special physical properties such as color, ferroelectricity or photoconductivity.

Current Research Activities with Azacrowns. (a) Ionic Channel. There is general interest in the preparation of synthetic ionic channels.[113-124] While success has been rather limited, there are a few reports about the increased ion permeation through membranes because of the formation of ion channels.[118,120]

The hexagonal columnar mesophase, the so-called "tubular mesophase," represents a molecular tube through which ions might flow. The potential development of phase-dependent ion-conducting channels, which may be turned on or off by some sort of external thermal, electric, or magnetic regulation, makes them an interdisciplinary research target. Different methods have been employed in order to reach and stabilize the columnar order. One way to prepare the tubular structure was reported by Mertesdorf, Ringsdorf, and Stumpe.[16] First they functionalized azamacrocycle [18]-N_6 with photo-sensitive cinnamoyl groups (Table I, **14**), and then the columnar aggregates were exposed to UV irradiation for an intracolumnar (2+2)-photocycloaddition between the adjacent molecules.

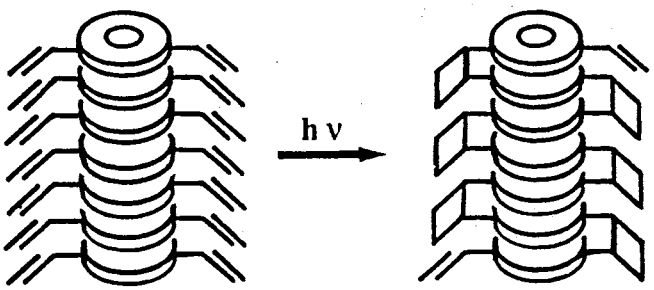

Figure 5. Schematic representation of intracolumnar crosslinking in the columnar ordered state. (The drawings are reproduced from reference 16).

The photoreaction was expected to stabilize the columnar order. However, in the columnar mesophase the liquid crystalline order was disturbed by E/Z-photoisomerization.

Another possible way to build an ion channel is to prepare Langmuir-Blodgett (LB) multilayers of macrocyclic ligands. With hydrocarbon wing groups and polar cores, [18]-N_6 derivatives are able to form ordered monomolecular layers by self-organization at the gas-water interface. This ordered monolayer structure can be transferred to form the so-called LB multilayers and lead to thin films with ordered columnar phases.[30,117,121,124]

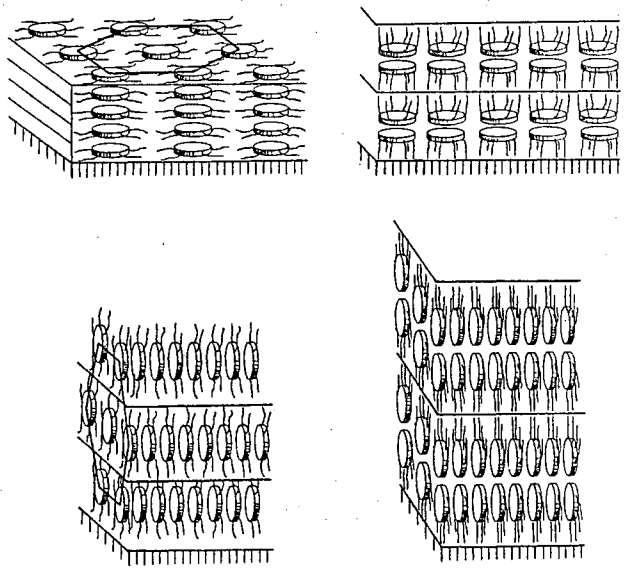

Figure 6. Hypothetical structures of Langmuir-Blodgett multilayers obtained from discotic liquid crystals. (The drawing is reproduced from reference 117).

(b) Polymer Bound Azamacrocycles. Macrocyclic ligands have been used to selectively separate metal ions from mixtures of metal ions in bulk liquid membrane or solvent extraction systems.[125,126] One of the problems is that the expensive macrocycles may slowly be lost from the organic layer of a liquid membrane or solvent extraction system. To solve this problem the macrocyclic ligands are covalently attached to polymers

or silica.[127-142] Usually the macrocyclic ligand bound to polymer or silica gel has approximately the same complexation properties as the corresponding unbound macrocycle for metal ions in aqueous solution.[96]

The high selectivity of azamacrocyclic compounds for transition metals over alkali and alkaline earth metal ions has made the immobilized azamacrocycles ideal candidates for difficult metal ion separations, recoveries, and determinations, such as column preconcentration of trace metals from sea-water or removal of toxic trace metals from industrial wastewater. Different separations can be performed with different macrocyclic ligands. The silica gel bound oxygen-only macrocycles can be used to concentrate alkali metal and alkaline earth metal cations according to size. With a silica gel-bound macrocyclic polyamine it was possible to separate ppb levels of heavy metal cations (Hg^{2+}, Ag^{+}, Pb^{2+}, Cu^{2+}, Cd^{2+}) from concentrated matrices of other cations, such as the alkali and alkaline earth cations.[96] The bound sulfur-containing macrocycles were good for Au^{3+}, Pd^{2+}, Ag^{+}, and Hg^{2+} cations.[142] The macrocycles with both nitrogen and oxygen have been used on a preparative scale to separate transition metal ions. These compounds are now available commercially from IBC Company. A macrocyclic ligand functionalized with a chiral group and bound to a polymer can be used for optical resolution.[138]

In recent years macrocyclic ligands have been successfully used in high performance ion chromatography. In this application typically the macrocyclic ligand must be adsorbed, covalently bonded or polymerized on particulate substrates.[143,144] The silica-bound azamacrocycles have been used to separate various phenolic compounds, nucleic acids, and proteins in the presence of K^{+} ions.[145,146]

(c) Radioactive Azamacrocyclic Complexes for Imaging and Therapy. Azacrown[18]-N_6 derivative **31** can be used for the dissolution of human urinary calculus, in which the major components are calcium phosphate and magnesium phosphate.[147]

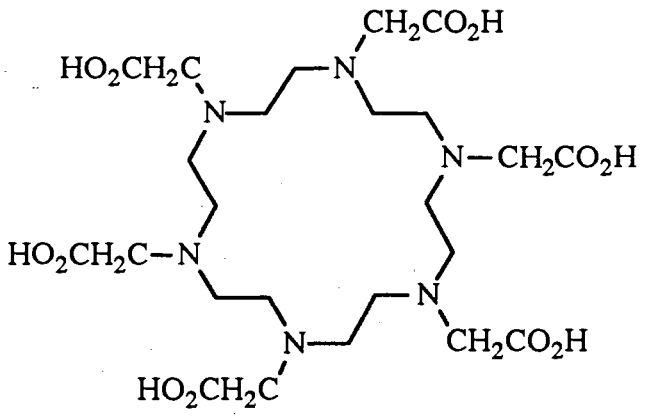

31

Mono-functionalized azamacrocycles have been conjugated with antibodies for tumor-targeting.[148-151] For example, the mono-functionalized azacrown **32**, which was obtained by a selective mono-N-alkylation process,[82] can form kinetically inert complexes with radioactive rhodium. These radioactive complexes are attached to antibodies and used for therapeutic or diagnostic purposes.

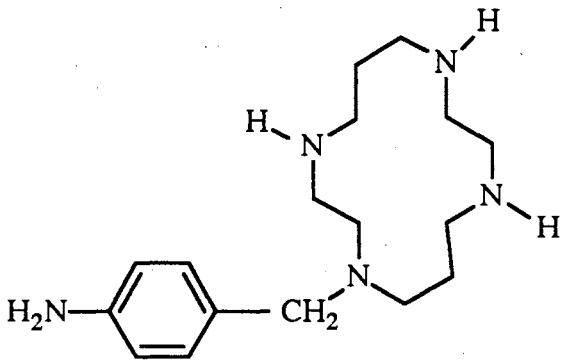

32

(d) Azamacrocycles as Fluorophores for Determination of Metal ions. Macrocyclic ligands functionalized with chromophores are useful as sensor materials for

the determination of metal ions. For example, azacrown **33** was prepared as a fluorescent reagent for determination of Cu^{2+} or Ag^{+} ions. In the presence of these metal cations the fluorescence intensity decreased.[152]

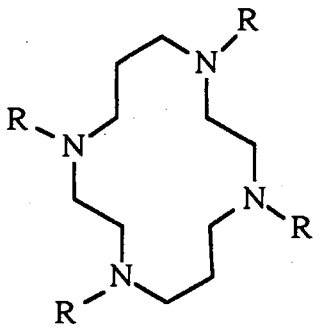

33: R = $-(CH_2)_3-NH-SO_2-$ 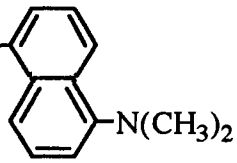 $-N(CH_3)_2$

(e) Modification of Architecture of Azamacrocycles. Kimura reported some methods for the modification of cyclams and other macrocyclic polyamines.[153]

(1) Conversion of amine into amide (lactam). This method will enhance the selectivities for metal ions, reversibilities of metal uptake controlled by pH and the stabilization of enclosed metals at higher oxidation state.

(2) Replacement of N donors by S donors to increase the selectivity for noble metal ions (such as Ag^{+} and Pt^{2+}).

(3) Replacement of skeletal C-H by C-F to obtain new complexes with special properties.

(4) Attachment of a side chain with a potential donor group, such as a cation-ligating donor

arm group. The incorporation of the side chain capable of further coordination will modify the complexation properties of the azamacrocyles.[154-158] When an armed macrocycle forms a host-guest complex, the guest cation is enclosed in such a way that the additional donor groups on the flexible arms further coordinate the guest cation trapped in the parent ligand ring. This method also has been used to change the reactivity of side chain functional groups in macrocyclic metal complexes. The examples include the promoted hydrolysis reactions of nitriles and esters and selective acylation.[158] Because of its coordination and photochemical properties, the 2,2'-bipyridine group has been attached to azacrown[18]-N_6 by Lehn and Ziessel to study their ability to form polynuclear complexes of potential use for catalysis.[154]

While there is intense effort in the synthesis of azacrown derivatives, the exploration for intelligent applications is still in its early stage. To better understand the special liquid crystalline properties and the relationship between molecular structure and liquid crystalline properties, there is need to synthesize azacrowns with different structures and to characterize the phases of the samples. To combine these liquid crystalline azacrowns with polymers for new polymeric liquid crystals and to study how the polymer environment affects the ordering of the macrocyclic mesogens in the liquid crystal state, mono-functionalized azacrowns and polymers need to be synthesized and characterized. To explore potential applications for ion transport or separation with liquid crystalline azacrowns, there is need to examine the complexing of the azacrowns in solution and the liquid crystalline properties of azacrowns in metal complexes. In this thesis we will report some of our research results on azacrown[18]-N_6 derivatives and polymers. The synthesis and characterization of these macrocyclic compounds and polymers will be reported in the Chapter II. The preparation of metal complexes of an azacrown[18]-N_6 hexamine and investigation of their liquid crystalline properties will be given in the Chapter III. The complexing of metal and organic cations with azacrowns in solution will be reported in Chapter IV.

References

(1) Gray, G. W. *Thermotropic Liquid Crystals*; John Wiley & Sons, Inc.: New York, 1987.

(2) Collings, P. J. *Liquid Crystals*; Princeton University Press: Princeton, 1990.

(3) Demus, A. *Liq. Cryst.* **1989**, *5*, 75.

(4) Destrade, C.; Mondon, M. C.; Malthete, J. *J. Phys.* **1979**, *C3*, 17.

(5) Destrade, C.; Foucher, P.; Gasparoux, H.; Tinh, N. H. *Mol. Cryst. Liq. Cryst.* **1984**, *106*, 121.

(6) Kreuder, W.; Ringsdorf, H.; Schonherr, O. H.; Wendorff, J. H. *Angew. Chem. Int. Ed. Engl.* **1987**, *26*, 1249.

(7) Ringsdorf, H.; Schlarb, B.; Venzmer, J. *Angew. Chem. Int. Ed. Engl.* **1988**, *27*, 113.

(8) Collard, D. M.; Lillya, C. P. *J. Am. Chem. Soc.* **1991**, *113*, 8577.

(9) Ohta, K.; Muroki, H.; Takagi, A.; Hatada, K.; Ema, H.; Yamamoto, I.; Matsuzaki K. *Mol. Cryst. Liq. Cryst.* **1986**, *140*, 131.

(10) Moller, M.; Tsukruk, V.; Wendorff, J. H.; Bengs, H.; Ringsdorf, H. *Liq. Cryst.* **1992**, *12*, 17.

(11) Lattermann, G.; Staufer, G.; Brezesinski, G. *Liq. Cryst.* **1991**, *10*, 169.

(12) Chandrasekhar, S.; Ranganath, G. S. *Rep. Prog. Phys.* **1990**, *53*, 57.

(13) Martin, I. G.; Durst, H.; Brzezinski, V.; Krug, H.; Kreuder, W.; Ringsdorf, H. *Angew. Chem. Int. Ed. Engl.* **1989**, *28*, 323.

(14) Paulus, W.; Ringsdorf, H. *Liq. Cryst.* **1991**, *9*, 807.

(15) Ringsdorf, H.; Urban, C. *Polym. Prepr.* **1992**, *33*, 1202.

(16) Mertesdorf, C.; Ringsdorf, H.; Stumpe, J. *Liq. Cryst.* **1991**, *9*, 337.

(17) Ringsdorf, H.; Wustefeld, R. *Philos. Trans. R. Soc. London* **1990**, *A330*, 95.

(18) McArdle, C. B. *Side Chain Liquid Crystal Polymers;* Chapman and Hall: New York, 1989.

(19) Kreuder, W.; Ringsdorf, H. *Makromol. Chem. Rapid Commun.* **1983**, *4*, 807.

(20) Wenz, G. *Makromol. Chem. Rapid Commun.* **1985**, *6*, 577.

(21) Herrmann-Schonherr, O.; Wendorff, J. H.; Kreuder, W.; Ringsdorf, H. *Makromol. Chem. Rapid Commun.* **1986**, *7*, 97.

(22) Huser, B.; Pakula, T.; Spiess, H. W. *Macromolecules* **1989**, *22*, 1960.

(23) Kranig, W.; Huser, B.; Speiss, H. W.; Kreuder, W.; Ringsdorf, H.; Zimmermann, H. *Adv. Mater.* **1990**, *2*, 36.

(24) Kohne, B.; Praefcke, K.; Ringsdorf, H.; Tschirner, P. *Liq. Cryst.* **1989**, *4*, 165.

(25) Percec, V.; Heck, J. *Polym. Bull.* **1991**, *25*, 431.

(26) Percec, H.; Cho, C. G.; Pugh, C.; Tomazos, D. *Macromolecules* **1992**, *25*, 1164.

(27) Lehn, J. M.; Malthete, J.; Levelut, A. M. *J. Chem. Soc., Chem. Commun.* **1985**, 1794.

(28) Lehn, J. M. *Angew. Chem. Int. Ed. Engl.* **1988**, *27*, 89.

(29) Malthete, J.; Poupinet, D.; Vilanove, R.; Lehn, J. M. *J. Chem. Soc., Chem. Commun.* **1989**, 1016.

(30) Mertesdorf, C.; Ringsdorf, H. *Liq. Cryst.* **1989**, *5*, 1757.

(31) Tatarsky, D.; Banerjee, K.; Ford, W. T. *Chem. Mater.* **1990**, *2*, 138.

(32) Idziak, S. H. J.; Maliszewskyj, N. C.; Heiney, P. A.; McCauley, J. P.; Sprengeler, P. A.; Smith, A. B. III *J. Am. Chem. Soc.* **1991**, *113*, 7666.

(33) Idziak, S. H. J.; Maliszewskyj, N. C.; Vaughan, G. B. M.; Heiney, P. A.; Mertesdorf, C.; Ringsdorf, H.; McCauley, J. P.; Smith, A. B. III *J. Chem. Soc., Chem. Commun.* **1992**, 98.

(34) Lattermann, G. *Mol. Cryst. Liq. Cryst.* **1990**, *182B*, 299.

(35) Mertesdorf, C.; Ringsdorf, H. *Mol. Eng.* **1992**, (in press).

(36) Lattermann, G.; Schmidt, S.; Kleppinger, R.; Wendorff, J. H. *Adv. Mater.* **1992**, *4*, 30.

(37) Malthete, J.; Levelut, A. M.; Lehn, J. M. *J. Chem. Soc., Chem. Commun.* **1992**, 1434.

(38) Shinkai, S.; Shimamoto, K.; Manabe, O.; Sisido, M. *Makromol. Chem., Rapid Commun.* **1989**, *10*, 361.

(39) Rodenhouse, R.; Percec, V.; Feiring, E. *J. Polym. Sci. C: Polym. Lett.* **1990**, *28*, 345.

(40) Rodenhouse, R.; Percec, V. *Macromolecules* **1989**, *22*, 2043.

(41) He, G.; Wada, F.; Kikukawa, K.; Matsuda, T. *J. Chem. Soc., Chem. Commun.* **1987**, 1294.

(42) Wen, J.; Hsiue, G. *Makromol. Chem., Rapid Commun.* **1990**, *11*, 151.

(43) Shinkai, S.; Nishi, T.; Ikeda, A.; Matsuda, T.; Shimamoto, K.; Manabe, O. *J. Chem. Soc., Chem. Commun.* **1990**, 303.

(44) Xie, M.; Chen, Y.; He, Y. *Mol. Cryst. Liq. Cryst.* **1991**, *209*, 213.

(45) Shinkai, S.; Nakamura, S.; Ohara, K.; Tachiki, S.; Manabe, O.; Kajiyama, T. *Macromolecules* **1987**, *20*, 21.

(46) Shinkai, S.; Torigoe, K.; Manabe, O.; Kajiyama, T. *J. Am. Chem. Soc.* **1987**, *109*, 4458.

(47) Shinkai, S.; Kajiyama, T. *Pure Appl. Chem.* **1988**, *60*, 575.

(48) Percec, V.; Rodenhouse, R. *Macromolecules* **1989**, *22*, 4408.

(49) Ungar, G.; Percec, V.; Rodenhouse, R. *Macromolecules* **1991**, *24*, 1996.

(50) Hsiue, G.; Wen, J. *Makromol. Chem.* **1991**, *192*, 2243.

(51) Kajiyama T.; Takahara, A.; Kikuchi, H. *Polym. J.* **1991**, *23*, 347.

(52) Rodenhouse, R.; Percec, V. *Makromol. Chem.* **1991**, *192*, 1873.

(53) Wen, J.; Hsiue, G.; Hsu, C. *Makromol. Chem., Rapid Commun.* **1990**, *11*, 151.

(54) Percec, V.; Johansson, G.; Rodenhouse, R. *Polym. Prepr.* **1992**, *33 (1)*, 219.

(55) Shinkai, S.; He, G.; Matsuda, T.; Shimamoto, K.; Nakashima, N.; Manabe, O. *J. Polym. Sci. C: Polym. Lett.* **1989**, *27*, 209.

(56) Neve, F.; Ghedini, M. *International Symposium on Macrocyclic Chemistry* **1992**, Abstracts, p 75.

(57) Zabirov, N. G.; Galyautdinov, N. I.; Shcherbakova, V. A.; Cherkasov, R. A. *Zh. Obshch. Khim.* **1990**, *60*, 1247 (*Chem. Abst.* **1991**, *114*, 6634).

(58) Xie, M.; Qin, J.; Hong, F.; Wang, L. *Mol. Cryst. Liq. Cryst.* **1991**, *209*, 309.

(59) He, G.; Wada, F.; Kikukawa, K.; Shinkai, S.; Matsuda, T. *J. Org. Chem.* **1990**, *55*, 541.

(60) Krakowiak, K. E.; Bradshaw, J. S.; Zamecka-Krakowiak, D. J. *Chem. Rev.* **1989**, *89*, 929.

(61) Atkins, T. J.; Richman, J. E.; Oettle, W. F. *Org. Synth.* **1978**, *58*, 86.

(62) Chavez, F.; Sherry, A. D. *J. Org. Chem.* **1989**, *54*, 2990.

(63) Jurczak, J.; Kasprzyk, S.; Salanski, P.; Stankiewicz, T. *J. Chem. Soc., Chem. Commun.* **1991**, 956.

(64) Kimura, E.; Kuramoto, Y.; Koike, T; Fujioka, H.; Kodama, M. *J. Org. Chem.* **1990**, *55*, 42.

(65) Tabushi, I.; Fujiyoshi, M. *Heterocycles* **1977**, *7*, 851.

(66) Hediger, M.; Kaden, T. A. *J. Chem. Soc., Chem. Commun.* **1978**, 14.

(67) Hediger, M.; Kaden, T. A. *Helv. Chim. Acta* **1983**, *66*, 861.

(68) Pilichowski, J. F.; Lehn, J. M. *Tetrahedron* **1985**, *41*, 1959.

(69) Hoesseini, M. W.; Lehn, J. M.; Duff, S. R.; Gu, K.; Mertes, M. P. *J. Org. Chem.* **1987**, *52*, 1662.

(70) Santis, G. D.; Casa, M. D.; Mariani, M.; Seghi, B.; Fabbrizzi, L. *J. Am. Chem. Soc.* **1989**, *111*, 2422.

(71) Gu, K.; Mertes, K. B.; Mertes, M. P. *Tetrahedron Lett.* **1989**, *30*, 1323.

(72) Bradshaw, J. S.; Krakowiak, K. E.; Izatt, R. M. *Tetrahedron Lett.* **1989**, *30*, 803.

(73) Krakowiak, K. E.; Bradshaw, J. S.; Izatt, R. M.; Zamecka-Krakowiak, D. J. *J. Org. Chem.* **1989**, *54*, 4061.

(74) Helps, I. M.; Parker, D.; Morphy, J. R.; Chapman, J. *Tetrahedron* **1989**, *45*, 219.

(75) Bradshaw, J. S.; Krakowiak, K. E.; Izatt, R. M. *J. Heterocyclic Chem.* **1989**, *26*, 565.

(76) Krakowiak, K. E.; Bradshaw, J. S.; Dalley, N. K.; Jiang, W.; Izatt, R, M. *Tetrahedron Lett.* **1989**, *30*, 2897.

(77) Krakowiak, K. E.; Bradshaw, J. S.; Izatt, R. M. *J. Org. Chem.* **1990**, *55*, 3364.

(78) Filali, A.; Yaouanc, J. J.; Handel, H. *Angew. Chem. Int. Ed. Engl.* **1991**, *30*, 560.

(79) Kruper W. J. U.S. Patent, **1991**, 4994560 (*Chem. Abst.* **1991**, *114*, 224663).

(80) Anelli, P. L.; Murru, M.; Uggeri, F.; Virtyani, M. *J. Chem. Soc., Chem. Commun.* **1991**, 1317.

(81) Yaouanc, J. J.; Bris, N. L.; Gall, G. L.; Clement, J. C.; Handel, H.; Abbayes, H. D. *J. Chem. Soc., Chem. Commun.* **1991**, 206.

(82) Bulach, V.; Mandon, D.; Weiss, R. *Angew. Chem. Int. Ed. Engl.* **1991**, *30*, 572.

(83) Qian, L.; Sun, Z.; Mertes, M. P.; Mertes, K. B. *J. Org. Chem.* **1991**, *56*, 4904.

(84) Pedersen, C. J. *J. Am. Chem. Soc.* **1970**, *92*, 391.

(85) Izatt, R.; Bradshaw, J. S.; Nielsen, S. A.; Lamb, J. D.; Christensen, J. J. *Chem. Rev.* **1985**, *85*, 271.

(86) Kodama, M.; Kimura, E.; Yamaguchi, S. J. *J. Chem. Soc. Dalton Trans.* **1980**, 2537.

(87) Bencini, A.; Bianchi, A.; Micheloni, M.; Paoletti, P.; Garcia-Espana, E; Nino, M. A. *J. Chem. Soc. Dalton Trans.* **1991**, 1171.

(88) Martin, L. Y.; Sperati, C. R.; Busch, D. H. *J. Am. Chem. Soc.* **1977**, *99*, 2968.

(89) Nagai, R.; Kodama, M. *Inorg. Chem.* **1984**, *23*, 4184.

(90) Kato, M.; Ito, T. *Inorg. Chem.* **1985**, *24*, 504.

(91) Kato, M.; Ito, T. *Inorg. Chem.* **1985**, *24*, 509.

(92) Tsukube, H. *J. Chem. Soc., Chem. Commun.* **1983**, 970.

(93) Tsukube, H.; Takagi, K.; Higashiyama, T.; Iwachido, T.; Hayama, N. *J. Chem. Soc. Perkin Trans. II* **1985**, 1541.

(94) Tsukube, H. *J. Coord. Chem.* **1987**, *16*, 101.

(95) Liebmann, A.; Mertesdorf, C.; Plesnivy, T.; Ringsdorf, H.; Wendorff, J. H. *Angew. Chem. Int. Ed. Engl.* **1991**, *30*, 1375.

(96) Izatt, R. M.; Bruening, R. L.; Tarbet, B. J.; Griffin, L. D.; Bruening, M. L.; Kradowiak, K. E.; Bradshaw, J. S. *Pure Appl. Chem.* **1990**, *62*, 1115.

(97) Cordier, D.; Hosseini, M. W. *New J. Chem.* **1990**, *14*, 611.

(98) Tsukube, H. *J. Chem. Soc., Perkin I*, **1985**, 615.

(99) Bencini, A.; Bianchi, A.; Garcia-Espana, E.; Giusti, M.; Mangani, S.; Micheloni, M.; Orioli, P.; Paoletti, P. *Inorg. Chem.* **1987**, *26*, 3902.

(100) Hosseini, M. W.; Lehn. J.; M. *Helv. Chim. Acta.* **1988**, *71*, 749.

(101) Bianchi, A.; Micheloni, M.; Paoletti, P. *Pure Appl. Chem.* **1988**, *60*, 525.

(102) Machida, R.; Kimura, E.; Kodama, M. *Inorg. Chem.* **1983**, *22*, 2055.

(103) Kimura, E.; Sakonaka, A.; Machida, R.; Kimura, M. *J. Am. Chem. Soc.* **1982**, *104*, 4255.

(104) Machida, R.; Kimura, E.; Kushi, Y. *Inorg. Chem.* **1986**, *25*, 3461.

(105) Kimura, E.; Machida, R.; Kodama, M. *J. Am. Chem. Soc.* **1984**, *106*, 5497.

(106) Hosseini, M. W.; Lehn, J. M.; Maggiora, L.; Mertes, K. B.; Mertes, M. P. *J. Am. Chem. Soc.* **1987**, *109*, 537.

(107) Lehn, J. M. *Angew. Chem.* **1988**, *100*, 91.

(108) Blackburn, G. M.; Thatcher, G. R. J.; Hosseini, M. W.; Lehn, J. M. *Tetrahedron Lett.* **1987**, *28*, 2779.

(109) Hosseini, M. W.; Lehn, J. M. *J. Coord. Chem.* **1987**, *109*, 7047.

(110) Collin, J. P.; Jouaiti, A.; Sauvage, J. P. *Inorg. Chem.* **1988**, *27*, 1986.

(111) Ebert, M.; Ringsdorf, H.; Wendorff, J. H.; Wustefeld, R. *Polym. Prepr.* **1989**, *30 (2)*, 479.

(112) Ebert, M.; Frick, G.; Baehr, C.; Wendorff, J. H. *Liq. Cryst.* **1992**, *11*, 293.

(113) Fragten, U. K.; Roks, M. F. M.; Nolte, J. M. *J. Chem. Soc., Chem. Commun.* **1985**, 1275.

(114) Gokel, G. W.; Hernandez, J. C.; Viscariello, A. M.; Arnold, K. A.; Campana, C. F.; Echegoyen, L.; Fronczek, F. R.; Gandour, R. D.; Morgan, C. R.; Trafton, J. E.; Miller, S. R.; Minganti, C.; Eiband, D.; Schultz, R. A.; Tamminen, M. *J. Org. Chem.* **1987**, *52*, 2963.

(115) Sirlin, C.; Bosio, L.; Simon, J. *Chem. Phys. Lett.* **1987**, *139*, 362.

(116) Simon, J.; Sirlin, C. *Pure Appl. Chem.* **1989**, *61*, 1625.

(117) Laschewsky, A. *Angew. Chem. Int. Ed. Engl.* **1989**, *28*, 1574.

(118) Shinkai, S.; He, G.; Matsuda, T; Shimamoto, K.; Nakashima, N.; Manabe, O. *J. Polym. Sci. C: Polym. Lett.* **1989**, *27*, 209.

(119) Lehn, J. M. *Angew. Chem. Int. Ed. Engl.* **1990**, *29*, 1304.

(120) Nakano, A.; Xie, Q.; Mallen, J. V.; Echegoyen, L.; Gokel, G. W. *J. Am. Chem. Soc.* **1990**, *112*, 1287.

(121) Ducharme, D.; Salesse, C.; Leblanc, R. M.; Meller, P.; Mertesdorf, C.; Ringsdorf, H. *Makromol. Chem. Macromol. Symp.* **1991**, *46*, 97.

(122) Vogtle, F.; Schroder, A.; Karbach, D. *Angew. Chem. Int. Ed. Engl.* **1991**, *30*, 575.

(123) Percec, V.; Heck, J. *Polym. Prepr.* **1992**, *33 (1)*, 217.

(124) Malthete, J.; Poupinet, D.; Vilanove, R.; Lehn, J. M. *J. Chem. Soc., Chem. Commun.* **1989**, 1016.

(125) Kirch, M.; Lehn, J. M. *Angew. Chem. Int. Ed. Engl.* **1975**, *8*, 555.

(126) Hernandez, J. C.; Trafton, J. E.; Gokel, G. W. *Tetrahedron Lett.* **1991**, *32*, 6269.

(127) Gramain, P.; Frere, Y. *Macromolecules.* **1979**, *12*, 1039.

(128) Yagi, K.; Ruiz, J.; Sanchez, M. C.; Guerrero, C. *Polym. Prepr.* **1982**, *23 (1)*, 169.

(129) Szczepaniak, W.; Kuczynski, K. *React. Polym.* **1985**, *3*, 101.

(130) Wohrle, D.; Nicolaus, V. *Polym. Bull.* **1986**, *15*, 185.

(131) Yokota, K.; Kakuchi, Toyoji.; Yamanaka, M.; Takada, Y. *Makromol. Chem., Rapid Commun.* **1986**, *7*, 633.

(132) Shirai, M.; Moriuma, H.; Tanaka, M. *Macromolecules* **1989**, *22*, 3186.

(133) Wienk, M. M.; Stolwijk, T. B.; Sudholter, J. R.; Reinhoudt, D. N. *J. Am. Chem. Soc.* **1990**, *112*, 797.

(134) Harris, S. J.; Barrett, G.; McKervey, M. A. *J. Chem. Soc., Chem. Commun.* **1991**, 1224.

(135) Delaviz, Y.; Gibson, H. W. *Polym. Mater. Sci. Eng.* **1992**, *66*, 301.

(136) Nicolaus, V.; Wohrle, D. *Angew. Makromol. Chem.* **1992**, *198*, 179.

(137) Bradshaw, J. S.; Krakowiak, K. E.; Tarbet, B. J.; Bruening, R. L.; Biernat, J. F.; Bochenska, M.; Izatt, R. M.; Christensen, J. J. *Pure Appl. Chem.* **1989**, *61*, 1619.

(138) Kakuchi, T.; Takaoka, T.; Yokota, K. *Polym. J.* **1990**, *22*, 199.

(139) Bartulin, J.; Parra, M.; Zunza, H. *Polym. Bull.* **1990**, *24*. 129.

(140) Blain, S.; Appriou, P.; Handel, H. *Analyst* **1991**, *116*, 815.

(141) Bruening, M. L.; Mitchell, D. M.; Bradshaw, J. S.; Izatt, R. M. *Anal. Chem.* **1991**, *63*, 21.

(142) Bradshaw, J. S.; Krakowiak, K. E.; Izatt, R. M.; Bruening, R. L.; Tarbet, B. J. *J. Heterocycl. Chem.* **1990**, *27*, 347.

(143) Lauth, M.; Gramain, P. *J. Chromatogr.* **1987**, *395*, 153.

(144) Lamb, J. D.; Smith, R. G. *J. Chromatogr.* **1991**, *546*, 73.

(145) Szczepaniak, W.; Szymanski, A. *Chem. Anal. (Warsaw)* **1987**, 273.

(146) Josic, D.; Reutter, W. *J. Chromatogr.* **1989**, *476*, 309.

(147) Kimura, E.; Haruto, F.; Atsuko, Y.; Hiromi, N.; Mutsuo, K. *Chem. Pharm. Bull.* **1985**, *33*, 655.

(148) Morphy, J. R.; Parker, D.; Alexander, R.; Bains, A.; Carne, A. F.; Eaton, M. A. W.; Harrison, A.; Millican, A.; Phipps, A.; Rhind, S. K.; Titmas, R.; Weatherby, D. *J. Chem. Soc., Chem. Commun.* **1988**, 156.

(149) Parker, D.; Morphy, J. R.; Jankowski, K.; Cox, J. *Pure Appl. Chem.* **1989**, *61*, 1637.

(150) William, K. Eur. Pat. **1988**, EP 374929 (*Chem. Abst.* **1991**, *114*, 6547).

(151) Takenochi, K.; Watanabe, K.; Takeshi, H.; Kato, Y.; Kimura, E. Jpn. Pat. **1991**, JP 03197468 (*Chem. Abst.* **1992**, *116*, 128980).

(152) Fujiwara, M.; Wakita, H.; Matsushita, T.; Shono, T. *Anal. Sci.* **1991**, *7*, 483.

(153) Kimura, E. *Pure Appl. Chem.* **1989**, *61*, 823.

(154) Lehn, J. M.; Ziessel, R. *J. Chem. Soc., Chem. Commun.* **1987**, 1292.

(155) Tschudin, D.; Basak, A.; Kaden, T. A. *Helv. Chim. Acta* **1987**, 1292.

(156) Tsukube, H.; Adachi, H.; Morosawa, S. *J. Chem. Soc. Perkin Trans. I* **1989**, 1537.

(157) Vaira, M. D.; Mani, F.; Stoppioni, P. *J. Chem. Soc., Chem. Commun.* **1989**, 126.

(158) Kaden, T. A.; Tschudin, D.; Studer, M.; Brunner, U. *Pure Appl. Chem.* **1989**, *61*, 879.

CHAPTER II

SYNTHESIS AND THERMOTROPIC LIQUID CRYSTALLINE PROPERTIES OF AZAMACROCYCLES

Introduction

The first azamacrocyclic liquid crystals were discovered by Lehn, Malthete, and Levelut in 1985.[1] In a search for novel liquid crystals by using macrocycles fitted with suitable lateral chains as basic units, they found three hexa-acylated azamacrocyclic compounds that exhibited mesophases. Based on the measurements of X-ray diffraction using low resolution techniques as well as optical microscopy, they suggested the new mesophases to have a hexagonal-tubular structure. In this "tubular mesophase" the macrocyclic molecules stack into parallel columns placed at the vertices of a hexagonal lattice. If the stacked disc-like macrocycles really form hollow columns, this kind of supramolecular architecture would be very interesting. They might be used as molecular or ionic channels and open ways for new properties of materials. One of the potential uses is phase-dependent ion-conducting channels for controllable cation-selective semipermeable membranes. Since then more effort has been made to synthesize and study liquid crystalline azamacrocycles.[2-8] To be able to form a columnar mesophase usually the disc-like molecule contains a rigid, flat core with six or more flexible aliphatic tails. For azamacrocyclic liquid crystals the conformation of the disc depends on the planar rigid substitutents. Only aromatic carboxylic acid derivatives of [18]-N_6 are known to be liquid crystalline. The optimized space filling of aliphatic hydrocarbon tails is also important. A minor change of molecular structure will lead to different liquid crystal properties. The hexagonal order in the "tubular mesophase" of two azacrown[18]-N_6 derivatives has been

confirmed by the existence of higher order diffraction peaks in high resolution powder X-ray diffraction.[6] So far the evidence of hexagonal order in compound **1** is still not clear, and there is argument about whether compound **1** forms a columnar mesophase.[3,7]

In this research project we have studied the liquid crystalline properties of low molar mass and polymeric [18]-N_6 derivatives. The target macrocycles **1-4** and side chain liquid crystalline polymer **5** are given in Figure 1. The goal is to better understand the relationship between molecular structure and liquid crystalline properties and how the polymer environment affects the ordering of the macrocyclic mesogens in the liquid crystal state.

Experimental Section

Materials and Analytical Methods. All organic reagents were obtained from Aldrich and were used without further purification unless otherwise stated. Triethylamine and dichloromethane were distilled from calcium hydride. 1,4,7,10,13,16-Hexaazacyclooctadecane (**[18]-N_6**) was prepared according to the method of Atkins, Richman, and Oettle.[9] 4-(10-Undecylenyloxy)benzoyl chloride, 4-dodecyloxybenzoyl chloride and 3,4-bis(dodecyloxy)benzoyl chloride were prepared as reported in the literature.[4] NMR spectra were recorded on a Varian XL-300 instrument at 300 MHz for ^1H or 75.43 MHz for ^{13}C. All spectra were recorded in $CDCl_3$ solution with TMS as internal standard unless otherwise specified. IR spectra were taken on a Perkin-Elmer 681 infrared spectrophotometer with KBr disks. A Varian DMS 200 UV-visible spectrophotometer was used for UV measurements. Thin layer chromatography was performed with silica gel high-performance TLC plates (HPTLC-HL, Analtech Inc.). Silica gel (40 μm, Baker) was used for flash chromatography. High pressure liquid chromatographic (HPLC) analyses were performed with a Waters 590 pump equipped with

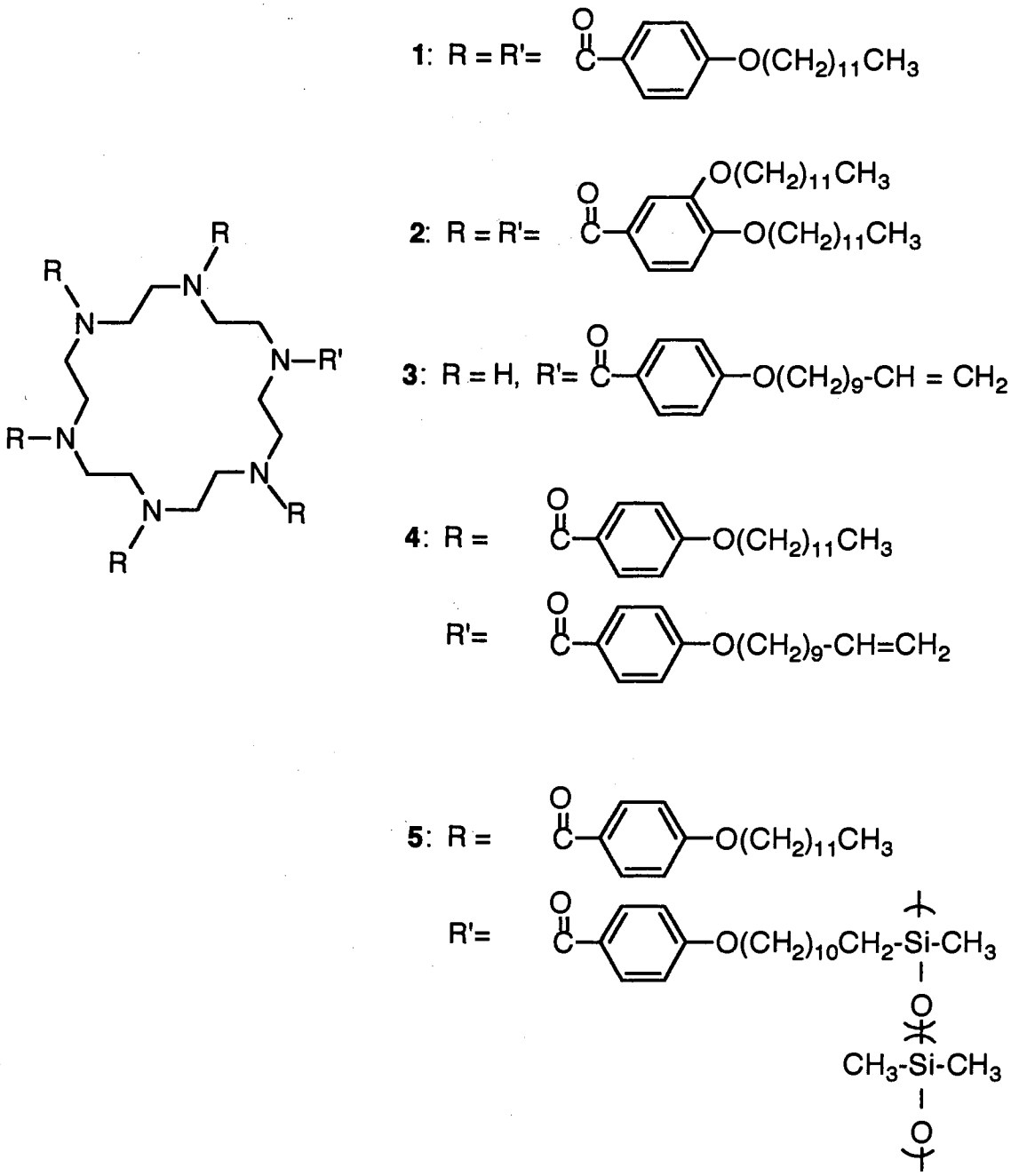

Figure 1. Structures of [18]-N_6 compounds.

a normal phase 5 μm silica column (length x ID = 250 mm x 4.6 mm, Whatman PARTISIL 5), a Beckman 153 analytical 254 nm UV detector, and an Interactive Microware data station. GPC analyses were performed using three PL (polystyrene) gel columns of 10^2, 10^3, 10^4 Å obtained from Polymer Laboratories, Ltd. Tetrahydrofuran (THF) was the solvent at a flow rate of 1mL/min, and monodisperse polystyrenes were used as standards. Elemental analyses were performed at Atlantic Microlab Inc. All X-ray diffraction experiments were done by S. Idziak and N. Maliszewskyj in the laboratory of Dr. Paul Heiney in the Department of Physics at the University of Pennsylvania.

1,4,7,10,13,16-Hexa-(4-dodecyloxybenzoyl)-1,4,7,10,13,16-hexaazacyclooctadecane (1). Synthesis was performed by treating **[18]-N_6** (0.52 g, 2.0 mmol) with 4-dodecyloxybenzoyl chloride (3.90 g, 12 mmol) in 30 mL of DMF (N,N-dimethylformamide) in the presence of DMAP [4-(N,N-dimethylamino)pyridine] for 14 h at 80 °C.[4] The crude product was crystallized from ethanol and finally dried by lyophilization of a benzene solution to yield pure product (72.9%). ^{1}H and ^{13}C NMR spectra were consistent with the structure. Anal. Calcd. for $C_{126}H_{198}N_6O_{12}$: C, 76.10; H, 10.03; N, 4.22. Found: C, 76.16; H, 10.03; N, 4.41.

1,4,7,10,13,16-Hexa-(3,4-bisdodecyloxybenzoyl)-1,4,7,10,13,16-hexaazacyclooctadecane (2). A solution of **[18]-N_6** (0.26 g, 1.0 mmol), the acid chloride from 3,4-bis(dodecyloxy)benzoic acid (3.50 g, 7.0 mmol), DMAP (1.71 g, 14.0 mmol), and 30 mL of DMF was stirred under nitrogen for 48 h at 80 °C. The DMF was removed under water aspirator vacuum and 50 mL of chloroform was added. The organic layer was washed twice with 100 mL of water and the concentrated mixture was separated by silica gel chromatography using 98/2 (v/v) chloroform/methanol as eluant. The crude product was crystallized from ethanol to yield 1.87 g (60.4%) of white product. ^{1}H NMR (50 °C): δ 0.89 (t, 36 H, CH_3), 1.28 (m, 192 H, CH_2), 1.45 (m, 24 H, CH_2), 1.78 (m, 24 H, CH_2), 3.74 (m, 24 H, NCH_2), 3.90, 3.98 (m, 24 H, CH_2O), 6.78 (m, 18 H, Ar).

^{13}C NMR (50 °C): δ 14.0 (CH_3), 22.6, 26.1, 29.3, 29.4, 29.5, 29.6, 31.9 (CH_2), 47-49 (br., NCH_2), 69.3, 69.6 (CH_2O), 113.1, 113.4, 120.0, 127.6, 149.4, 151.1 (Ar), 172.3 (C=O). IR (KBr): 2935 (s), 2860 (s), 1635 (m), 1470 (m), 1274 (s) cm^{-1}. Anal. calcd. for $C_{198}H_{342}N_6O_{18}$: C, 76.84; H, 11.14; N, 2.72. Found: C, 76.80; H, 11.18; N, 2.69. Mass spectrum (FAB, 2-nitrophenyl octyl ether/p-toluenesulfonic acid 2/1 v/v) m/z 3096 [$(M+H)^+$, calcd for $C_{198}H_{343}N_6O_{18}$: 3095.91].

1-[4-(10-Undecylenyloxy)benzoyl]-1,4,7,10,13,16-hexaazacyclooctadecane (3). A solution of 4-(10-undecylenyloxy)benzoyl chloride (3.08 g, 10.0 mmol) in 0.5 L of dichloromethane was added dropwise over 3 h at 40 °C to a stirred solution of **[18]-N_6** (7.83 g, 30.0 mmol), triethylamine (4.04 g, 40.0 mmol) and 2 L of dichloromethane. After 14 h the solid residue was removed by filtration, and the mixture was concentrated and washed with water. Dichloromethane was removed and residual oil (about 6 g) was separated by flash chromatography using 20/5/1 (volume) chloroform/ methanol/ 28% ammonium hydroxide as eluent. Pure product, 1.14 g (22%), was obtained as a viscous oil. ^1H NMR: δ 1.33 (m, 12 H, CH_2), 1.75 (m, 2 H, CH_2), 2.05 (m, 7 H, CH_2, NH), 2.70, 2.85, 3.58 (m, 24 H, NCH_2), 3.95 (t, 2 H, CH_2O), 4.95 (m, 2 H, $=CH_2$), 5.80 (m, 1 H, CH=), 6.88, 7.38 (m, 4 H, Ar). ^{13}C NMR: δ 25.9, 28.8, 29.0, 29.1, 29.2, 29.3, 29.4, 33.6 (CH_2), 48.3, 48.8, 49.0 (NCH_2), 68.1 (CH_2O), 114.0 ($=CH_2$), 139.0 (CH=), 114.3, 128.5, 129.0, 160.0 (Ar), 172.4 (C=O).

4,7,10,13,16-Penta-(4-dodecyloxybenzoyl)-1-[4-(10-undecylenyloxybenzoyl)]-1,4,7,10,13,16-hexaazacyclooctadecane (4). A solution of compound **3** (0.66 g, 1.2 mmol), triethylamine (2.40 g, 24.0 mmol), 4-dodecyloxybenzoyl chloride (3.00 g, 9.2 mmol), and 60 mL of dichloromethane was stirred at 40 °C for 72 h. The solvent and excess triethylamine were removed by aspirator vacuum, and 30 mL of chloroform was added. The organic layer was washed twice with 100 mL of water, and the concentrated mixture was separated by chromatography using

98/2 (v/v) chloroform/methanol as eluent. The product was recrystallized from ethanol to give 1.27 g (53%) of white solid. ^{13}C NMR (50 °C): δ 14.0 (CH_3), 22.5, 25.9, 29.0, 29.1, 29.2, 29.3, 29.4, 29.5, 31.8, 33.2 (CH_2), 47.5 (br. CH_2N), 68.2 (CH_2O), 114.4 (=CH_2), 139.0 (CH=), 114.5, 126.9, 128.7, 160.5 (Ar), 171.9 (C=O). The ^1H NMR spectrum was the same as that of compound **1**, except that there were small peaks at 4.95 and 5.82 ppm (CH_2=CH-). Anal. Calcd. for $C_{125}H_{194}N_6O_{12}$: C, 76.10; H, 9.91; N, 4.26. Found: C, 76.00; H, 9.74; N, 4.17.

Polymer (5a). Compound **4** (0.81 g, 0.41 mmol), random poly(methylhydrosiloxane-co-dimethylsiloxane) (0.19 g, 0.40 mmol Si-H) and 5 mL of dry toluene were added to a 10 mL glass tube containing a micro stirring bar. The starting polymer was supplied from Petrarch, M_n = 2000-2500, containing 15-18% of repeating units of hydromethylsiloxane as reported by the supplier, calcd. DP_n = 29. While a stream of argon was bubbled through the solution for 15 min, 4 μL of platinum-divinyltetramethyldisiloxane catalyst (3.0-3.5% platinum solution in xylene from Petrarch) was added. The tube was sealed and kept at 100 °C for 48 h. The Si-H IR absorption at 2140 cm^{-1} had totally disappeared. The polymer was precipitated into 60 mL of methanol with stirring. The precipitate was separated by centrifugation and dissolved in chloroform. The polymer was precipitated from a solution of chloroform by the slow addition of methanol with continuous stirring. After 12 precipitations to remove residual compound **4**, which comprised about 40% of the initial product by GPC analysis, 80 mg (8%) of purified polymer was obtained.

Polymer (5b). The procedure was followed as described above using compound **4** (0.45 g, 0.23 mmol), an ethanol solution of chloroplatinic acid catalyst (H_2PtCl_6, 0.1 mg) and copolysiloxane (0.03 g, 0.2 mmol Si-H). The starting polymer was supplied from Petrarch, M_n = 900-1000, containing 50-55% of repeating units of hydromethylsiloxane as reported by the supplier, calc. DP_n = 14. The polymer was

analyzed also by ^{29}Si NMR and by GPC, M_n = 1050 as determined by GPC, and M_n = 1300, DP_n = 17, containing 53% hydromethylsiloxane as determined by ^{29}Si NMR.[10] The polymer was separated by 3 precipitations from chloroform to methanol and purified by GPC to yield 11% of purified product. The separation was done by 14 x 0.1 mL injections of a THF solution containing a total of 200 mg of the polymer into the GPC at a flow rate of 1 mL/min to yield 53 mg (11%) of purified **5b**.

The purities and molecular weights of the polymers were determined by GPC. The residual compound **4** in each polymer was less than 2%. The molecular weights of the polymers are given in Table I. There was no Si-H ^1H NMR spectral line at 4.7 ppm or CH_2=CH- spectral line at 5.0 or 5.6 ppm. The percentage of macrocyclic side groups on each polymer chain was calculated from the intensity ratio of the Si-CH_3 signal (0.15 ppm) to that of the aromatic signal (6.8-7.4 ppm). In polymer **5a** 79% of the Si-H bonds reacted with compound **4**, and in polymer **5b** 32% of the Si-H bonds reacted with compound **4**.

Table I. Characterization of Side Chain Copolymers

polymer	**5a**	**5b**
M_n (M_w/M_n)[a]	7830 (1.56)	7430 (1.36)
% substitution of Si-H bonds[b]	79%	32%
wt % of mesogenic group on polymer	75%	84%

[a] by GPC. [b] by ^1H NMR.

Characterization of the Phase Behavior. The phase behaviors of the co-polymers, and the corresponding low molar mass azamacrocyclic derivatives **1**, **2** and **4** were studied using differential scanning calorimetry (DSC) and optical polarizing microscopy. Thermal transitions were determined with a Perkin-Elmer DSC-2C differential scanning calorimeter equipped with a TADS 3600 data station. Heating and cooling rates were 20 °C/min, unless noted otherwise. The sample sizes were 5-10 mg. Two separate scans were done for polymer samples. The first scan was done from about -100 °C to 50 °C under nitrogen. The second scan was done from 20 °C to about 180 °C under air. The first order transitions were read at the maximum of the endothermic or exothermic peaks. Glass transition temperatures (T_g) were read at the midpoint of the change in the heat capacity. The temperature and ΔH were calibrated with indium as the standard. The thermal transitions and anisotropic textures were observed on a Nikon 104 optical polarizing microscope fitted with a Nikon 35 mm automatic camera and an Instec hot stage controlled by an Apple II computer. X-ray powder diffraction measurements were done by Stefan H. J. Idziak and Nicholas C. Maliszewskyj in the laboratory of Dr. Paul A. Heiney at the University of Pennsylvania.

Results

Synthesis. The hexacyclen derivatives **1**, **2**, **3**, **4** and polymer **5** were synthesized as shown in Scheme I.

One major problem in the synthesis of monosubstituted azamacrocyclic compounds is the how to minimize and separate the multisubstituted by-products. In the synthesis of mono-N-acylated azamacrocyclic compound **3**, a large excess of azacrown[18]-N_6 was used to limit the multi-N-acylation. Even at a molar ratio of **[18]-N_6**/acyl chloride of 3/1, there were about 30% of multi-N-acylated by-products. The analysis by TLC and NMR indicates that the major byproducts were the three isomeric disubstituted macrocycles, and there were also trisubstituted compounds in the reaction mixture.

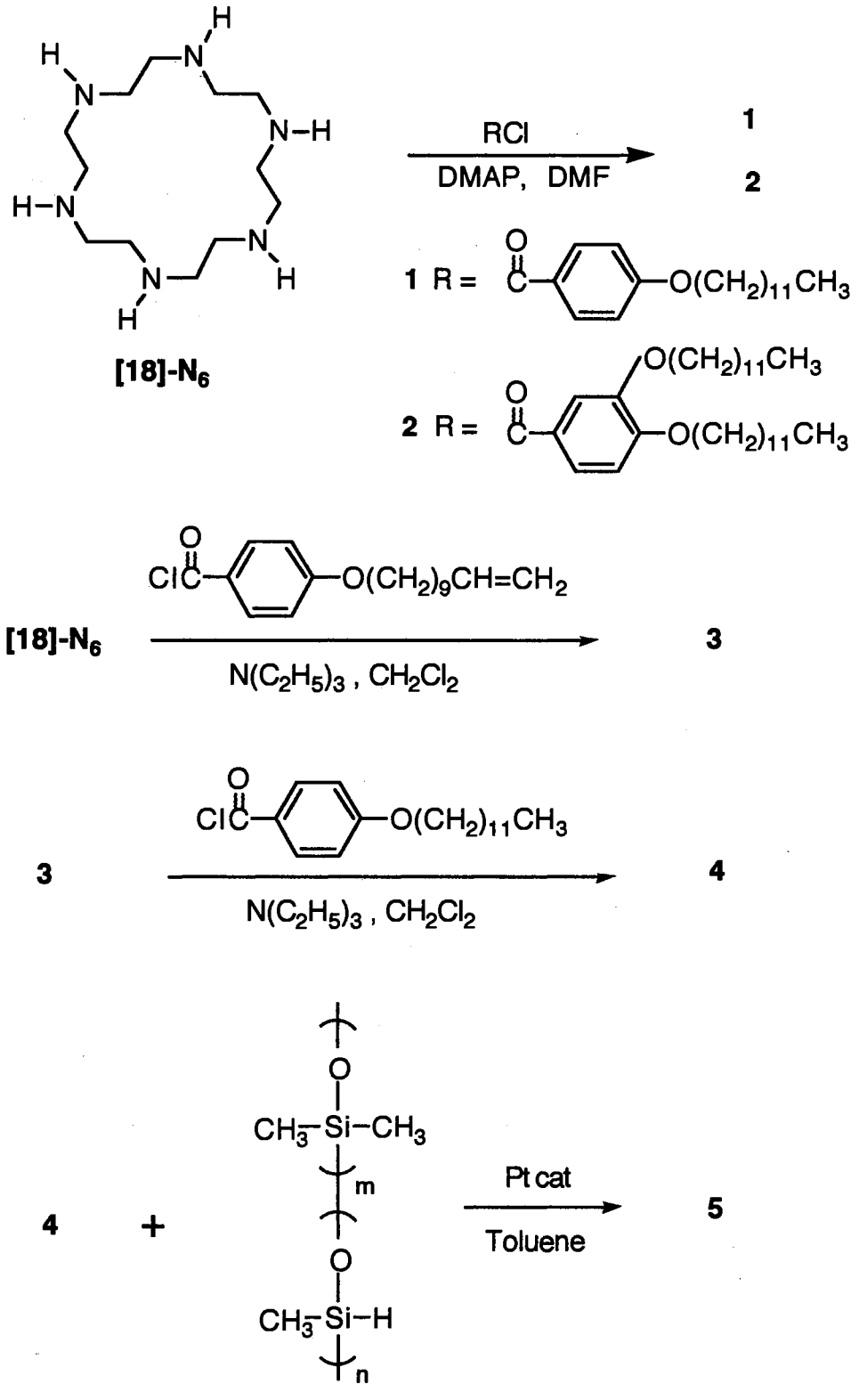
[18]-N6
RCl
DMAP, DMF
1
2
1 R =
2 R =
O(CH2)11CH3
[18]-N6
ClC
O(CH2)9CH=CH2
N(C2H5)3 , CH2Cl2
3
4
CH3–Si–CH3
CH3–Si–H
m
n
Pt cat
Toluene
5

Scheme I

The side chain polymers were prepared by standard hydrosilylation of copolysiloxane. To reduce the steric hindrance, copolysiloxanes with 15-18% and 50-55% Si-H bonds was used as starting polymers in these experiments. Both ^{1}H NMR and GPC analysis show that about 32%-79% of Si-H bonds were grafted with azamacrocyclic groups. It is possible to improve the yield of polymer substitution by hydrosilylation with large excess of compound **4**. Because of the high molecular weight of mesogen, the weight percentages of the mesogenic functional group are 75% and 84% for polymer **5a** and **5b**.

Liquid Crystalline Phases. Hexamide 1. The DSC analysis shows that the first heating curves of the compound **1** were not only different from the second one, but also were affected by recrystallization conditions and thermal history. Different DSC results have been reported for this compound prepared in different laboratories. Table II summarizes the phase transitions of hexamide **1**. The DSC thermograms of compound **1** are given in Figure 2. Figure 3 shows polarizing micrographs of the textures. When a sample was cooled from isotopic melt at a rate of 0.5 °C/min or faster, only a featureless grainy birefringent texture was observed. The cooled sample usually contained a small amount of liquid crystal and a large amount of amorphous substance. If the sample was sheared during cooling, the amount of the liquid crystal increased and a better texture was observed (Figure 3). This texture resembles the texture reported originally.[1] When the sample was annealed at about 100 °C for 3 days, a spherulitic texture developed (Figure 4).

To study the annealing effect, compound **1** was sandwiched between two cover glass slips of thickness of about 50 μm and cooled from the 170 °C isotopic melt at 0.1 °C/min to 105 °C. The spherulite textures were developed by isothermal annealing at 105 °C on the hot stage of the microscope. To observe the morphology and the spherulite growth rate, photomicrographs were taken at different times. Figure 5 displays typical growing spherulites. The spherulites with a maltese cross pattern grow out from primary nuclei and result in irregular polygons.

Table II. DSC Phase Transitions of Macrocyclic Amide **1**.

	transitions, °C (ΔH, kcal/mol)[a]	reference
first heating	C 121.5 (35.7) D 141.5 (0.7) I	1
	C 108.0 (25.4) D 140.0 (0.6) I	2
	C 102.0 (30.4) D 131.0 (0.7) I	4
	C 110.0 (7.0) D_1 118.0 (17.4) D_2 140.0 I	3
	C 110.0 (28.8) D 138.4 (0.7) I	b
	C 107.7 (13.7) D_1 119.4 (20.4) D_2 138.7 (0.6) I	c
second heating	G 75.0 D 140.0 I	3
	G 80.0 D 137.0 (0.5) I	4
	G 75.0 D 138.6 (0.6) I	b
	G 70.0 D 138.5 (0.6) I	c
	C 138.6 (18.6) I	d
	C 141.0 (18.8) I	e

[a] C = crystal, D = discotic mesophase, I = isotropic liquid, G = glass. [b] This work, recrystallization from ethanol. [c] This work, recrystallization from chloroform/ethanol (1:1). [d] Annealed at 100 °C for 3 days. [e] Sample with spherulitic texture removed from cover glass slips.

In the process of crystallization the spherulites grow together, stopping with more or less straight boundaries. During spherulite growth at 105 °C no new nuclei were observed. When the temperature was further reduced after some growth, new nuclei started growing in the amorphous phase between the existing spherulites. The resulting mesophase included two different textures (Figure 5g). When spherulite crystals were heated, no mesophase was observed before melting to the isotropic phase as shown at Figure 6. The growth rate of spherulites at 105 °C was calculated from the measurement of the size of spherulite as a function of time during the isothermal crystallization process. Figure 7 is a typical plot of the radius R of spherulites against crystallization time. The growth rate was 18 μm/h. The induction period of nucleations was about 10 h. A sample with the spherulitic texture under the polarizing microscope was removed form the cover glass slips and analyzed by DSC (Figure 8). There was an endothermic peak at 142 °C with a ΔH_i of 18.8 kcal/mol, while the ΔH_i for an unannealed sample was only 0.6 kcal/mol. NMR analysis showed that the macrocyclic amide **1** was stable during annealing process; there was no change in the ^1H NMR spectrum after annealing. The ΔH_i value of the melt-crystallized sample is less than the sum of all ΔH_i values of solution-crystallized samples.

The scanning electron microscope (SEM) photographs showed a difference between the annealed sample with spherulitic texture and the unannealed sample with grainy texture (Figure 9). Well developed lamellae were clearly visible for the annealed sample. The unannealed sample looks more amorphous. A similar scanning electron microscopic photo was reported by Shibaev for a polymer with frozen smectic multilayer aggregates.[11] The spherulite sample of hexamide **1** still on the glass slide was examined with low-resolution X-ray powder measurements (Figure 10). The X-ray also revealed the multilayer crystal structure, with the layers parallel to the surface of the glass slides.

a

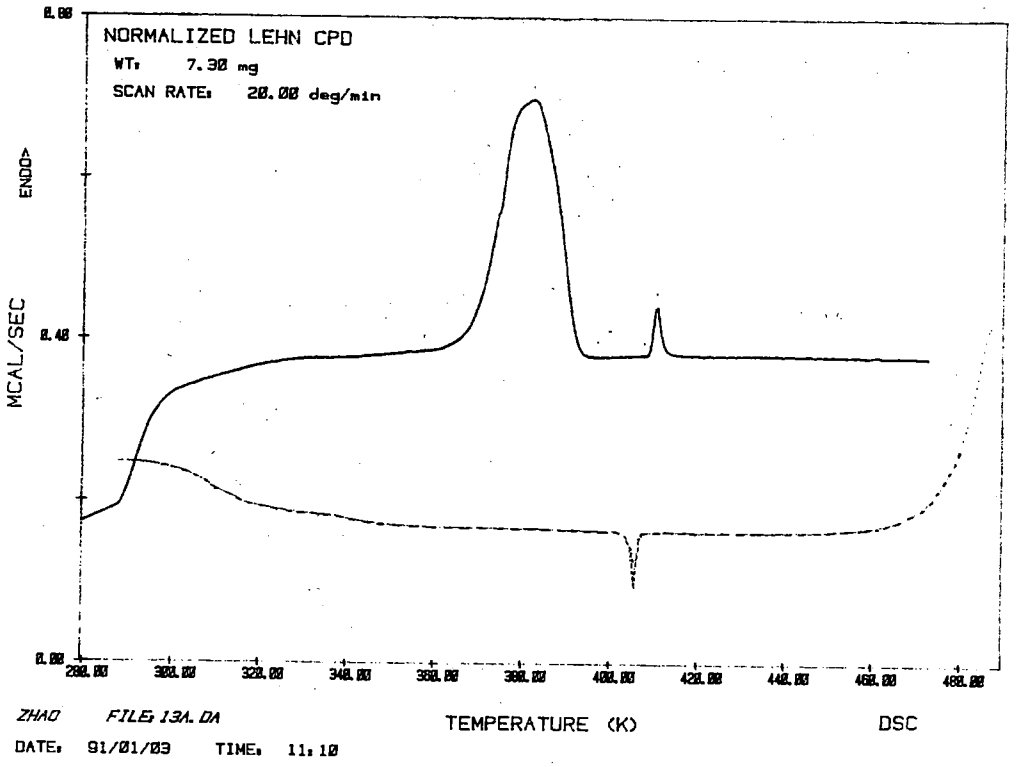

Figure 2. DSC thermograms of **1**: (a) first heating and cooling scan of the sample obtained by recrystallization from ethanol; (b) first heating and cooling scan of the sample obtained by recrystallization from chloroform/ethanol (v/v, 1/1); (c) second heating and cooling scan of the both samples obtained by recrystallization from ethanol or chloroform/ethanol; (d) first heating and cooling scan of the sample obtained by annealing at 100 °C for 3 days.

b

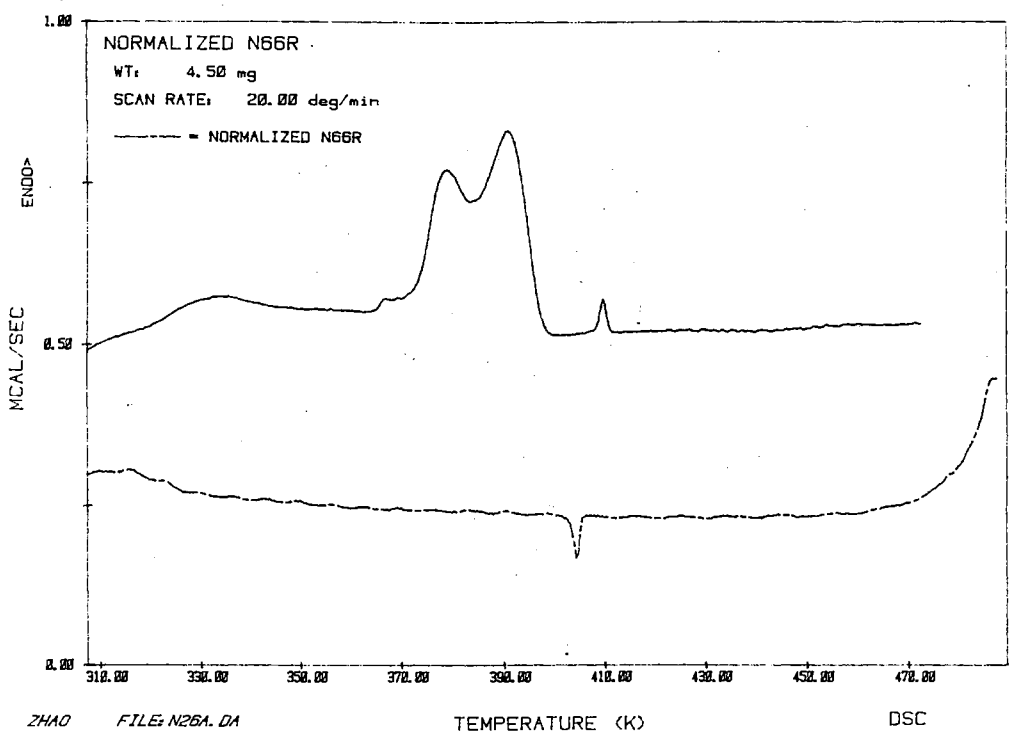
NORMALIZED N66R
WT: 4.50 mg
SCAN RATE: 20.00 deg/min
——— = NORMALIZED N66R
ENDO>
MCAL/SEC
1.00
0.50
0.00
310.00
330.00
350.00
370.00
390.00
410.00
430.00
450.00
470.00
ZHAO FILE: N26A.DA
TEMPERATURE (K)
DSC

c

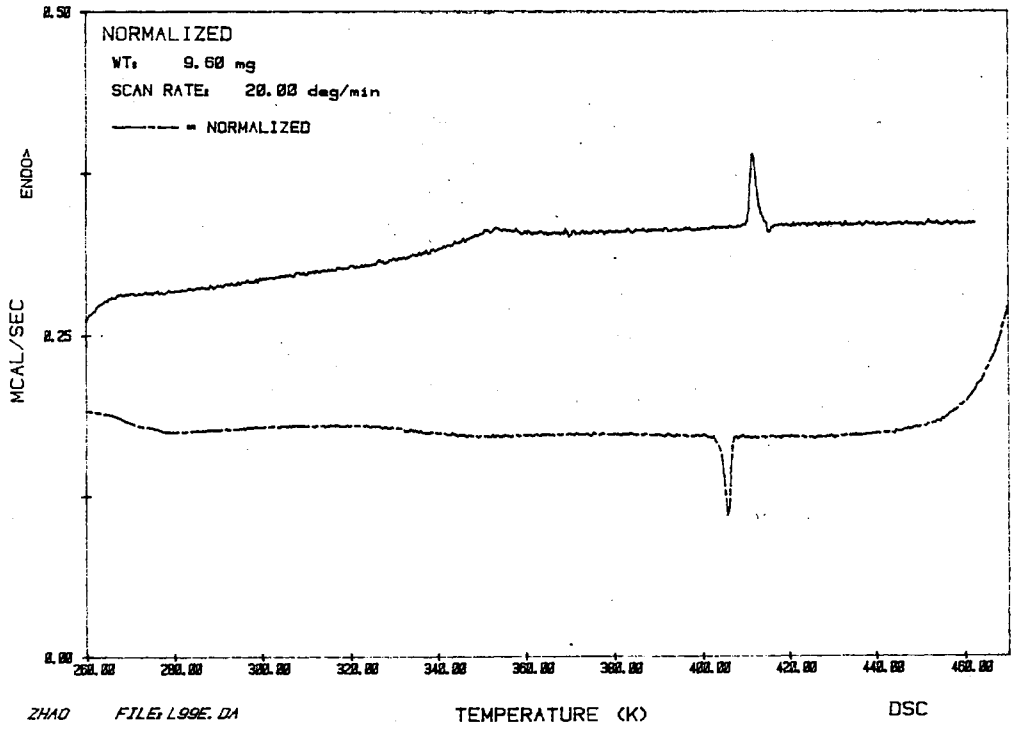
NORMALIZED
WT: 9.60 mg
SCAN RATE: 20.00 deg/min
——— = NORMALIZED
ENDO>
MCAL/SEC
0.50
0.25
0.00
260.00
280.00
300.00
320.00
340.00
360.00
380.00
400.00
420.00
440.00
460.00
ZHAO FILE: L99E.DA
TEMPERATURE (K)
DSC

d

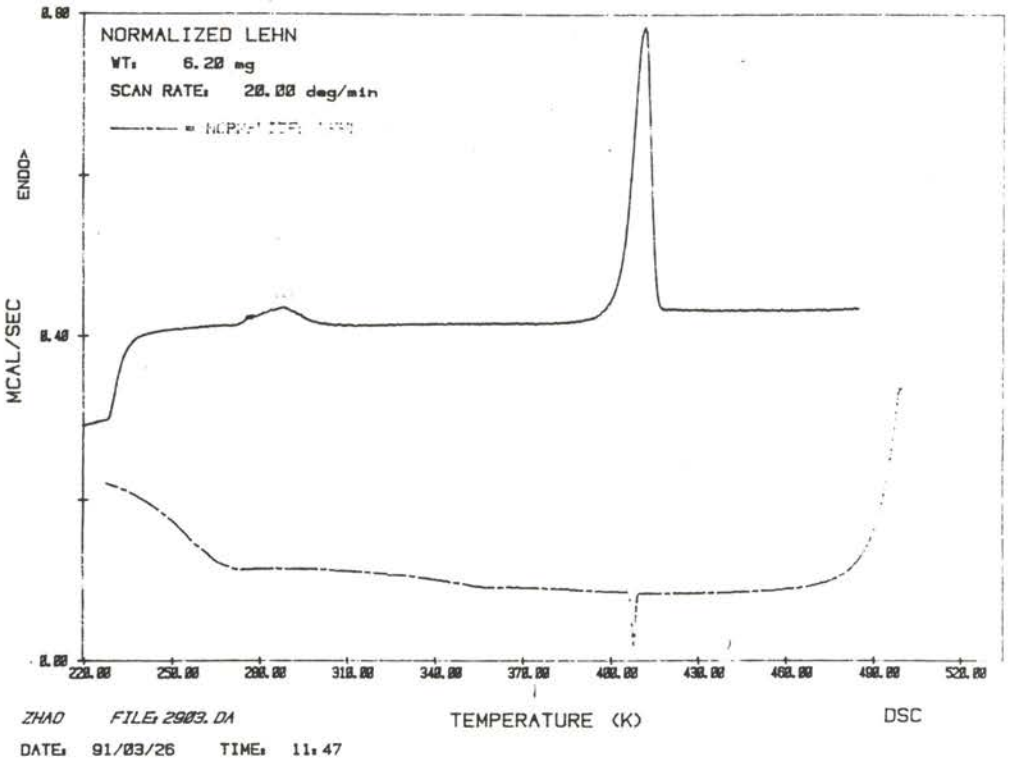

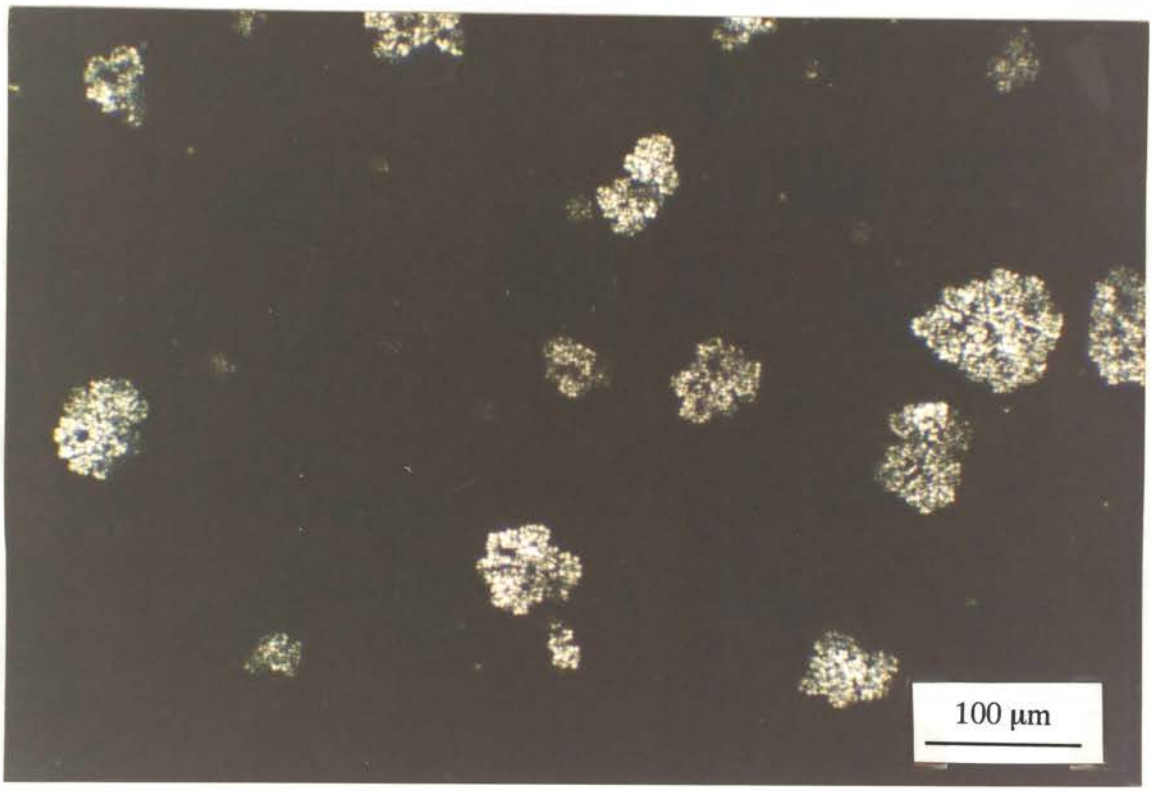

Figure 3. Polarizing micrograph of **1** at 30 °C, cooled from the isotropic liquid at 5 °C/min to 30 °C without annealing.

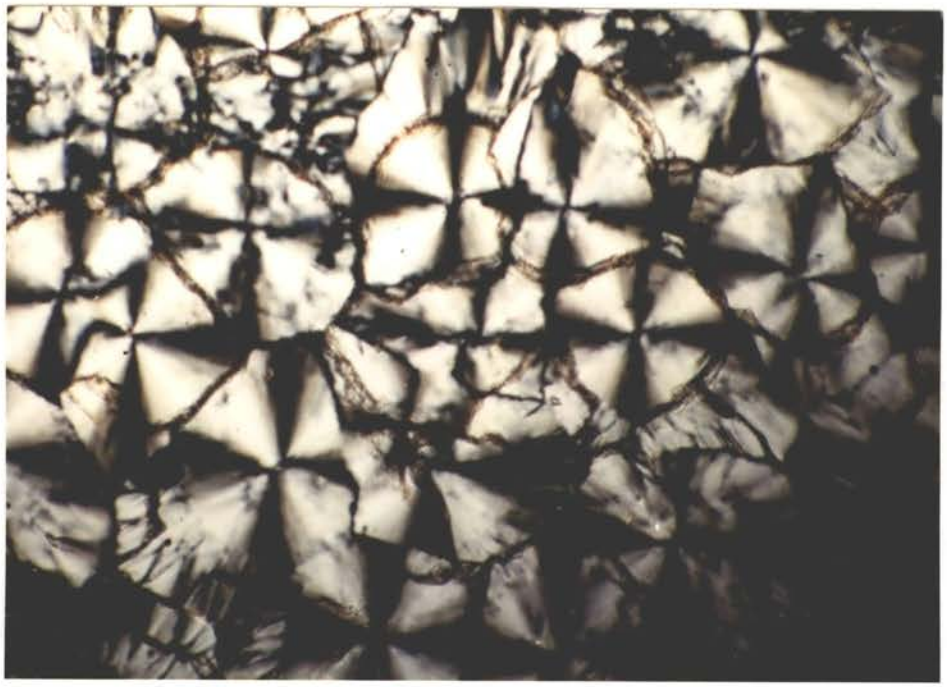

Figure 4. Polarizing micrograph of **1** at 30 °C, annealed at 100 °C for 3 days.

a

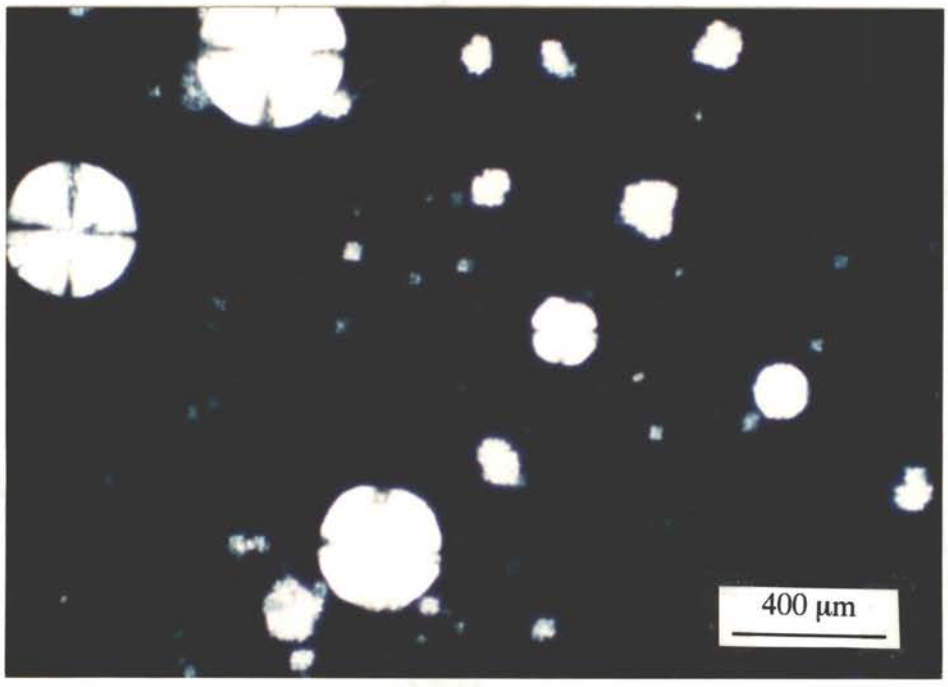

Figure 5. Polarizing micrographs showing the spherulite growth at different times at 105 °C: (a) 20 h; (b) 29 h; (c) 35 h; (d) 46 h; (e) 59 h; (f) 69 h; (g) sample obtained after 20 h annealing cooled to 25 °C at 5 °C/min.

b

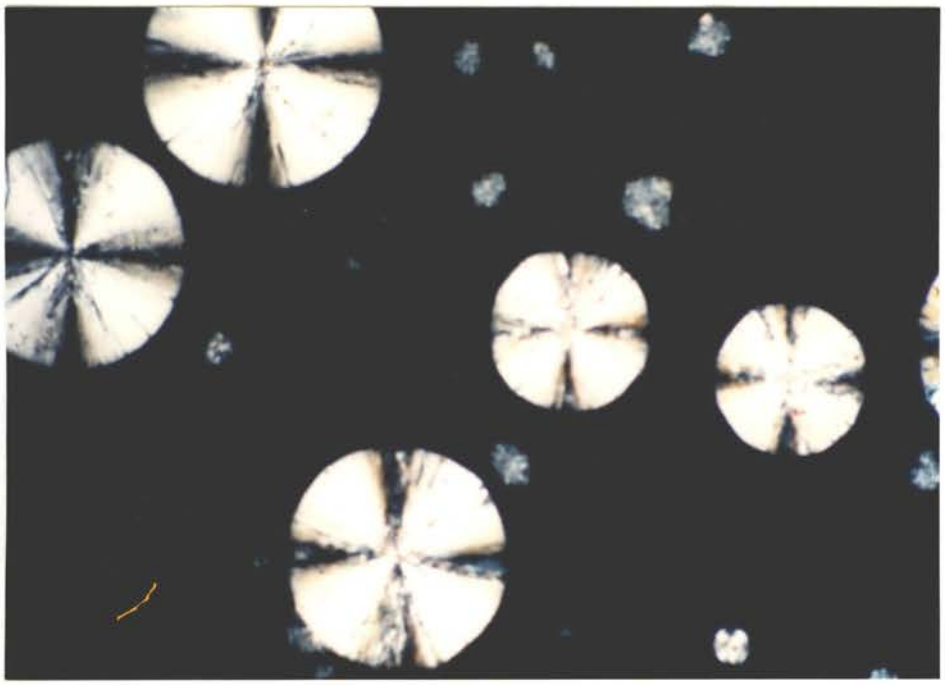

c

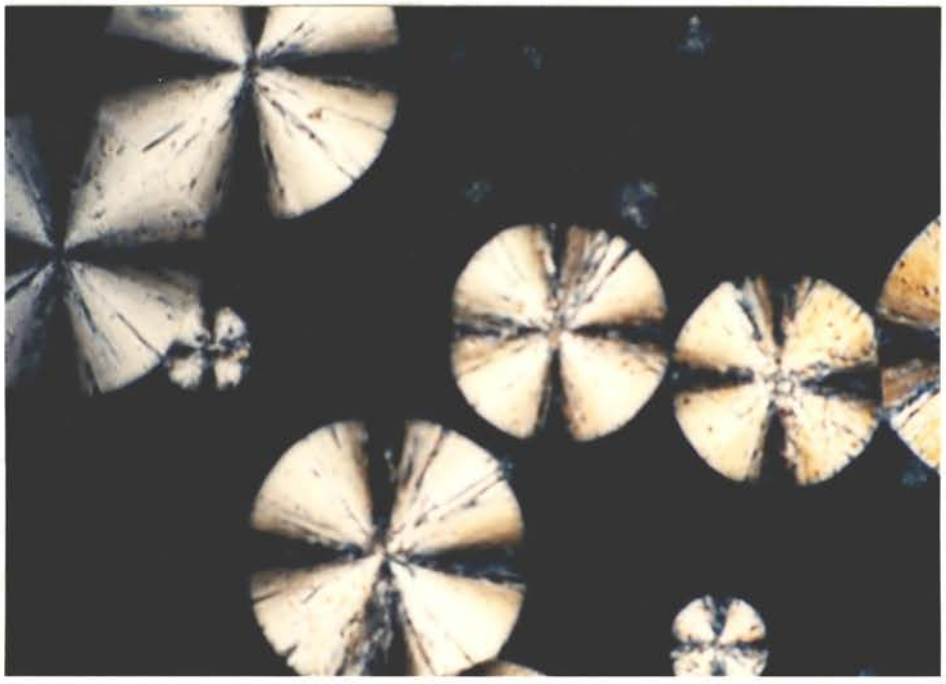

d

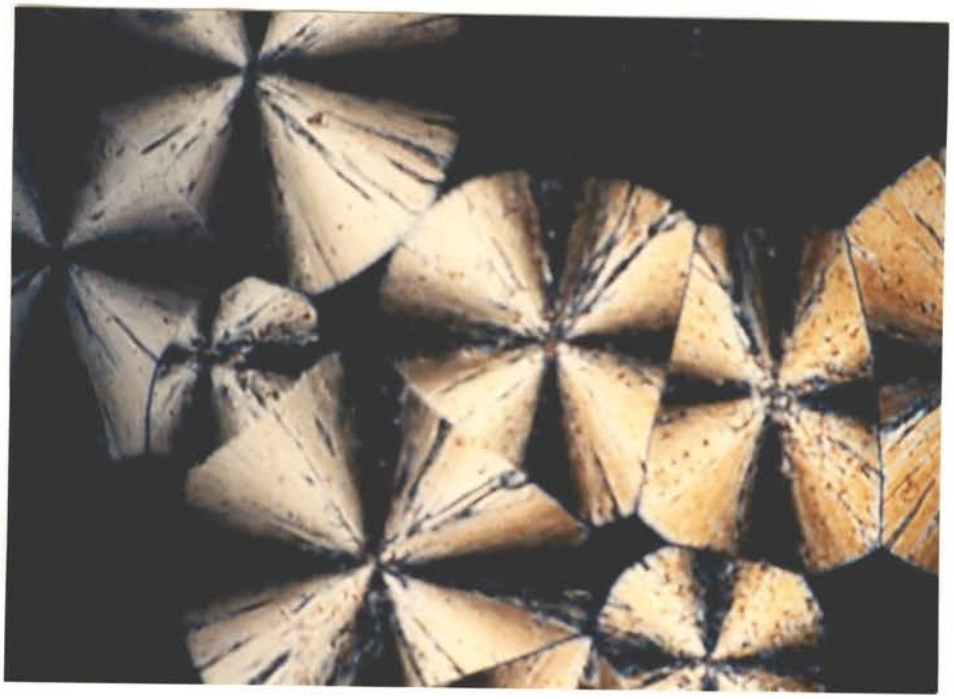

e

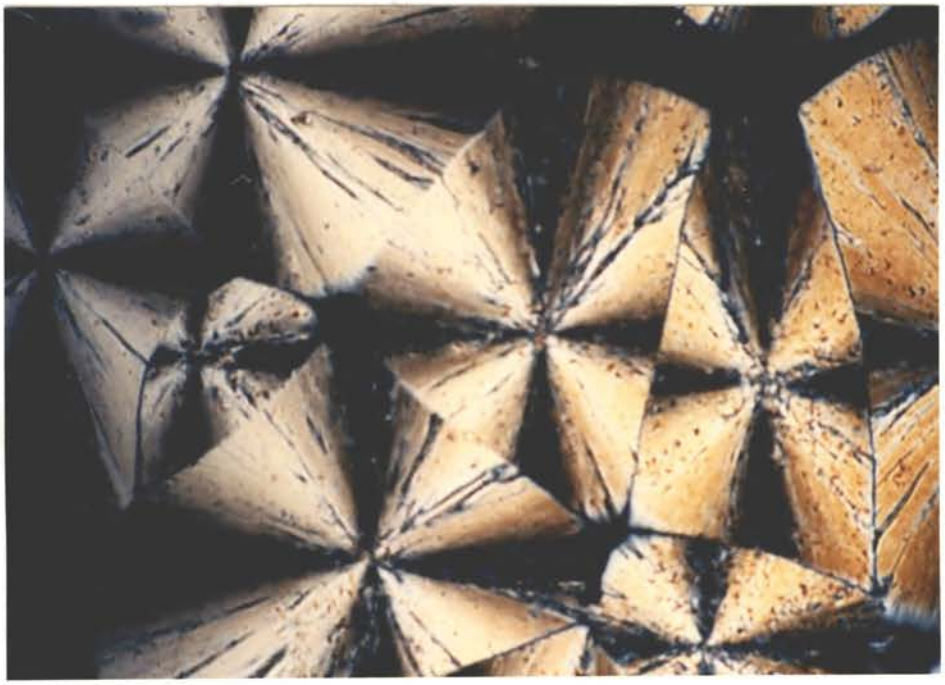

f

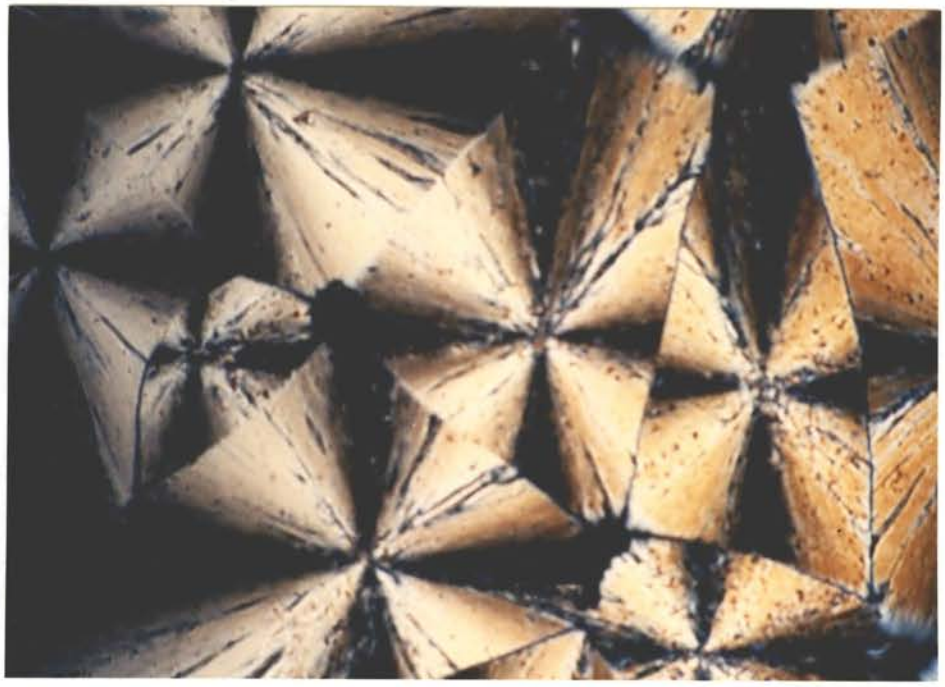

g

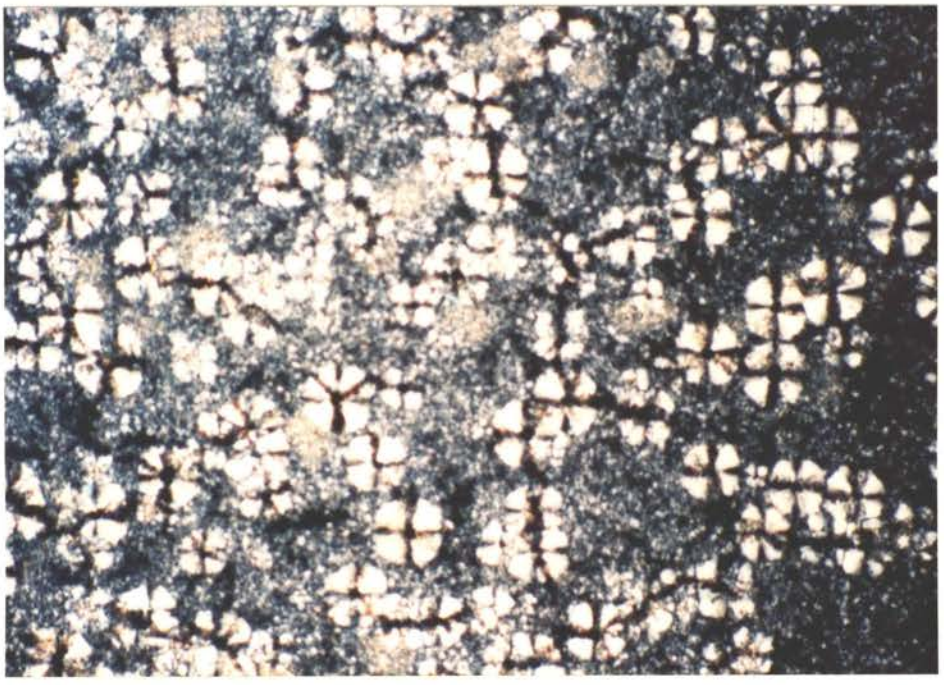

a

b

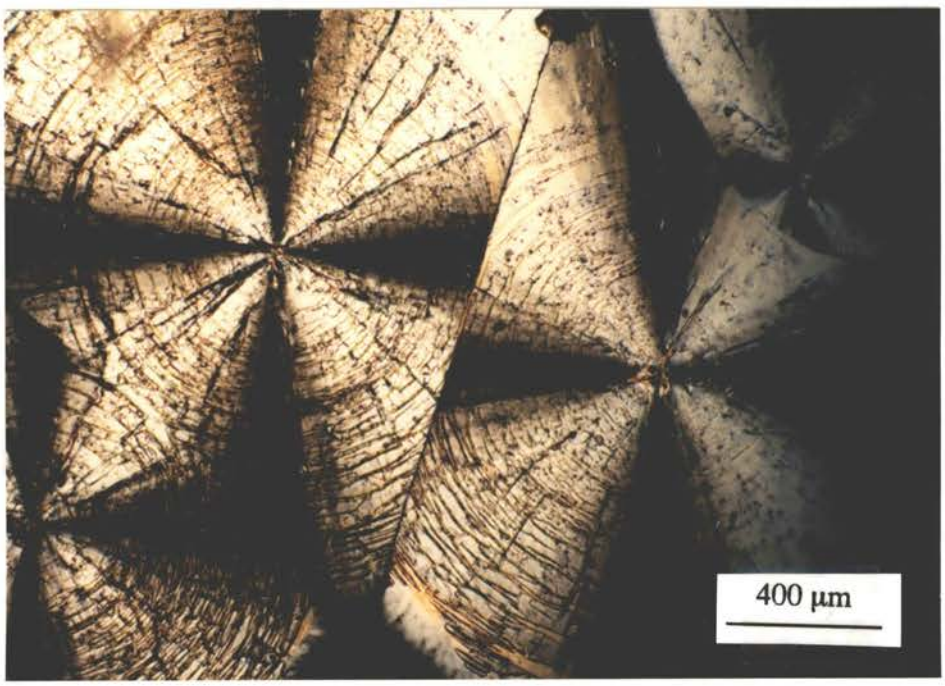

Figure 6. Polarizing micrographs showing the melting process of spherulitic crystals of **1**: (a) 90 °C; (b) 135 °C; (c) 138 °C; (d) 145 °C.

c

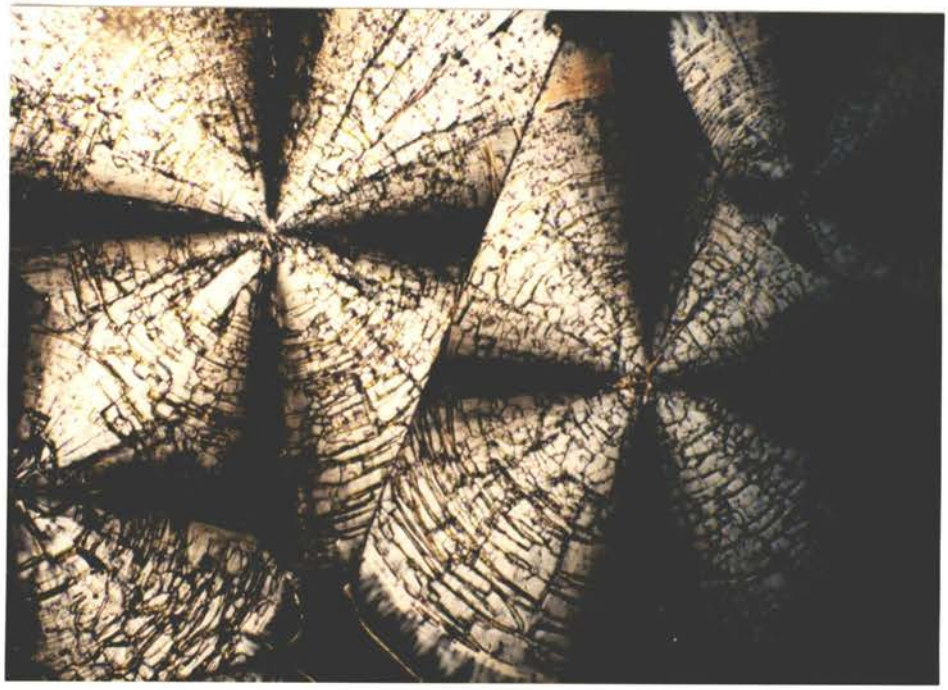

d

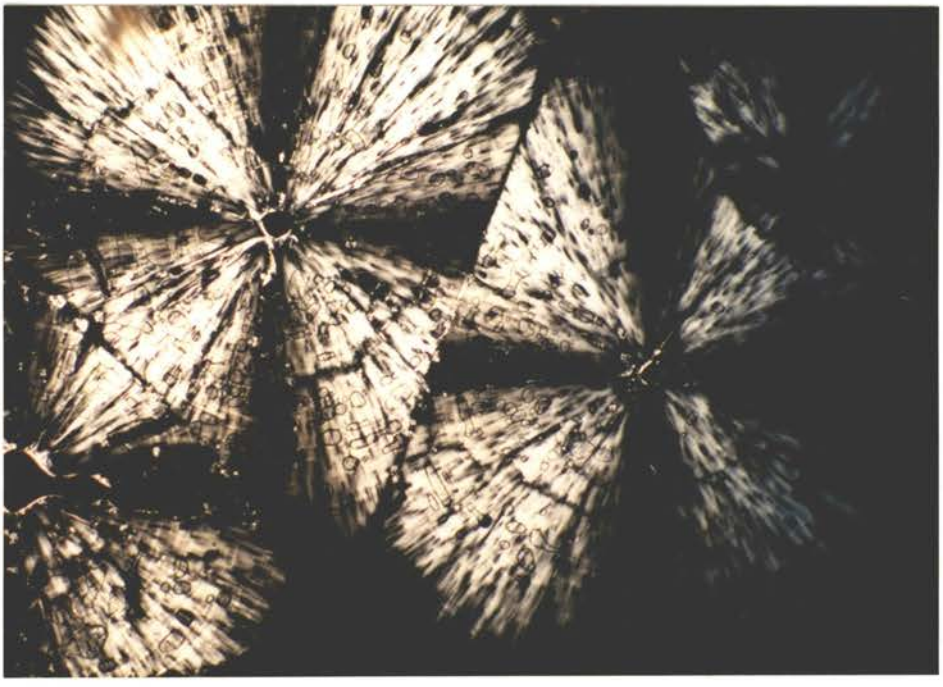

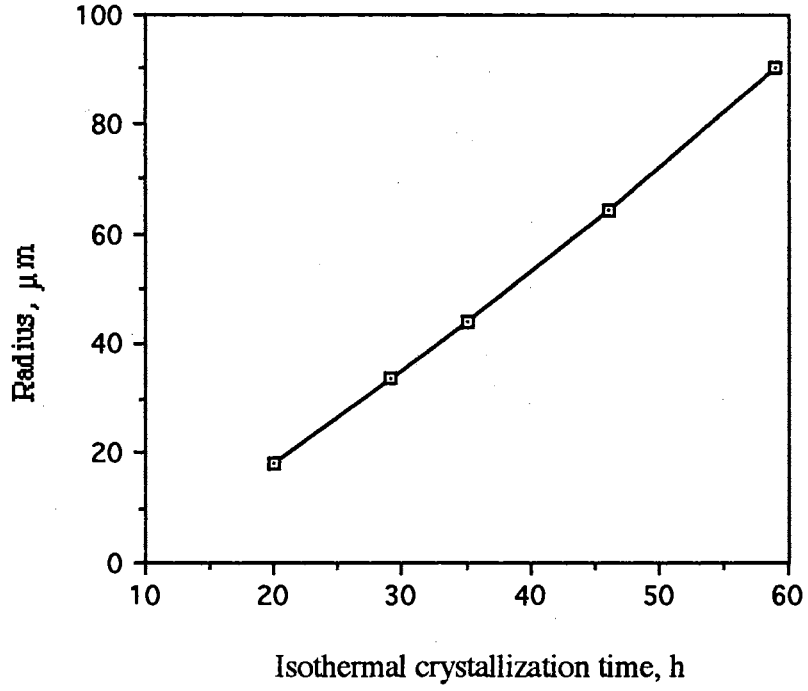

Figure 7. Radius of spherulites of **1** versus crystallization time at 105 °C.

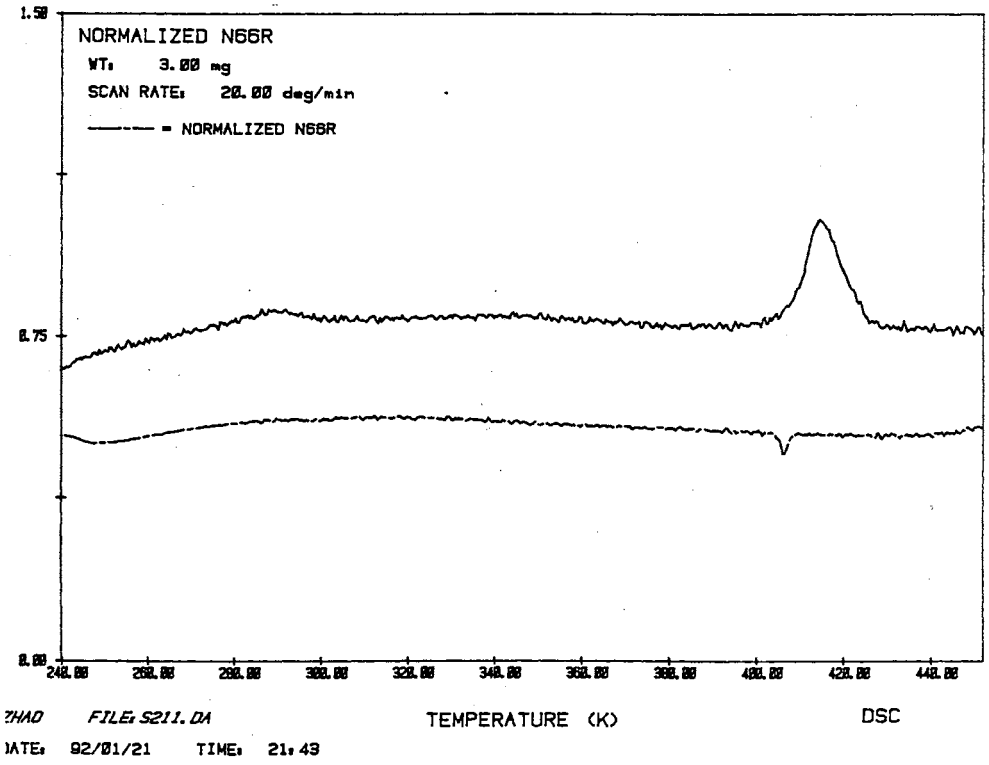

Figure 8. DSC thermograms of annealed **1** with spherulitic texture removed from cover glass slips.

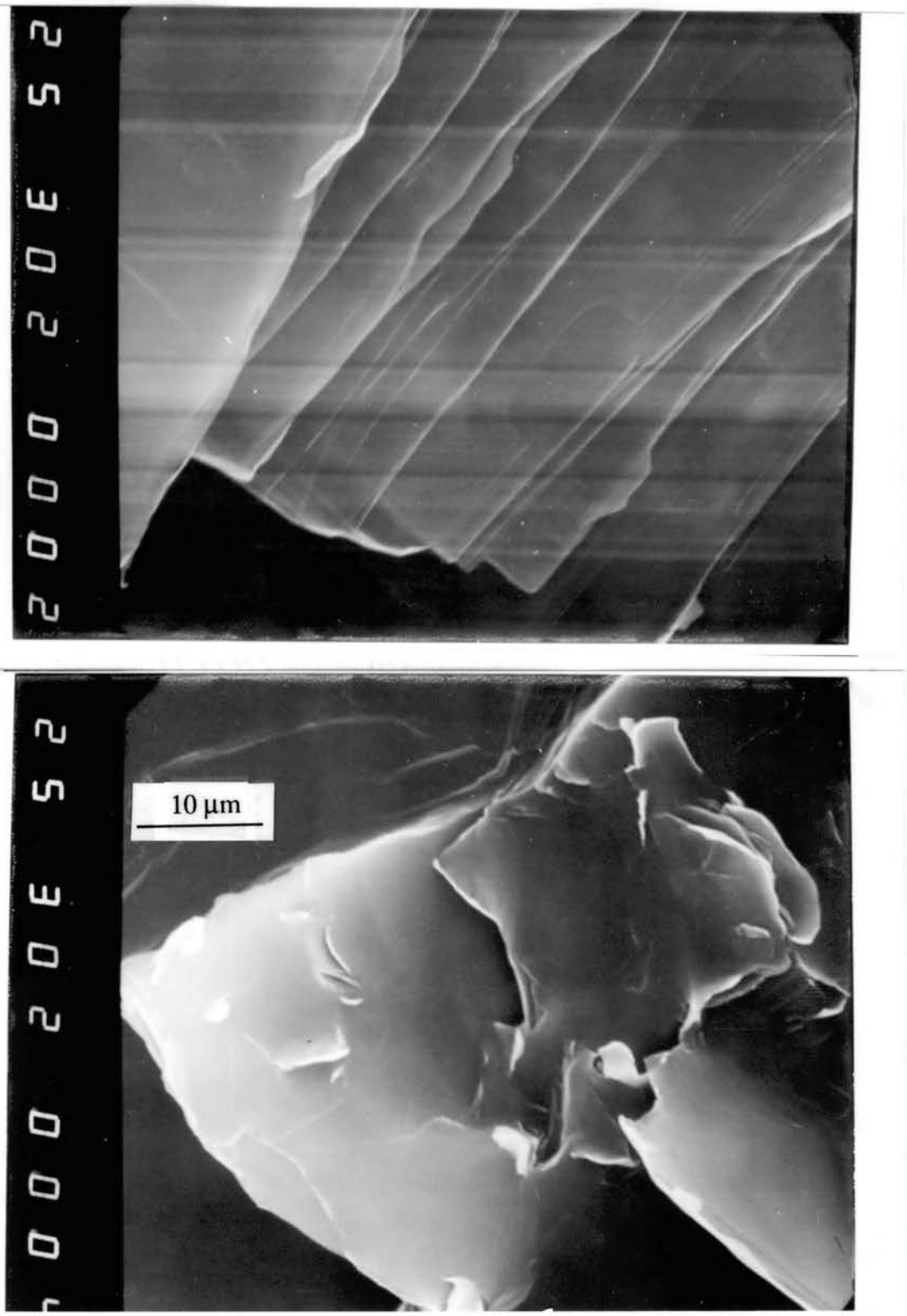

Figure 9. Scanning electron micrographs of **1**: (a) annealed sample with spherulitic texture; (b) unannealed sample.

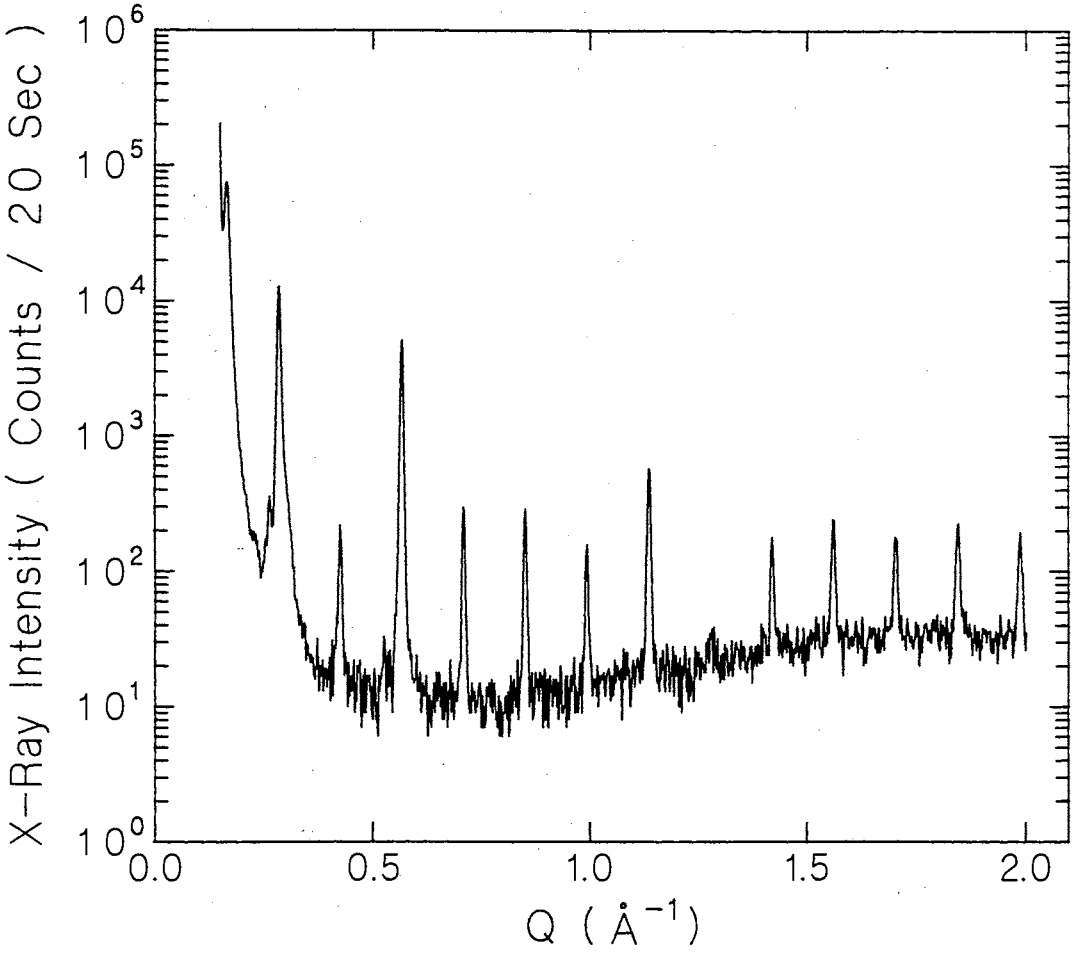

Figure 10. X-ray diffractogram at 27 °C of a sample of **1** annealed on a glass slide.

Hexamide 2. The liquid crystalline properties of hexamide **2** were very clear as shown in the reproducible DSC thermogram (Figure 11). There was no difference between the first scan and the second scan. The phase transition temperatures determined by DSC were (in brackets: ΔH in kcal/mol):

$$C_1\ 8\ (11.5)\ C_2\ 107\ (6.1)\ D\ 127\ (2.2)\ I$$

$$\rightleftharpoons$$

$$C_1\ -5\ (10.9)\ C_2\ 90\ (3.7)\ D\ 117\ (2.5)\ I$$

On cooling the isotropic melt of hexamide **3** the mesophase grows from digitated stars, which then develop to a focal conic texture with spherulitic domains (Figure 12). This texture is similar to those of the discotic liquid crystals with hexagonal columnar (D_{hd}) phases.[2,12] There was no obvious change of the texture from 80 °C to 5 °C, and there was a continuous change in the color of the texture during cooling. During the second heating a texture change was observed between 100 °C to 130 °C. Some streak like texture appeared in the focal conic domains (Figure 13). The change of color and the streak texture have been reported by Lattermann for the D_{hd} mesophase of 3,5-dihydroxycyclohexyl-3,4,5-tris(decyloxy)benzoate.[12]

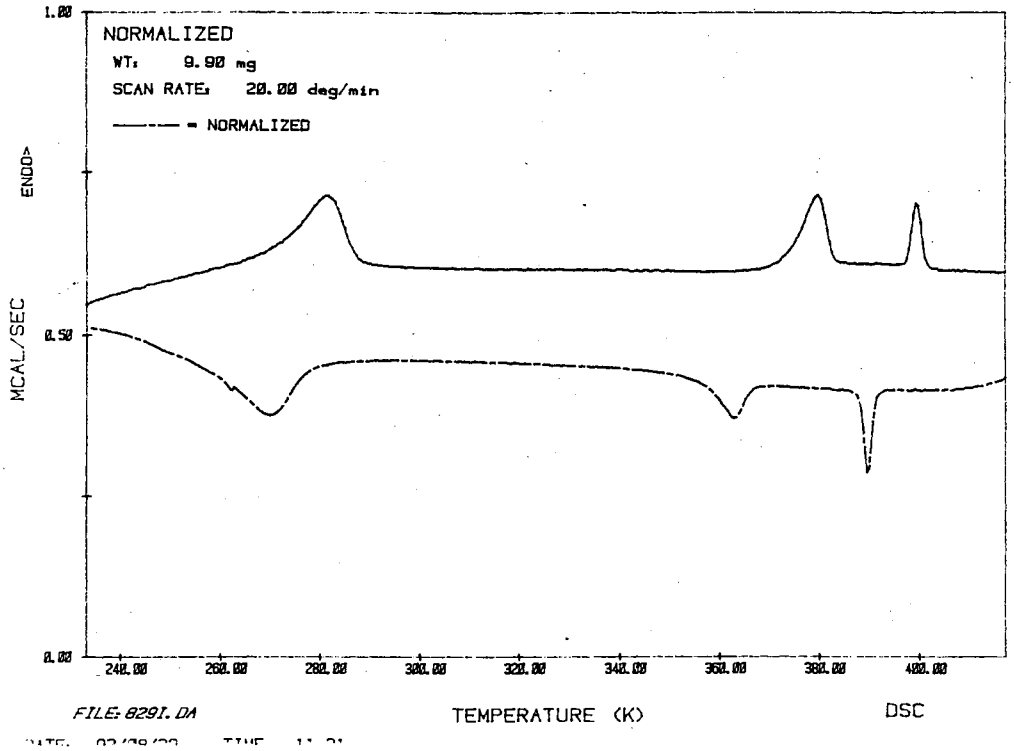

Figure 11. DSC thermograms of **2**, the second heating and cooling.

a

b

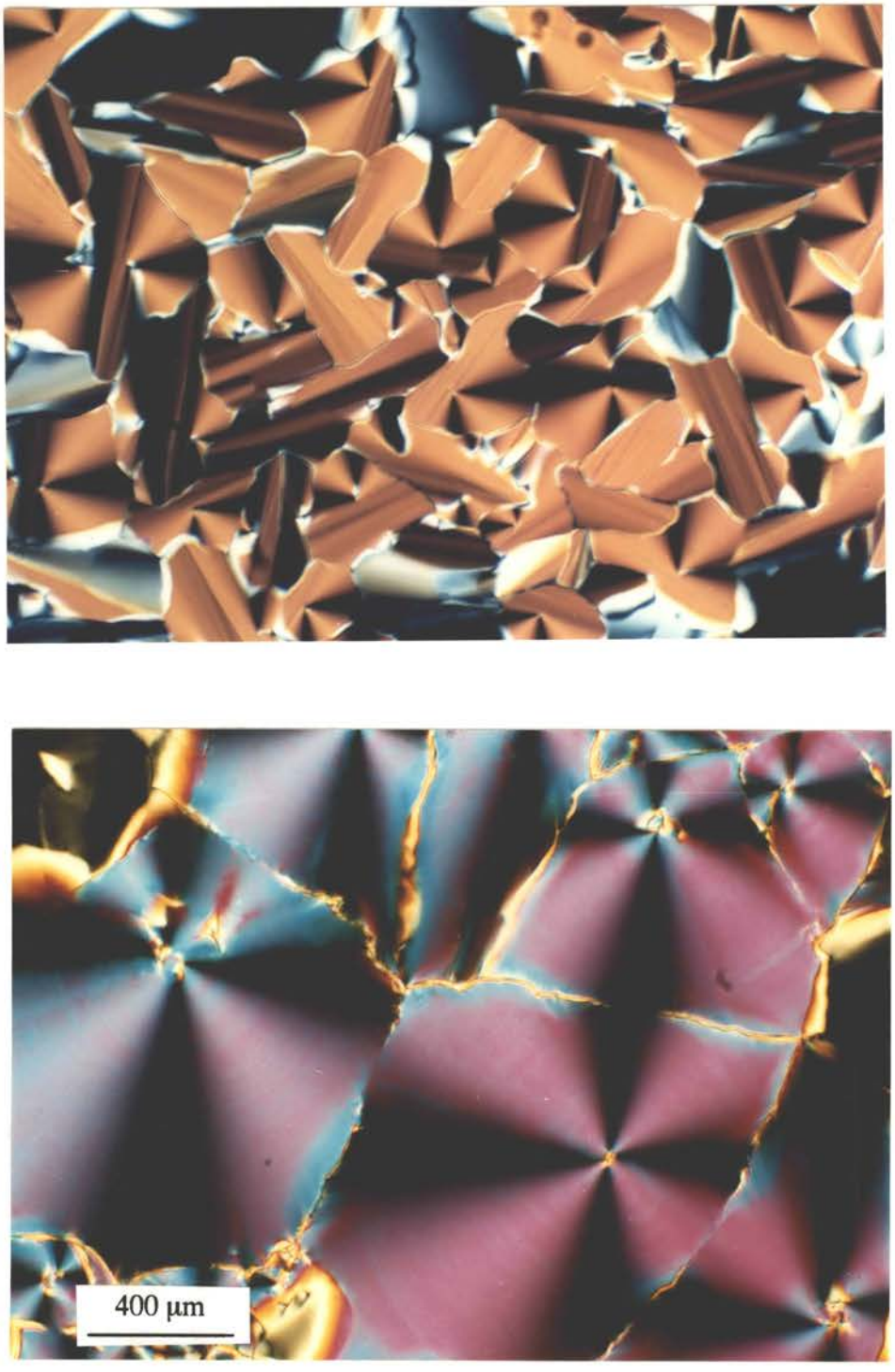

Figure 12. Polarizing micrographs of the textures of **2** cooled from the isotropic liquid: (a) cooled to 120 °C; (b) cooled to 5 °C.

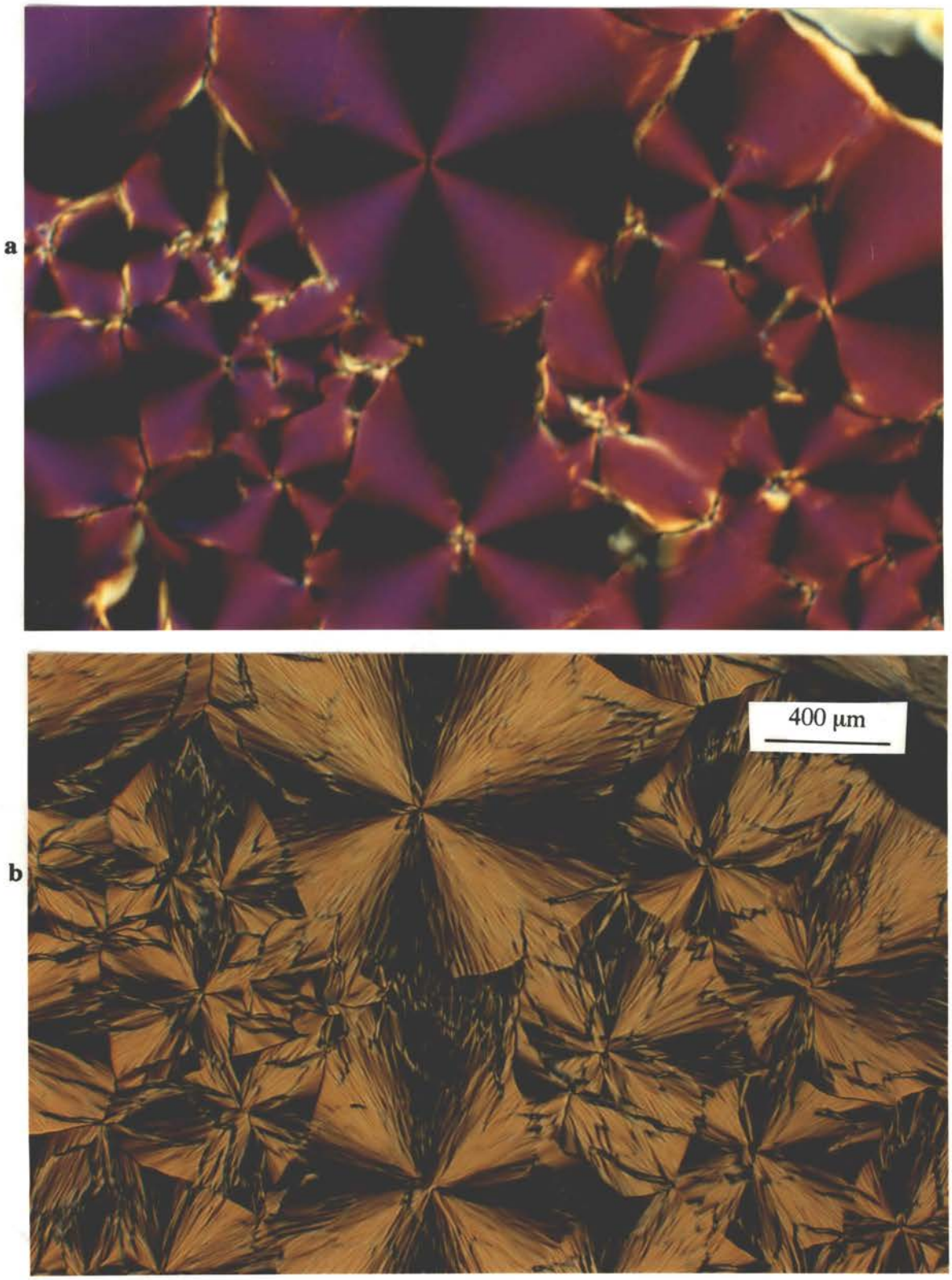

Figure 13. Polarizing micrographs of the textures of **2** during the second heating: (a) heated to 80 °C; (b) heated to 120 °C.

Compound 4. The DSC thermogram and the polarizing micrograph of compound **4** are given in Figures 14 and 15. The first and second DSC scans were different, and the phases transition was similar to that of hexamide **1**. There was only a small isotropic phase transition peak at 122 °C. A spherulitic texture was also observed for the annealed sample.

a

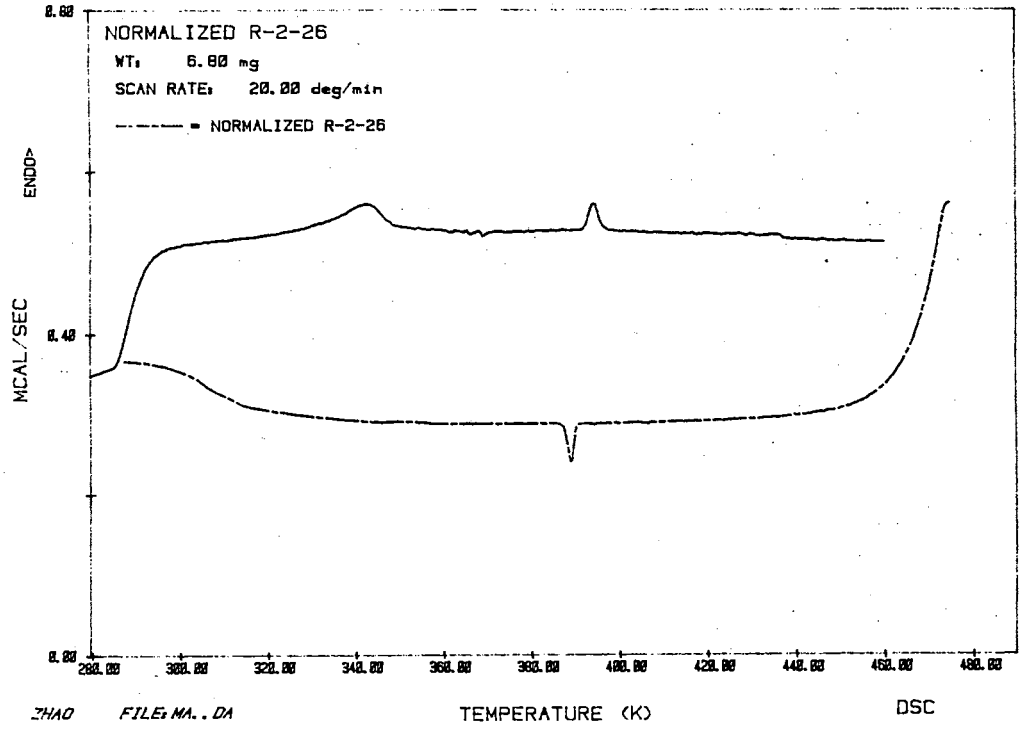

Figure 14. DSC thermograms of macrocycle **4** : (a) first heating and cooling; (b) second heating and cooling; (c) heating and cooling of the sample annealed at 80 °C for 10 h.

b

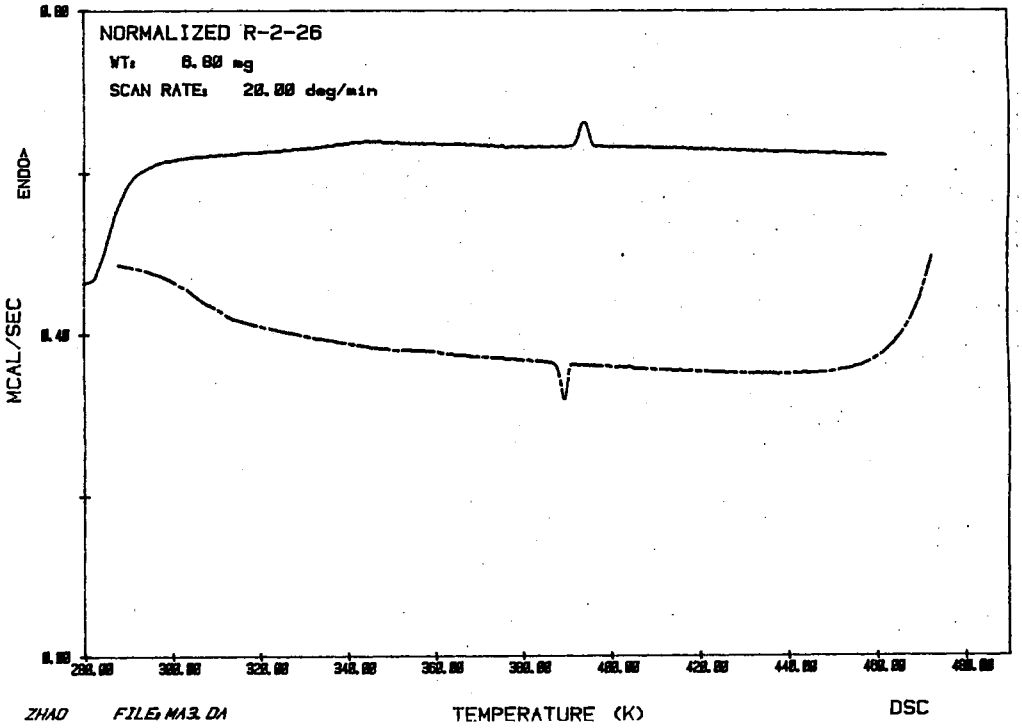
NORMALIZED R-2-26
WT: 6.80 mg
SCAN RATE: 20.00 deg/min
ENDO>
MCAL/SEC
TEMPERATURE (K)
DSC
ZHAO FILE: MA3.DA

c

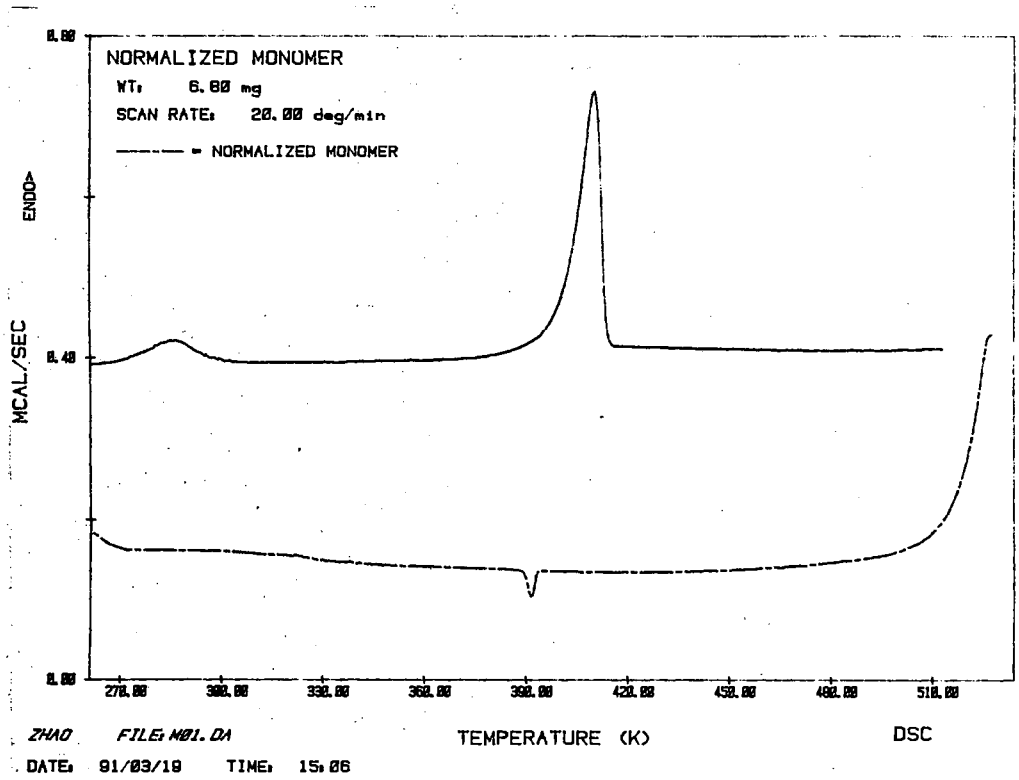
NORMALIZED MONOMER
WT: 6.80 mg
SCAN RATE: 20.00 deg/min
= NORMALIZED MONOMER
ENDO>
MCAL/SEC
TEMPERATURE (K)
DSC
ZHAO FILE: M01.DA
DATE: 91/03/19 TIME: 15:06

a

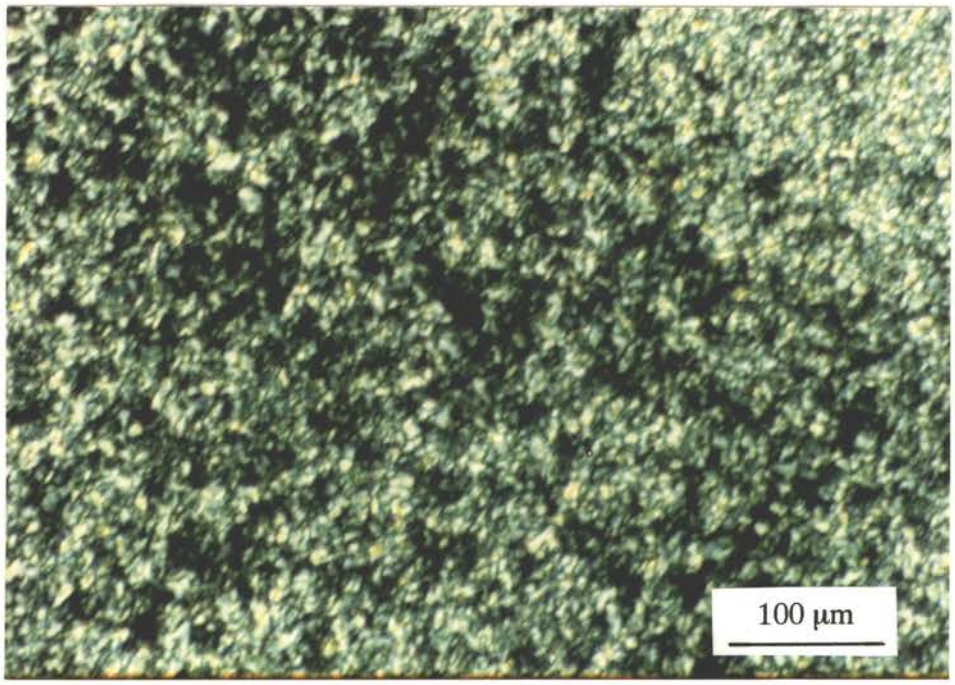

b

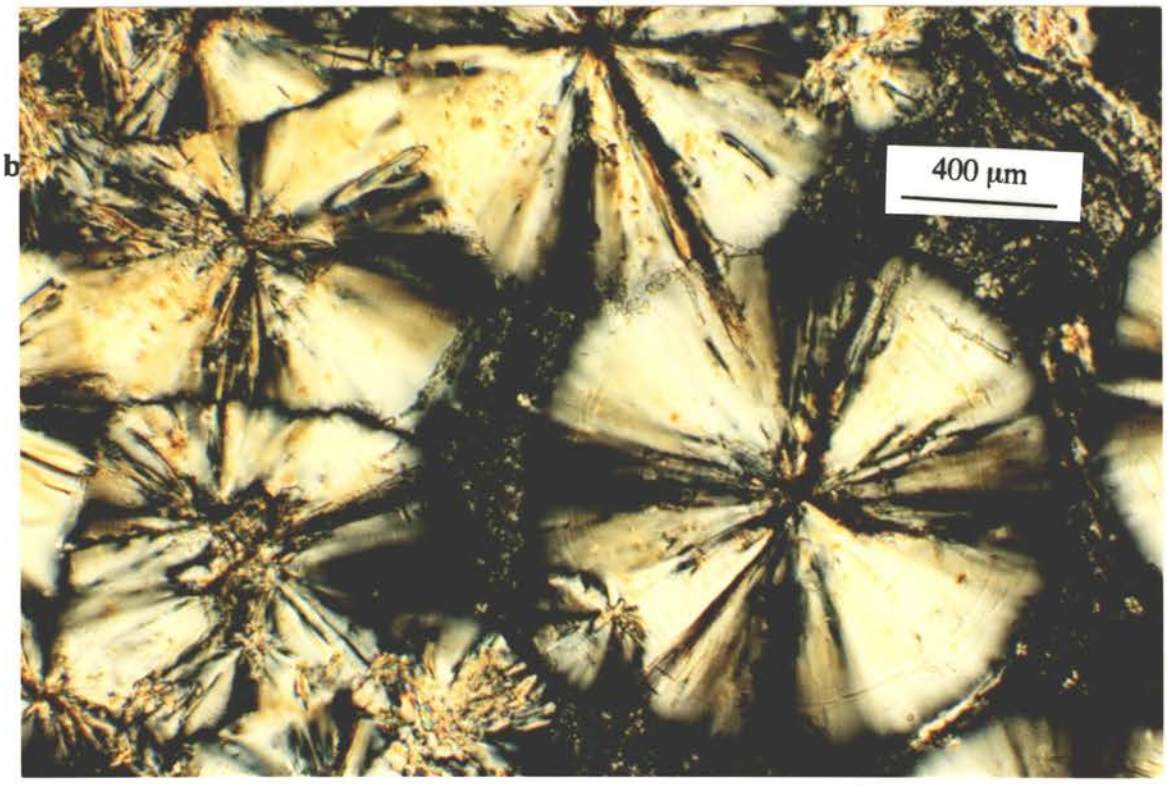

Figure 15. Polarizing micrographs of the textures of **4** obtained by cooling from the isotropic liquid: (a) cooled to 90 °C; (b) annealed at 100 °C for 48 h.

Polymers 5a and 5b. The polymers **5a** and **5b** are birefringent waxy solids at room temperature. Figure 16 shows the DSC thermograms of the polymers. The DSC curves of the first heating of the polymers consisted of a glass transition at about 70-80 °C and an isotropic transition at 90-110 °C. Without annealing the polymer exhibited only a featureless grainy birefringent texture. The annealed and sheared sample displayed a schlieren texture (Figure 17) that was stable at room temperature for at least 6 months. Preliminary X-ray diffractograms of the polymer **5a** are given in Figure 18. The first peak in the x-ray diffractogram at 22 °C indicates a plane spacing of 41.8 Å. There seems to be a barely resolved second peak, which might or might not indicate a hexagonal structure. At 99 °C there is a liquid crystalline phase with a plane spacing of 39.9 Å. The broad peak in the diffractogram at 122 °C indicates an isotropic phase. More X-ray work will be done in the future for a detailed structure identification of the polymers.

a

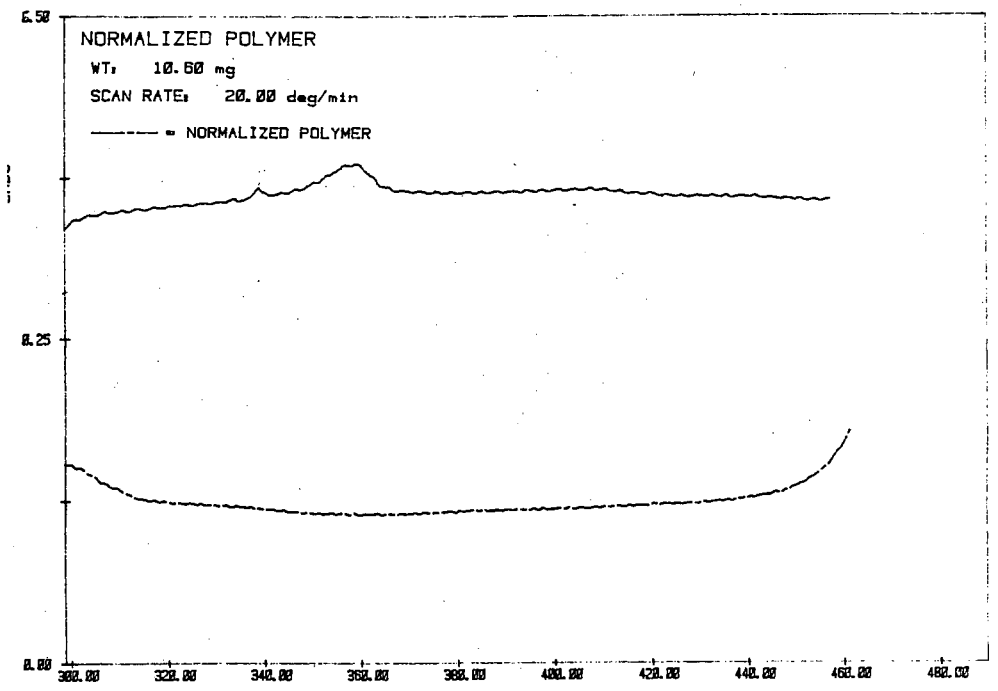

b

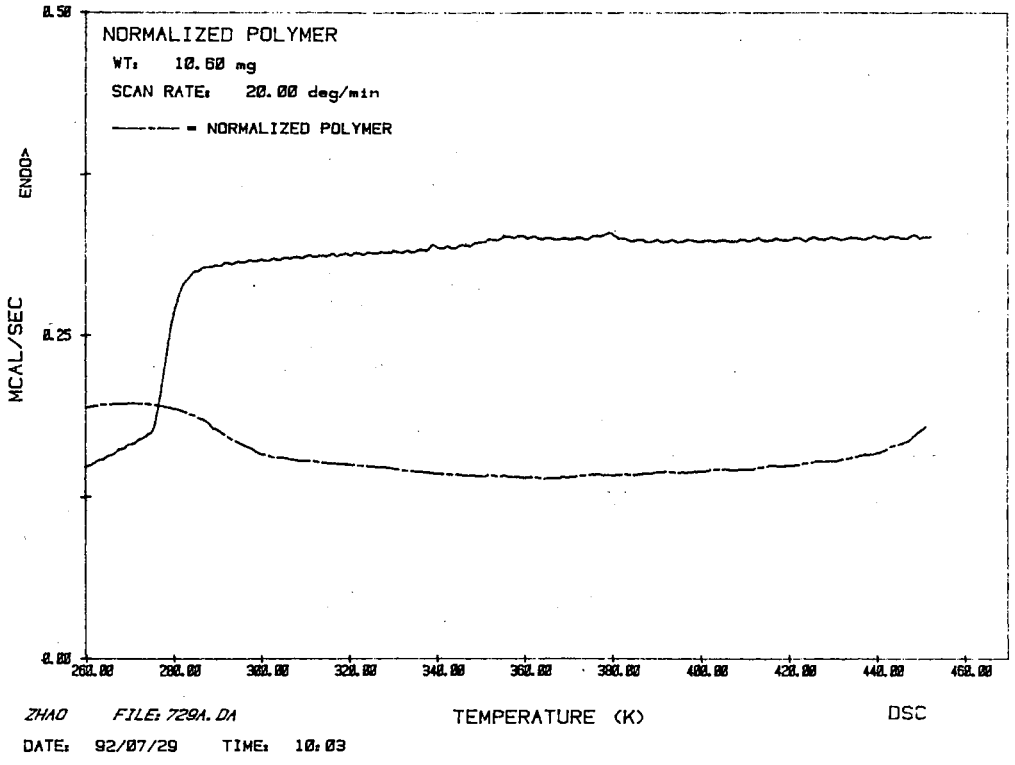

Figure 16. DSC thermograms of polymers: (a) first scan of polymer **5a**; (b) second scan of polymer **5a**, annealed at 80 °C for 48 h; (c) first scan of polymer **5b**; (d) second scan of polymer **5b**.

c

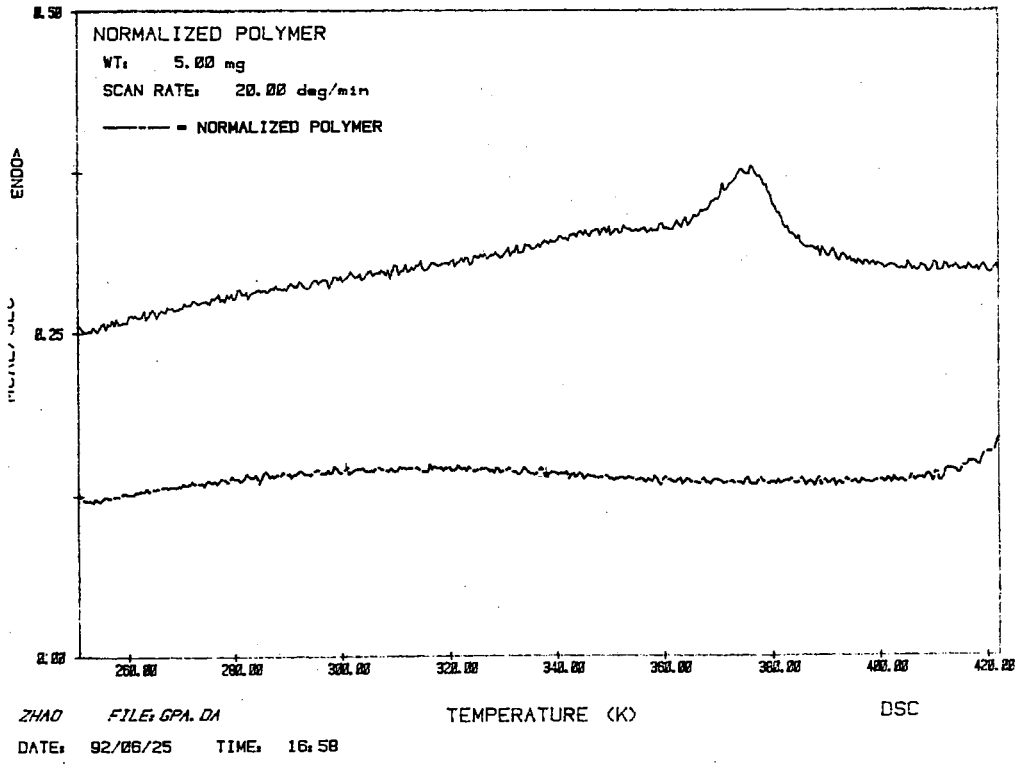
NORMALIZED POLYMER
WT: 5.00 mg
SCAN RATE: 20.00 deg/min
——— = NORMALIZED POLYMER
ENDO>
0.25
0.00
260.00
280.00
300.00
320.00
340.00
360.00
380.00
400.00
420.00
ZHAO FILE: GPA.DA
TEMPERATURE (K)
DSC
DATE: 92/06/25 TIME: 16:58

d

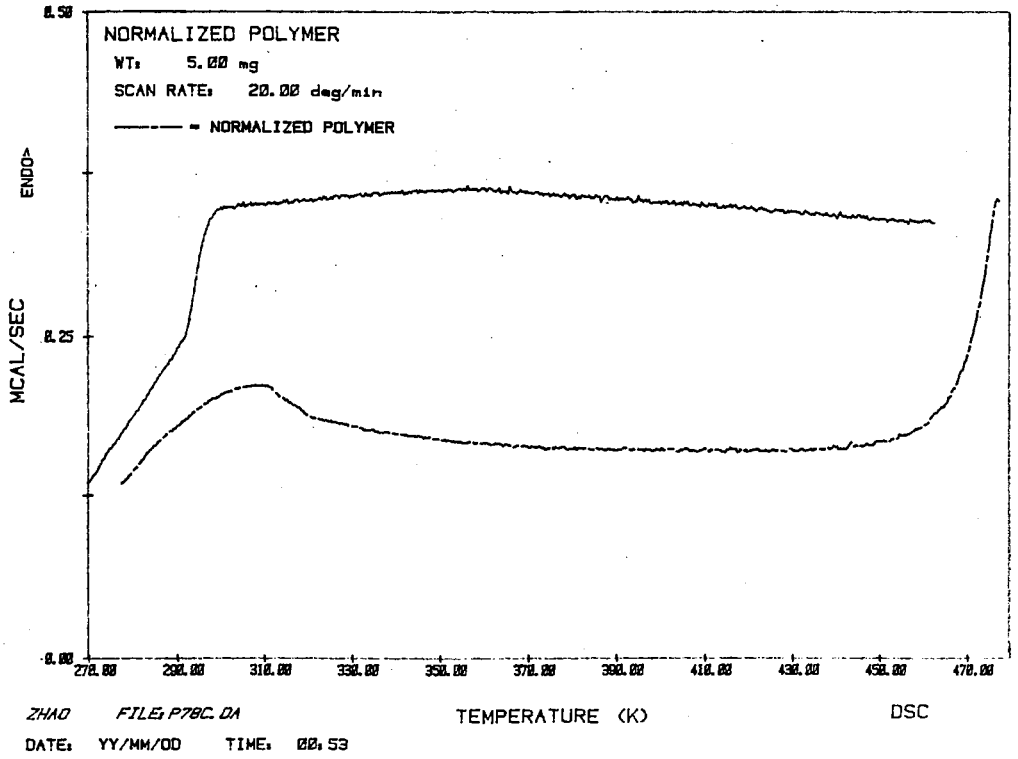
NORMALIZED POLYMER
WT: 5.00 mg
SCAN RATE: 20.00 deg/min
——— = NORMALIZED POLYMER
ENDO>
MCAL/SEC
0.25
0.00
270.00
290.00
310.00
330.00
350.00
370.00
390.00
410.00
430.00
450.00
470.00
ZHAO FILE: P78C.DA
TEMPERATURE (K)
DSC
DATE: YY/MM/DD TIME: 00:53

a

b

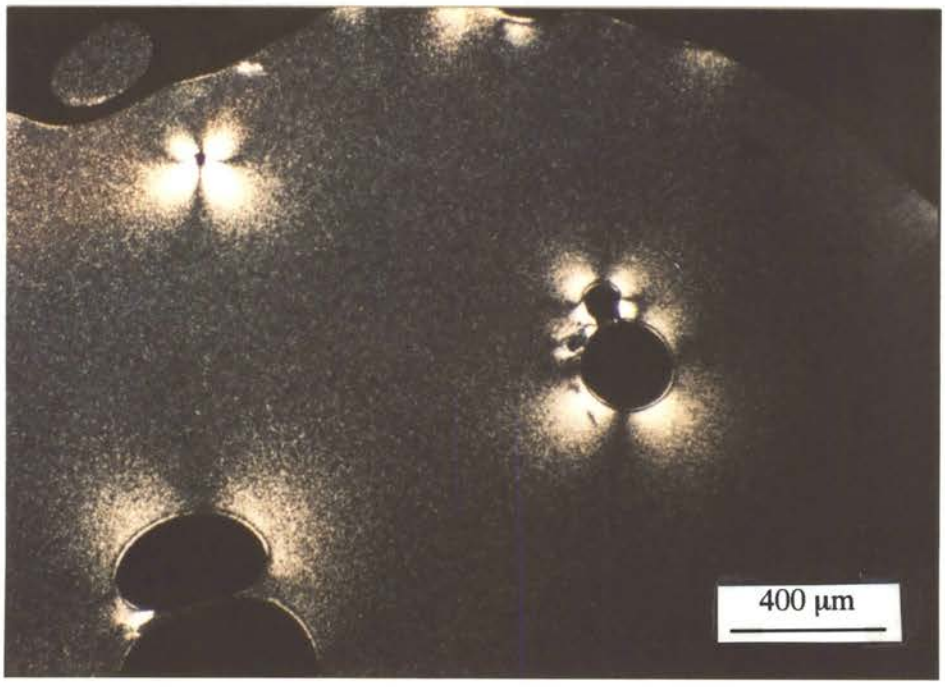

Figure 17. Polarizing micrographs of the textures of polymer **5b**: (a) virgin sample at 23 °C before heating; (b) cooled from isotropic melt at 0.1 °C/min, and annealed at 100 °C for 2 days; (c) annealed at 100 °C for 5 days.

c

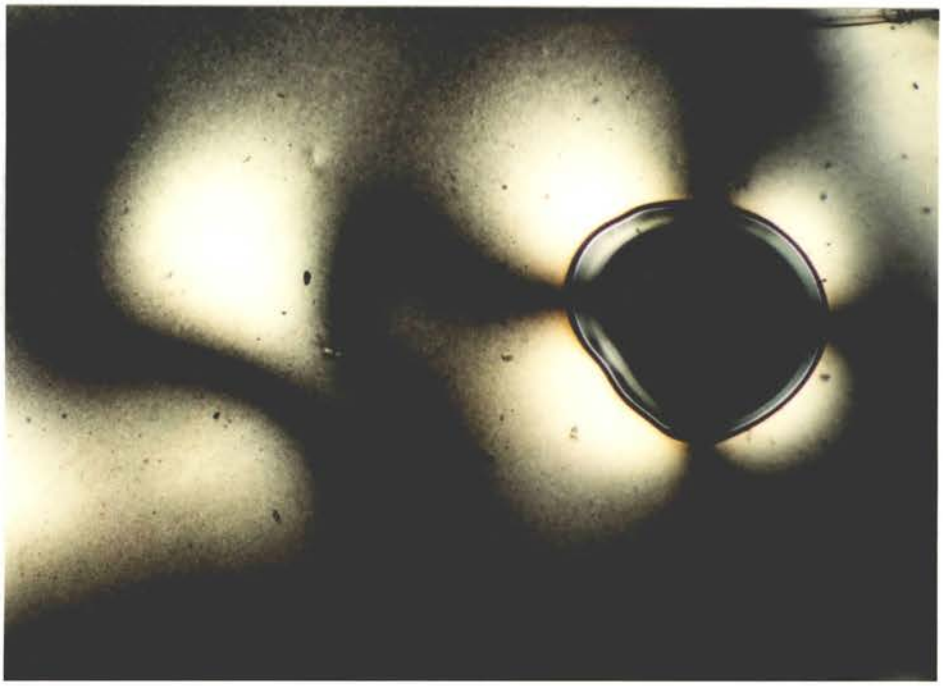

a

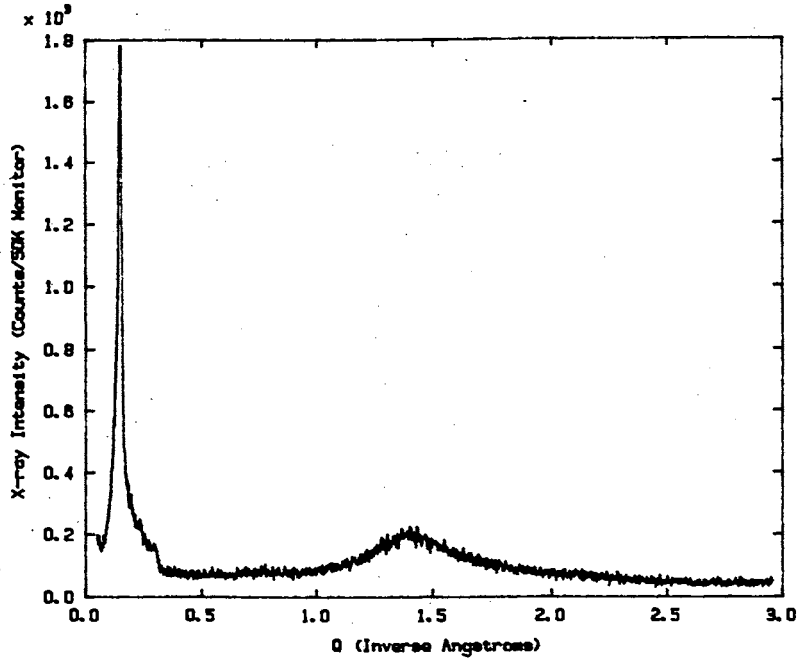

b

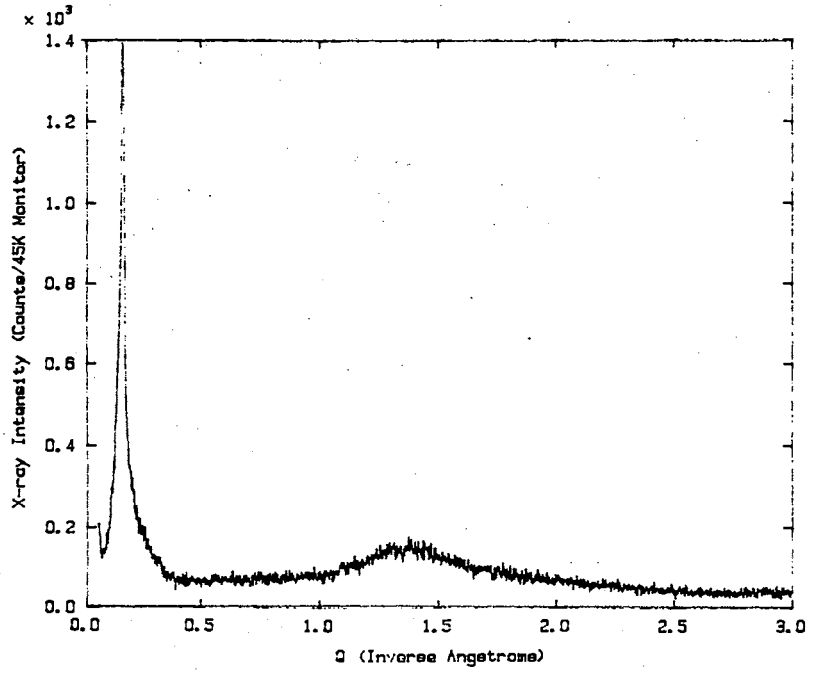

Figure 18. X-ray diffractograms of polymer **5a.** (a) obtained at 23 °C; (b) obtained at 99 °C; (c) obtained at 122 °C.

c

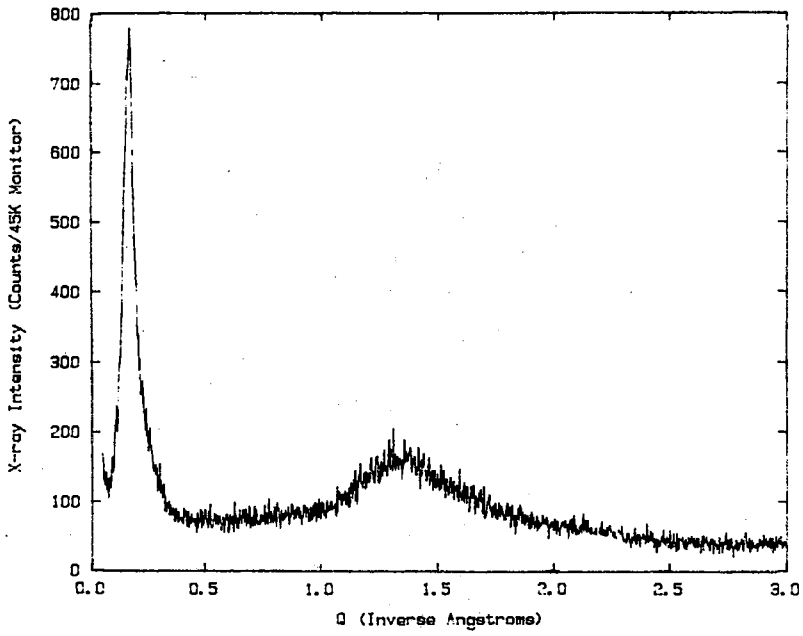

4-Dodecyloxybenzoic acid and 4-(10-undecylenyloxy)benzoic acid. These substituted benzoic acids have been synthesized as intermediates in our experiments. Both benzoic acids have been reported to be liquid crystalline compounds with nematic and smectic (S_C) mesophases.[13,14] Their mesophases were observed with the optical polarizing microscope, and the typical textures are presented in Figures 19-20.

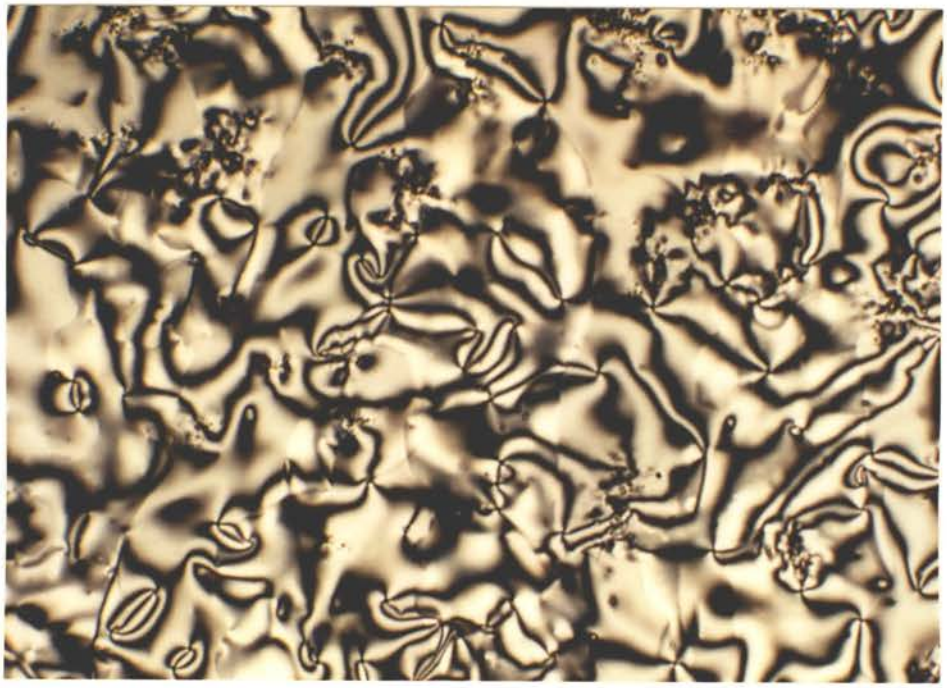

Figure 19. Polarizing micrograph of the texture of 4-dodecyloxybenzoic acid obtained on cooling from isotropic melt to 110 °C in nematic phase.

a

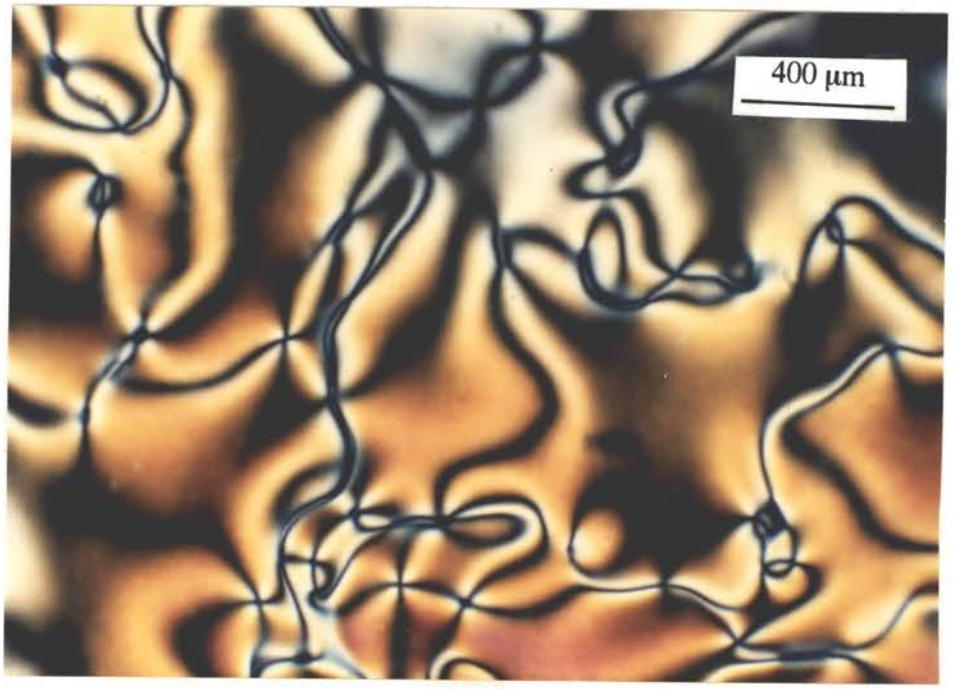

Figure 20. Polarizing micrographs of the textures of 4-(10-undecylenyloxy)benzoic acid: (a) obtained on heating to 125 °C in nematic phase; (b) obtained on cooling to 80 °C in the smectic C (S_C) phase.

b

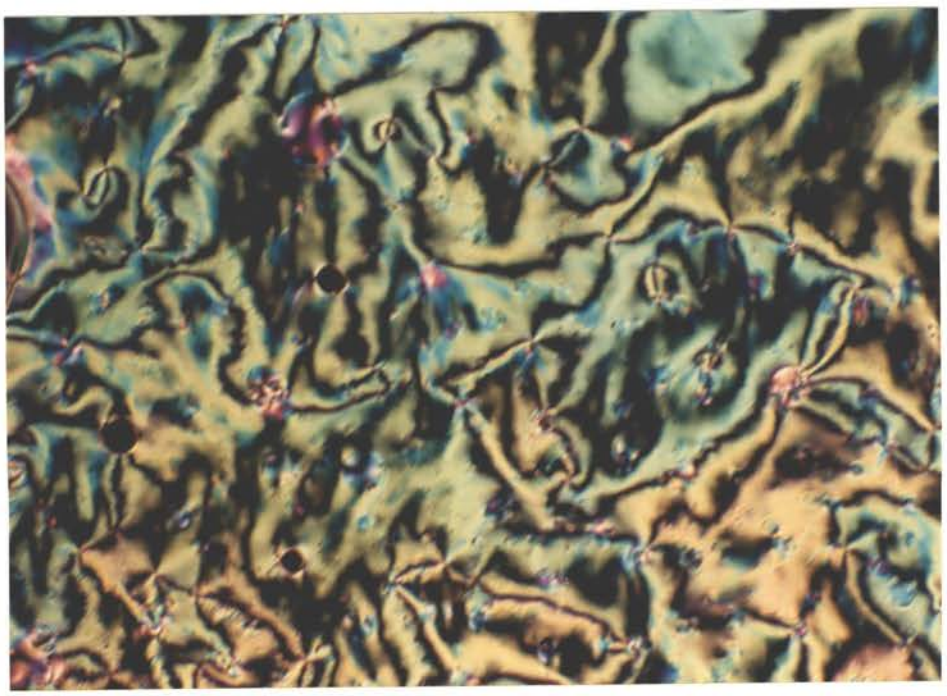

Discussion

The liquid crystalline behavior of the macrocyclic hexamide **1** has been investigated several times.[1-4] The mesomorphic behavior of this derivative of azacrown[18]-N_6 depends on the method of purification and the thermal history of the sample. While the compound **1** shows different, irreproducible first DSC scans, the second and the following scans all show a broad phase transition at about 75 °C and a small sharp peak at about 140 °C. The slow phase transition at 75 °C appears to be a glass transition. Without annealing, the sample obtained by cooling the isotropic melt quickly to room temperature was a glass containing only small amounts of liquid crystals. For a well annealed sample there was no 75 °C transition, and only a melting of the spherulitic crystals to the isotropic phase was observed by DSC and by microscopy. The transition enthalpy, ΔH_i, of 16-19 kcal/mol indicates that the spherulitic crystalline structure is a well-organized phase. The melting transition of spherulitic crystal was at about 140 °C, the same temperature as the mesophase

to isotropic transition during the second DSC heating of the unannealed **1**. The same transition temperature might indicate that the small sharp phase change in the second DSC heating is related to the spherulitic crystal. The crystallization of hexamide **1** from the mesophase was very slow, with a growth rate of spherulitic crystals of about 18 μm/h. In DSC analysis a sample cooled at 5 °C or 20 °C per minute formed only very small amounts of liquid crystal or crystal. This is why in the DSC second heating scan only a small sharp peak was detected at 139 °C. In the investigation of the liquid crystalline azacrown[18]-N_6 derivatives some difficulty is attributed to their slow and usually incomplete phase transitions, which lead to irreproducible DSC curves and cooling to mixtures of liquid crystal and isotropic glass. Figure 21 shows structural models of hexamide **1** in ordered and disordered states. These structures were created using the program Chem3D on a Macintosh IIci computer. The conformational energies of ordered states are minimized. Because of its bulky side chains and rigid ring the ordered hexagonal tube-like mesophase is not so easy to form.

The X-ray analysis of the annealed sample showed a d-spacing of 45.2 Å, which was calculated from the lamellar reflections with a periodicity in $q = 0.1416$ Å^{-1} in Figure 10. The X-ray data suggest a monoclinic unit cell with sides of 45.2, 28.1 and 9.6 Å with a 118° angle between the shorter sides. This gives a unit cell volume of 10800 Å^3. Assuming 4 molecules per cell and 3.7×10^{20} molecules per cm^3, the density of the crystal is calculated as 1.222 g/cm^3. In a hexagonal structure the d spacing is 37.7 Å,[1] in a smectic layered structure the d spacing is 32.0 Å,[6] and the fully extended end-to-end length of hexamide **1** is about 50 Å.[6] The 45.2 Å spacing of the spherulitic crystal is less than the calculated end-to-end distances of about 50 Å. A spacing of 32.6 Å has been reported for a hexagonal structure of hexamide **1**.[1] So it seems that the melt-grown phase is more like a linear smectic structure than a discotic hexagonal structure.

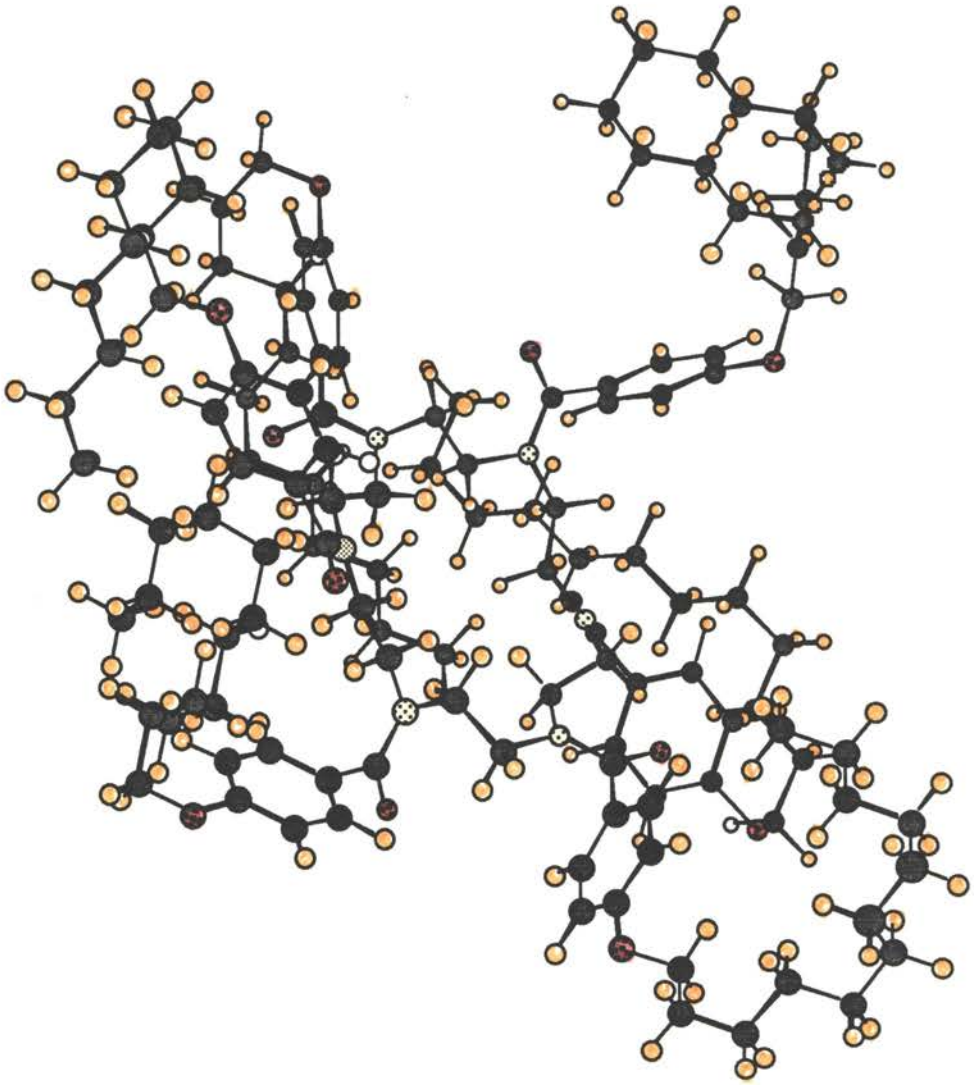

a

Figure 21. Three-dimensional molecular model of hexamide **1**: (a) a disordered conformation; (b) an ordered conformation; (c) a magnified ordered conformation.

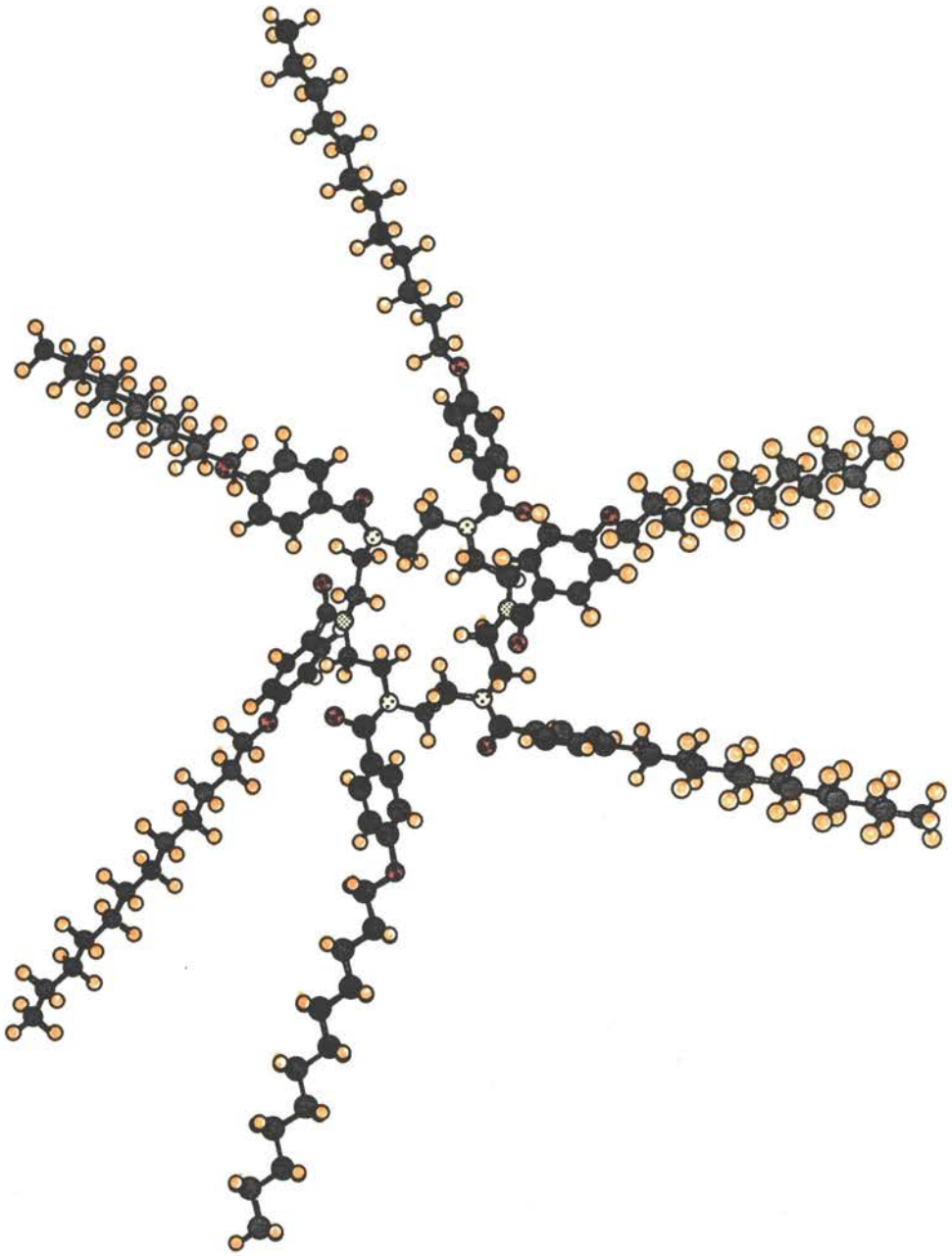

b

Figure 21. (b) an ordered conformation.

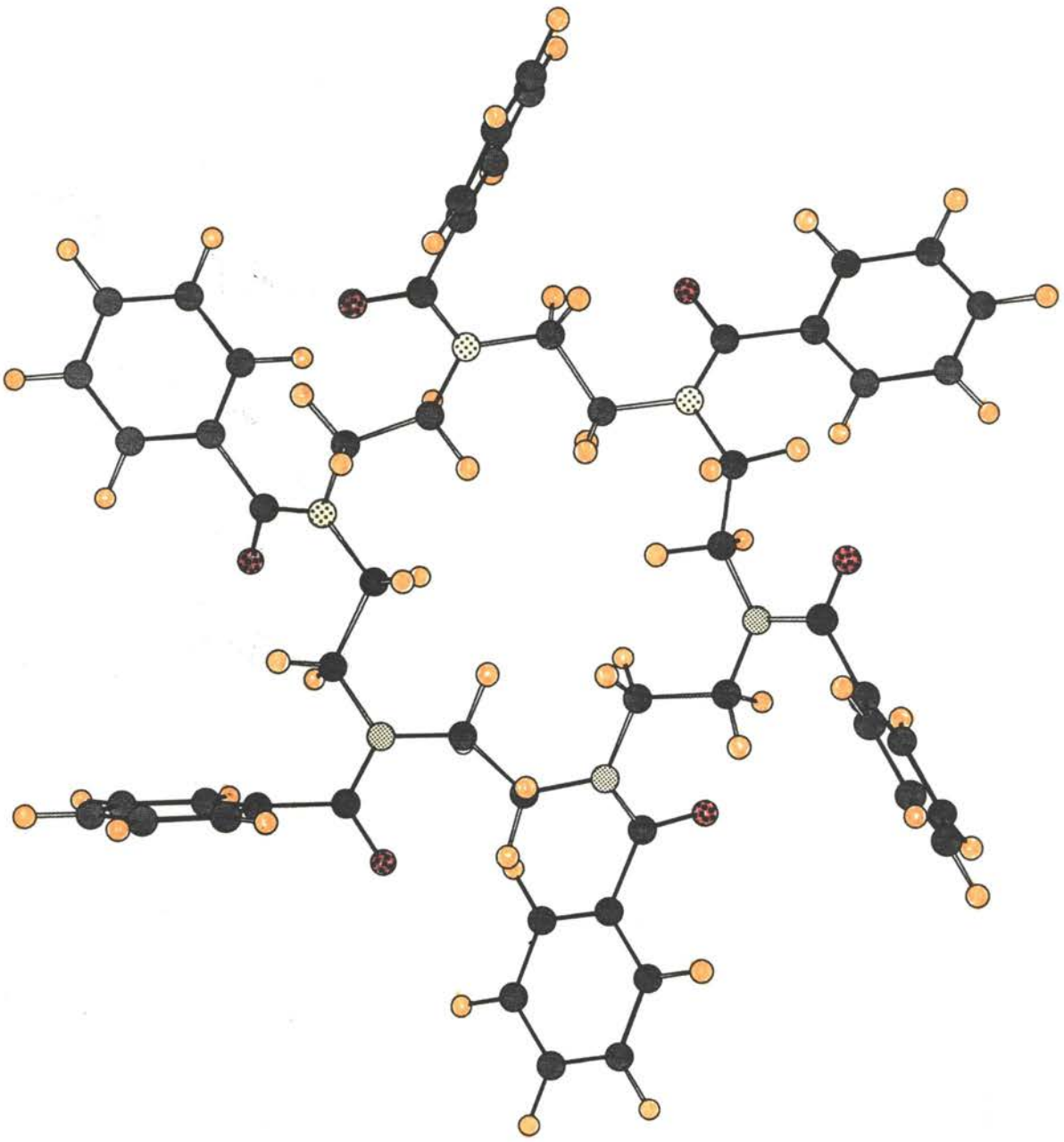

c

Figure 21. (c) a magnified ordered conformation.

Hexamide **2** is the liquid crystalline [18]-N_6 derivative with the highest reported number of carbons in alkyl chains. It showed liquid crystalline properties similar to those of Lattermann's analogous C_{10} hexamide, which exhibited a discotic mesophase between 97.5 and 141 °C.[5] The fan-like texture and high entropy of the isotropic transition of **2** might indicate a columnar mesophase between 106.7 °C and 126.5 °C.[12] The X-ray diffraction showed one sharp peak corresponding to d = 33 Å and a diffuse halo at 110 °C, which suggested a columnar or smectic mesophase. The phase between 8.4 °C and 106.7 °C was an unidentified crystal.

There are phase relationships between the [18]-N_6 discotic mesogens and the rod-like mesogens in the side chains. From the comparison of the liquid crystalline properties of hexamides **1** and **2** with 4-dodecyloxybenzoic acid and 3,4-bis(dodecyloxy)benzoic acid, it is clear that the improved liquid crystallinity of **2** is based on the better liquid crystallity of its substitutent benzoic acid. The ΔH_i of 3,4-bis(dodecyloxy)benzoic acid is 12.3 kcal/mole, while the ΔH_i of 4-dodecyloxybenzoic acid is only about 1.0 kcal/mol. Small ΔH_i is also true for the other [18]-N_6 derivatives (see Table I in Chapter I).

The *p*-alkoxybenzoic acids with 4 or 6 carbons in the alkyl chain show only less ordered nematic mesophases, and their [18]-N_6 derivatives are not liquid crystals. The benzoic acids with 11, 12, and 14 carbon alkyl chains show highly ordered smectic mesophases and lead to [18]-N_6 liquid crystals. By incorporating these good mesogens into azacrown compounds, liquid crystalline [9]-N_3, [12]-N_3, and [14]-N_4 derivatives have been successfully prepared.[5] Since the rod-like benzoic acid mesogens and other acid compounds, such as cinnamic acid and phenylazobenzoic acid, have been well studied for their liquid crystallinities, it should be possible to use this knowledge to design new discotic macrocycles with controlled liquid crystallinities. To design a new liquid crystalline macrocyclic ligand, the optimum combination of the liquid crystallinity of the

side chain substituents and the complexing properties of the macrocycle will be a key point for success.

The mesomorphic behavior of compound **4** was similar to that of hexamide **1**, because of the similarity of their structures. Both annealed samples show the spherulitic texture. Like the similar monofunctionalized discotic compounds, the unsymmetrical compound **4** showed a lower isotropic transition temperature than those of unfunctionalized compound.[15,16] The difference between the two compounds was decreased by annealing (Figures 2 and 14).

In the polymer preparation the steric hindrance may cause difficulty in the hydrosilylation because of the bulky mesogenic groups. Kreuder and Ringsdorf prepared the first liquid crystalline side chain polymer with disc-like mesogens.[15] In their homopolymer about 74% of the Si-H bonds were grafted with a bulky mesogenic group of molecular weight 827. The molecular weight of compound **4** is 1973. To our knowledge this is the largest mesogenic group ever used for a side chain polysiloxane.

The polymers **5a** and **5b** showed similar phase behavior. The DSC curve in the first heating consisted of a glass transition at about 78 °C and an isotropic transition at about 100 °C. There was no exotherm in cooling scans. In the second scan only a weak glass transition was detected (Figure 16). Both polymer samples annealed at 80-100 °C for long time showed a nematic schlieren texture with an isotropic transition temperature at about 110 °C. The X-ray measurements also confirmed that polymer **5a** has mesophase at 99 °C and an isotropic phase at 122 °C. Under a polarizing microscope, the polymers look like anisotropic glasses at room temperature. As expected the oriented structure was frozen below the glass transition temperature as indicated by a stable schlieren texture over at least 6 months. The less flexible unsymmetrical structure of the polymer might result in the destruction of the columnar structure to give a polymer with a nematic discotic phase. The weight percentage of hexamide group of the polymer was 75% and 84% for polymer

5a and **5b**. It is much higher than the weight percentage of the mesogenic functional group in most other liquid crystalline polymers. So the properties of the new polymers **5** depend more on the properties of hexamide **1**, which is a poor or metastable liquid crystal. The high ratio of hexamide to polysiloxane also leads to a poor film-forming property of this liquid crystalline polymer.

Conclusion

The [18]-N_6 derivatives **1**, **2**, **3**, **4** and polymer **5** were prepared and investigated for their liquid crystalline properties. Hexamide **1** has only a monotropic liquid crystalline phase. The spherulitic crystal phase of hexamide **1** was observed in annealing and isothermal crystallization. The intrinsic properties of high viscosity of hexamide **1** lead to a slow crystallization. Purification methods, annealing and shearing have great effects on the orientation of these bulky macrocycles. Hexamide **2** showed an enantiotropic liquid crystalline phase. The differences of the liquid crystalline properties between hexamide **1** and **2** suggest the important relationship between the liquid crystallinity of the substitutent mesogen and the liquid crystallinity of the azacrown derivative. The liquid crystallinity of hexamide **4** was similar to hexamide **1**, but the isotropic transition temperature was lower. The polymer shows a mesophase between a glass transition at about 75 °C and the isotropic transition at about 110 °C.

References

(1) Lehn, J. M.; Malthete, J.; Levelut, A. M. *J. Chem. Soc., Chem. Commun.* **1985**, 794.

(2) Mertesdorf, C.; Ringsdorf, H. *Liq. Cryst.* **1989**, *5*, 1757.

(3) Idziak, S. H. J.; Maliszewskyj, N. C.; Heiney, P. A.; Maccauley, J. P.; Sprengeler, P. A.; Smith, A. B. *J. Am. Chem. Soc.* **1991**, *113*, 7666.

(4) Tatarsky, D.; Banerjee, K.; Ford, W. T. *Chem. Mater.* **1990**, *2*, 138.

(5) Lattermann, G. *Mol. Cryst. Liq. Cryst.* **1990**, *182B*, 299.

(6) Idziak, S. H. J.; Maliszewskyj, N. C.; Vaughan, G. B. M.; Heiney, P. A.; Mertesdorf, C.; Ringsdorf, H.; McCauley, J. P.; Smith, A. B. *J. Chem. Soc., Chem. Commun.* **1992**, 98.

(7) Malthete, J.; Levelut, A. M.; Lehn, J. M. *J. Chem. Soc., Chem. Commun.* **1992**, 1434.

(8) Mertesdorf, C.; Ringsdorf, H. *Mol. Eng.* **1992** (in press).

(9) Atkins, T. J.; Richman, J. E.; Oettle, W. F. *Org. Syn.* **1978**, *58*, 86.

(10) Bautista, M. O.; Duran, R. S.; Ford, W. T. *Macromolecules* **1993**, *26*, 659.

(11) Shibaev, V. P.; Kostromin, S. G.; Plate, N. A. *Eur. Polym. J.* **1982**, *18*, 651.

(12) Staufer, G.; Lattermann, G. *Makromol. Chem.* **1991**, *192*, 2421.

(13) Hatakeyama, H.; Ikeda, M. *Mol. Cryst. Liq. Cryst.* **1978**, *45*, 275.

(14) Kelly, S. M.; Buchecker, R. *Helv. Chim. Acta* **1988**, *71*, 461.

(15) Kreuder, W.; Ringsdorf, H. *Makromol. Chem. Rapid Commun.* **1983**, *4*, 807.

CHAPTER III

LIQUID CRYSTALLINE METAL COMPLEXES OF HEXA-(4-DODECYLOXYBENZYL)-[18]-N_6

Introduction

In recent years research interest in liquid crystalline azacrown[18]-N_6 derivatives has increased and different compounds were synthesized.[1-11] Some of these nitrogen-containing macrocycles are macrocyclic ligands, which show complexing ability for transition metals.[12] The combination of the selective complexing with self assembling structures will lead to some interesting properties. A tube-like structure consisting of macrocyclic ligands might be used as a phase-dependent metal ion channel for many applications.[4] It is important to understand the relationship between liquid crystalline properties and complexation of metal. What kind of metal ions will be complexed by these macrocyclic ligands? How will liquid crystalline properties be affected by complexation of metal ions? The complexation properties of some azacrown[18]-N_6 compounds have been studied by Ringsdorf's research group.[13] They found that non-liquid crystalline azacrown[18]-N_6 hexamines can be changed to columnar liquid crystals after complexation with $Co(NO_3)_2$ and $Ni(NO_3)_2$. The new mesophases were attributed to the stiffening of the molecular conformation and interaction between the central metals. In Chapter II we reported the synthesis and liquid crystalline properties of azacrown[18]-N_6 hexamide **1**. In this chapter we report the preparation of complexes of metal ions with azacrown[18]-N_6 hexamine **2** and investigation of their phase behavior. Tetraamide **3** and tetraamine **4** were prepared also.

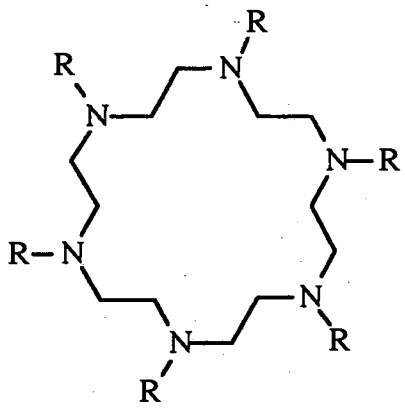

1: R = 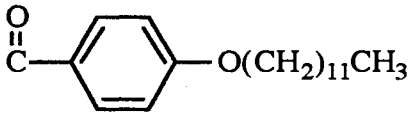

2: R = 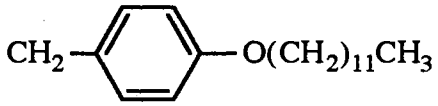

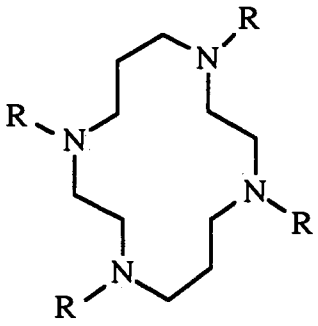

3: R = 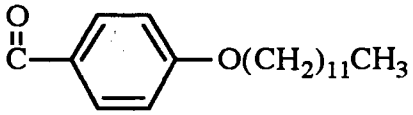

4: R = 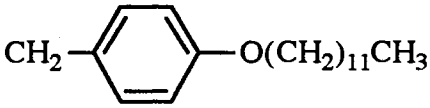

Experimental Section

Materials and Analytical Methods. All organic reagents were obtained from Aldrich and were used without further purification unless otherwise stated. 1,4,7,10,13,16-Hexa-(4-dodecyloxybenzoyl)-1,4,7,10,13,16-hexaazacyclooctadecane (**1**) was prepared using the procedure in Chapter II. Thermogravimetry measurements were done with a Perkin-Elmer model TGS-2 thermogravimetric analyzer. NMR spectra were recorded on a Varian XL-300 instrument at 300 MHz for ^{1}H or 75.43 MHz for ^{13}C. All spectra were recorded in $CDCl_3$ solution with TMS as internal standard unless otherwise specified. FT-IR spectra were taken on a Nicolet Impact 400 spectrometer with KBr disks.

Characterization of the Phase Behavior. The phase behaviors of the metal complexes were studied using differential scanning calorimetry (DSC) and optical polarizing microscopy. Thermal transitions were determined with a Perkin-Elmer DSC-2C differential scanning calorimeter equipped with a TADS 3600 data station. Heating and cooling rates were 20 °C/min, unless noted otherwise. The sample was heated from -10 °C to 150 °C at 20 deg/min, held 2 min at 150 °C, cooled to -10 °C at 20 deg/min using solid CO_2 in the DSC heat exchange system, held 15 min at -10 °C, heated from -10 °C to 150 °C at 20 deg/min, and cooled as before for a total of 2 heating and cooling scans. The sample sizes were 5-10 mg. The thermal transitions and anisotropic textures were observed on a Nikon 104 optical polarizing microscope fitted with a Nikon 35 mm automatic camera and an Instec hot stage controlled by an Apple II computer. The sample was heated from 20 °C to 110 °C (isotropic melt) at 5 °C/min, held 2 min at 110 °C, cooled to 20 °C at 5 °C/min, held about 10 min at 20 °C, and heated and cooled as before for a total of 2 heating and cooling observations.

1,4,7,10,13,16-Hexa-(4-dodecyloxybenzyl)-1,4,7,10,13,16-hexaazacyclooctadecane (2). Synthesis was performed by reduction of hexamide **1** (2.29 g, 1.20 mmol) with $LiAlH_4$ (0.83 g, 21.0 mmol)[7], in 72.9% yield. ^1H NMR (50 °C): δ 0.88 (t, 18 H, CH_3), 1.27 (m, 96 H, CH_2), 1.42 (m, 12 H, CH_2), 1.76 (t, 12 H, CH_2), 2.58 (br, 24 H, NCH_2), 3.38 (br, 12 H, CH_2Ar), 3.91 (t, 12 H, CH_2O), 6.76 (d, 12 H, Ar), 7.06 (d, 12 H, Ar). ^{13}C NMR (50 °C): δ 14.0 (CH_3), 22.6, 26.1, 29.3, 29.4, 29.6, 29.9, 31.9 (CH_2), 52.5 (NCH_2), 58.8 (CH_2Ar), 68.1 (CH_2O), 114.2, 129.9, 131.7, 158.1 (Ar). IR (KBr): 2930 (s), 2860 (s), 1615 (m), 1518 (s), 1470 (m), 1255 (s) cm^{-1}. Mass spectrum (FAB, 2-nitrophenyloctyl ether/*p*-toluenesulfonic acid, 2/1 v/v) 1906 [$(M+H)^+$, calcd. for $C_{126}H_{211}N_6O_6$: 1906]. Anal. Calcd. for $C_{126}H_{210}N_6O_6$: C, 79.43; H, 11.12; N, 4.41. Found C, 78.48; H, 11.08; N, 4.32.

1,4,8,10,11-Tetra-(4-dodecyloxybenzyl)-1,4,8,11-tetraazacyclooctadecane (4). Tetraamide **3** was prepared as reported.[5] Synthesis of tetraamine **4** was performed by reduction of tetraamide **3** with $LiAlH_4$. ^1H NMR (50 °C): δ 0.92 (t, 12H, CH_3), 1.34 (m, 64H, CH_2), 1.49 (m, 8H, CH_2), 1.80 (t, 12H, CH_2), 2.52 (m, 8H, NCH_2), 2.60 (m, 8H, CH_2N), 3.40 (m, 8H, CH_2Ar), 3.95 (m 8H, CH_2O), 6.82 (d, 8H, Ar), 7.18 (d, 8H, Ar). ^{13}C NMR (50 °C): δ 14.0 (CH_3), 22.6, 26.1, 29.3-29.6, 31.9 (CH_2), 50.7 (NCH_2), 51.6 (CH_2N), 59.0 (CH_2Ar), 68.1 (CH_2O), 114.2, 129.9, 131.9, 158.1 (Ar).

Procedure for Complexation of the Metal Ions with Hexamine 2. All metal salts (purity ≥ 98%) were obtained from Aldrich. The appropriate equivalents of hexamine **2** and metal salt (such as 0.03 mmol, 10.9 mg of $Cu(O_3SCF_3)_2$ and 0.03 mmol, 57.2 mg of hexamine **2**) were stirred in 5 mL of dry tetrahydrofuran (THF) at 25 °C for 48 h. The THF was removed and the residue was dried in vacuum at 50 °C for 24 h.

Results and Discussion

Selection of Metal Salts. To select some metal salts for preparation of metal complexes of hexamine **2**, a very simple experiment was done by testing the solubility and color of different metal salts (about 5 mg) in THF solutions (1 mM, 2mL) of hexamine **2**. The results are reported in Table I. Based on the above results, only metal salts that were highly soluble in THF containing **2** were chosen for preparation of metal complexes of hexamine **2**.

Table I. Results of Preliminary Experiments of Metal Salts

metal salt	color of solid metal salt	solubility in THF without **2**	solubility in THF with **2**	color of solution without **2**	color of solution with **2**
$Mg(O_3SCF_3)_2$	white	medium	high	colorless	colorless
$MgCl_2 \cdot H_2O$	white	medium	medium	colorless	colorless
$Mg(O_2CCH_3)_2 \cdot 4H_2O$	white	medium	medium	colorless	colorless
KI	white	low	low	colorless	colorless
$Cr(NO_3)_3 \cdot 9H_2O$	white	low	low	colorless	colorless
$MnCl_2 \cdot 4H_2O$	white	low	low	colorless	colorless
$FeCl_3$	brown	high	high	yellow	yellow
$Fe(NO_3)_3 \cdot 9H_2O$	white	medium	medium	colorless	colorless
$FeSO_4 \cdot 7H_2O$	white	low	low	colorless	colorless
$Co(O_2CCH_3)_2 \cdot 4H_2O$	pink	low	low	colorless	colorless
$CoCl_2 \cdot 6H_2O$	pink	medium	high	blue	blue
$Co(OH)_2$	pink	low	low	colorless	colorless
$Ni(O_2CCH_3)_2 \cdot 4H_2O$	green	low	medium	colorless	colorless
$Ni(OH)_2$	green	low	low	colorless	colorless
$Cu(O_3SCF_3)_2$	white	medium	high	colorless	blue
$Cu(O_2CCH_3)_2$	green	medium	high	green	green
$CuBr_2$	green	high	high	green	green
$CuCl_2 \cdot 2H_2O$	green	high	high	green	yellow
$Zn(O_3SCF_3)_2$	white	medium	high	colorless	colorless
$Pd(O_2CCH_3)_2$	brown	high	high	yellow	yellow
AgO_3SCF_3	white	high	high	colorless	colorless

Table I. (continued)

metal salt	color of solid metal salt	solubility in THF without **2**	with **2**	color of solution without **2**	with **2**
$HgCl_2$	white	low	high	colorless	colorless
$Pb(O_2CCH_3)_2{\cdot}3H_2O$	white	medium	medium	colorless	colorless
$PbCl_2$	white	low	low	colorless	colorless
$Pb(NO_3)_2$	white	low	low	colorless	colorless

Characterization of the Metal Complexes. All THF solutions, from which new complexes were isolated, were clear without residual undissolved metal salts. The dry samples were studied by thermogravimetry, NMR and FT-IR for their purity and structures.

By thermogravimetric measurements, the weight loss of all samples in the temperature range 30-100 °C was less than 1%, which indicates that there were no large amounts of water or THF in the samples, and the complexes were composed of hexamine **2** and bound metal salts. Figure 1 shows typical thermogravimetric curves of the complexes. There was about 10% and 25% weight loss at 250 °C and 300 °C for the copper triflate complex and most of other complexes. As expected the complexes were not stable at high temperature.

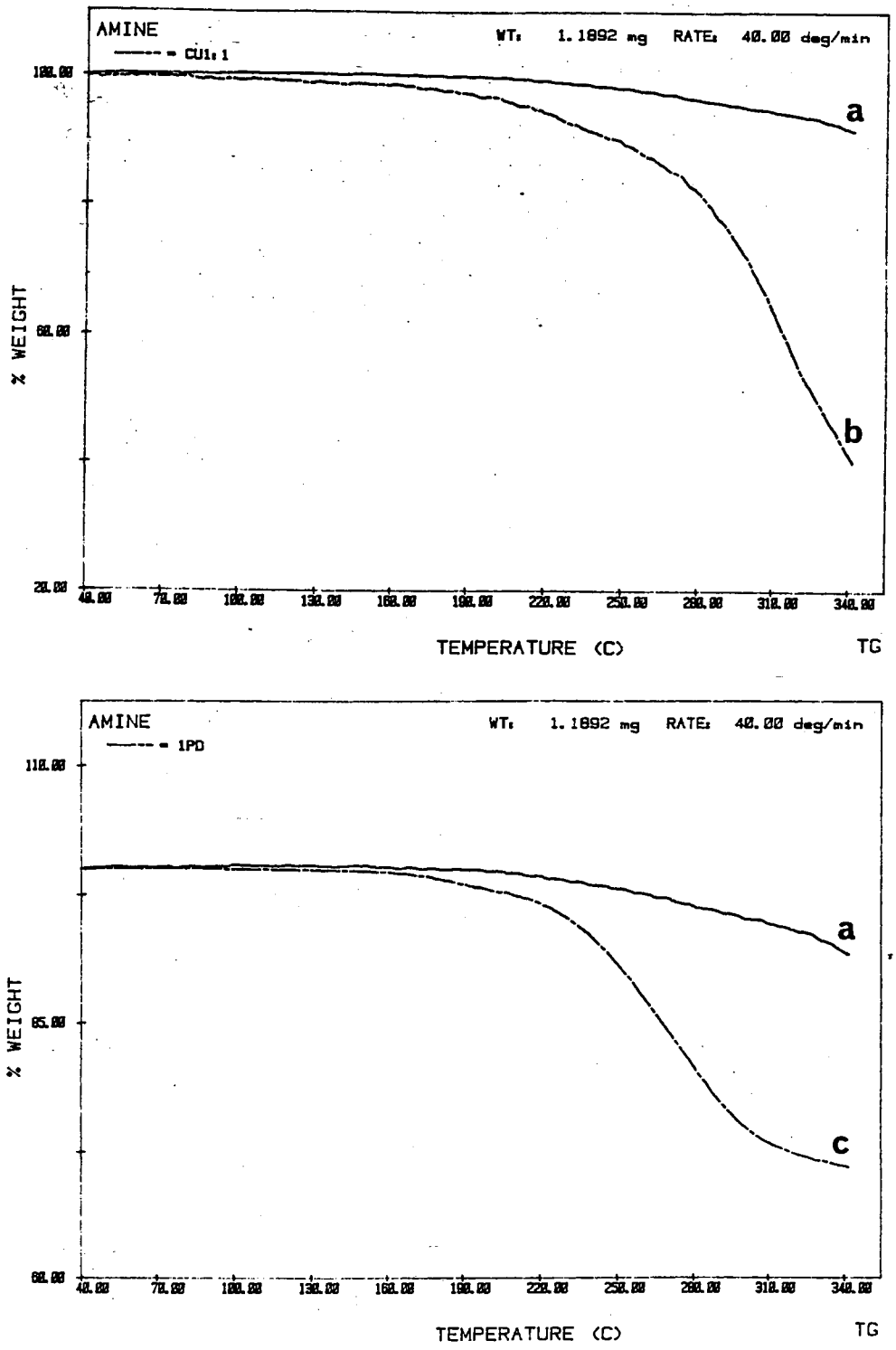

Figure 1. Thermogravimetric recordings. (a) hexamine **2**; (b) complex of hexamine **2** and $Cu(O_3SCF_3)_2$; (c) complex of hexamine **2** and $Pd(O_2CCH_3)_2$.

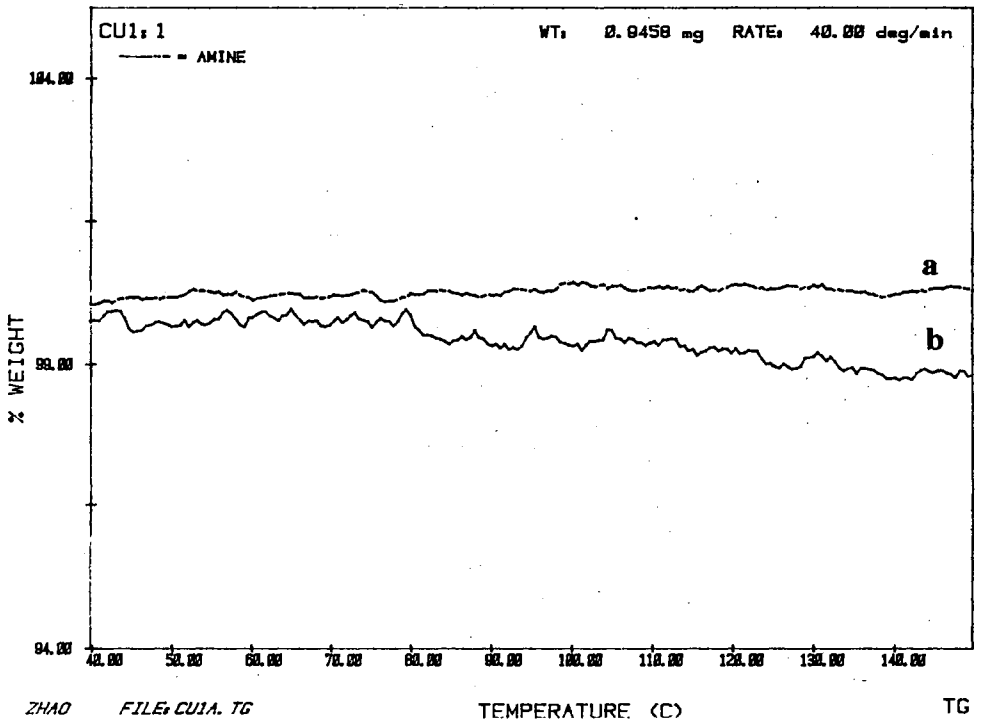
CU1: 1
WT: 0.9458 mg
RATE: 40.00 deg/min
---- = AMINE
104.00
99.00
94.00
% WEIGHT
a
b
40.00
50.00
60.00
70.00
80.00
90.00
100.00
110.00
120.00
130.00
140.00
ZHAO
FILE: CU1A.TG
TEMPERATURE (C)
TG

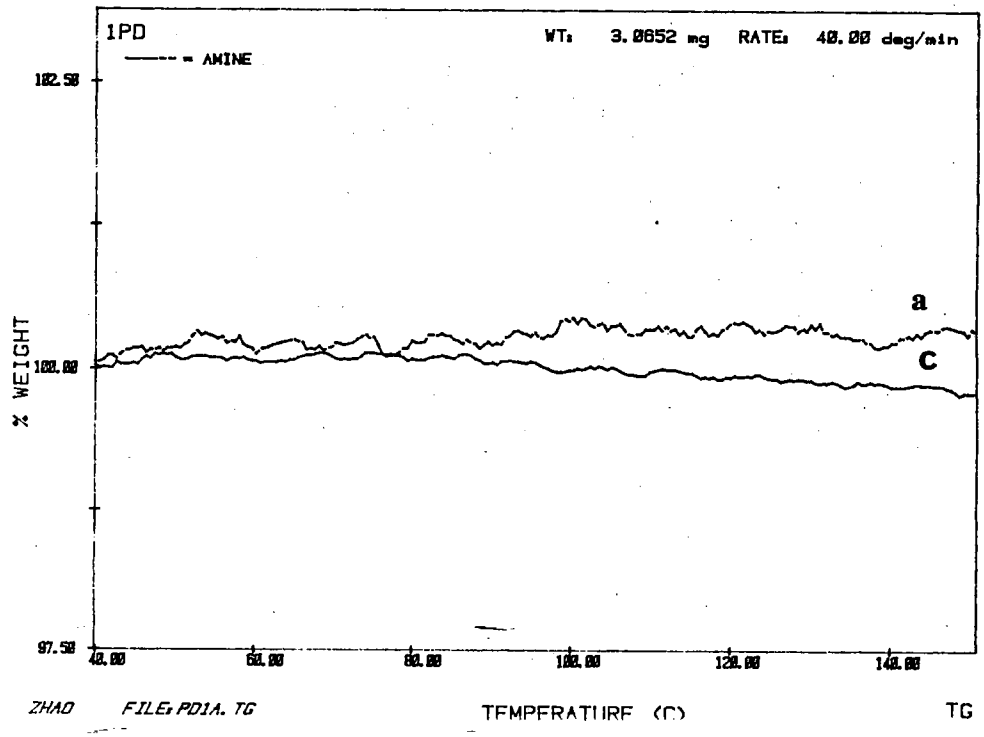
1PD
WT: 3.0652 mg
RATE: 40.00 deg/min
---- = AMINE
102.50
100.00
97.50
% WEIGHT
a
c
40.00
60.00
80.00
100.00
120.00
140.00
ZHAO
FILE: PD1A.TG
TEMPERATURE (C)
TG

Why is hexamine **2** a non-liquid crystalline compound but hexamide **1** a discotic liquid crystalline compound? One reason is that hexamide **1** has a more rigid central ring, which is the result of the restricted rotation about amide C(O)-N bonds. For hexamine **2** free rotation about the corresponding CH_2-N bonds leads to flexible conformations, which do not help discotic liquid crystalline properties. The restricted or unrestricted rotation of CO-N or CH_2-N bonds can be detected by ^1H NMR analysis of the benzene ring signals in spectra of the macrocyclic amide and amine. Figure 2 shows the different aromatic signals of hexamide **1** and hexamine **2**, and for further comparison tetraamide **3** and tetraamine **4** are also presented. Because of the restricted rotation, the aromatic protons neighboring the PhCO-N bond give a broad signal, while the aromatic protons near the flexible $PhCH_2$-N bond give a sharp signal. The rigid macrocyclic conformations also can be confirmed by the broad signals of $N(CH_2)_2$ of the central rings.

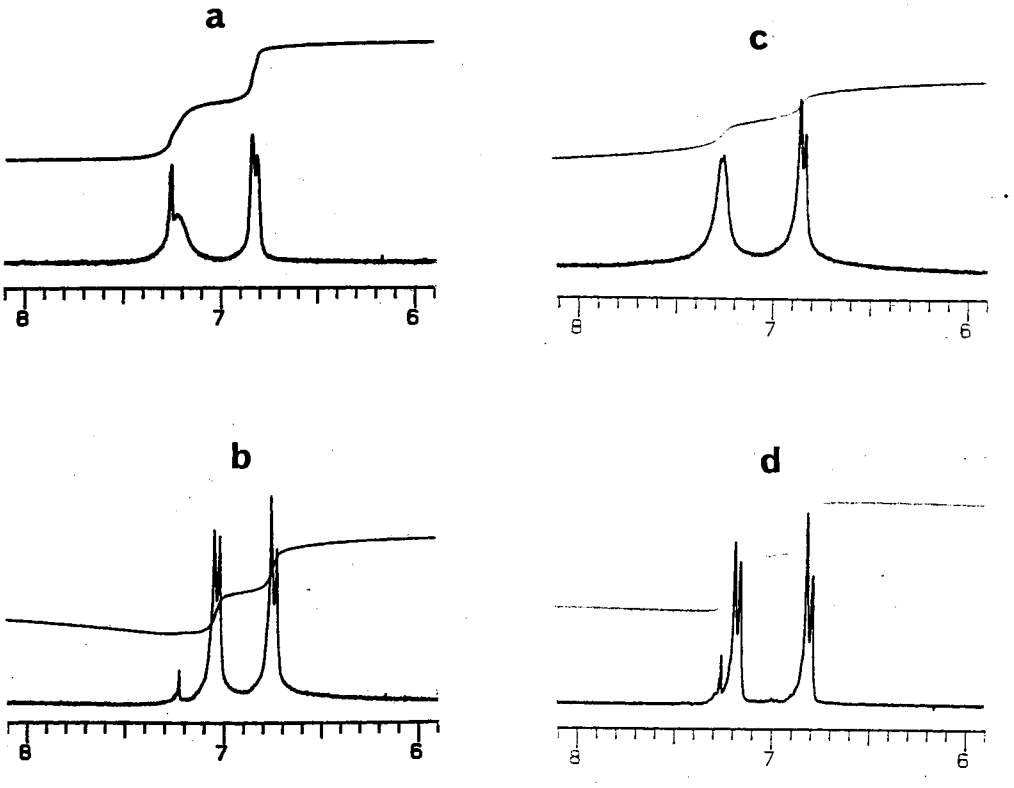

Figure 2. ^1H NMR spectra in aromatic region of macrocycles ($CDCl_3$, 50 °C). (a) hexamide **1**; (b) hexamine **2**; (c) tetraamide **3**; (d) tetraamine **4**.

Figure 3 presents the ^1H NMR spectra of hexamine **2** and its complexes. After complexation all peaks became broad, except the peaks of alkyl tails. This indicates slow conformational changes and stiffened molecular conformations. Large changes in chemical shifts and linewidths in the ^1H NMR spectra of **2** in the presence of metal salts show that the macrocycle coordinates to the metal ions. For most complexes the macrocycle ring signals at 2.58 ppm move to about 3.0 ppm. NMR chemical shifts have been used to study complex stability constants.[15,16] In a control experiment hexamine **2** and $Cu(O_3SCF_3)_2$ (1:1 mole ratio) were dissolved in $CDCl_3$, and the ^1H NMR spectrum is presented at Figure 3h. The complexation can be confirmed by the broad peaks and chemical shift. It may be a simple method to select metal salts for binding.

The complexation also can be detected by FT-IR spectra. For example the FT-IR spectrum (Figure 4) of the $Cu(O_3SCF_3)_2$-hexamine **2** complex shows that the shoulder peak at 2850-2950 cm^{-1}, which is due to the C-H stretching vibration of the $N\text{-}CH_2$ groups, disappeared after hexamine **2** complexed with $Cu(O_3SCF_3)_2$. This is evidence for complete complexation of Cu^{2+} by hexamine **2**. Upon complexation some IR peaks became broad, and there were some changes in the fingerprint region.

Phase Behavior. The complexes were examined for their liquid crystalline properties by DSC and polarizing microscopy. The phase behavior of the complexes is summarized in Table II. DSC thermograms and polarizing microscopic textures of the complexes are presented in Figures 5-17.

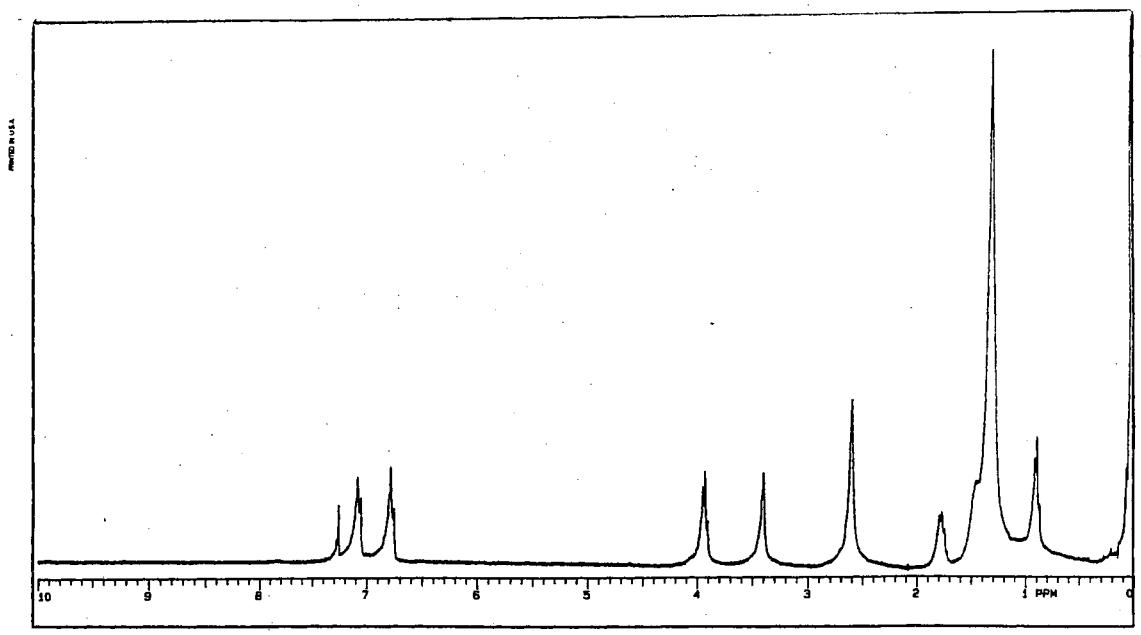

a

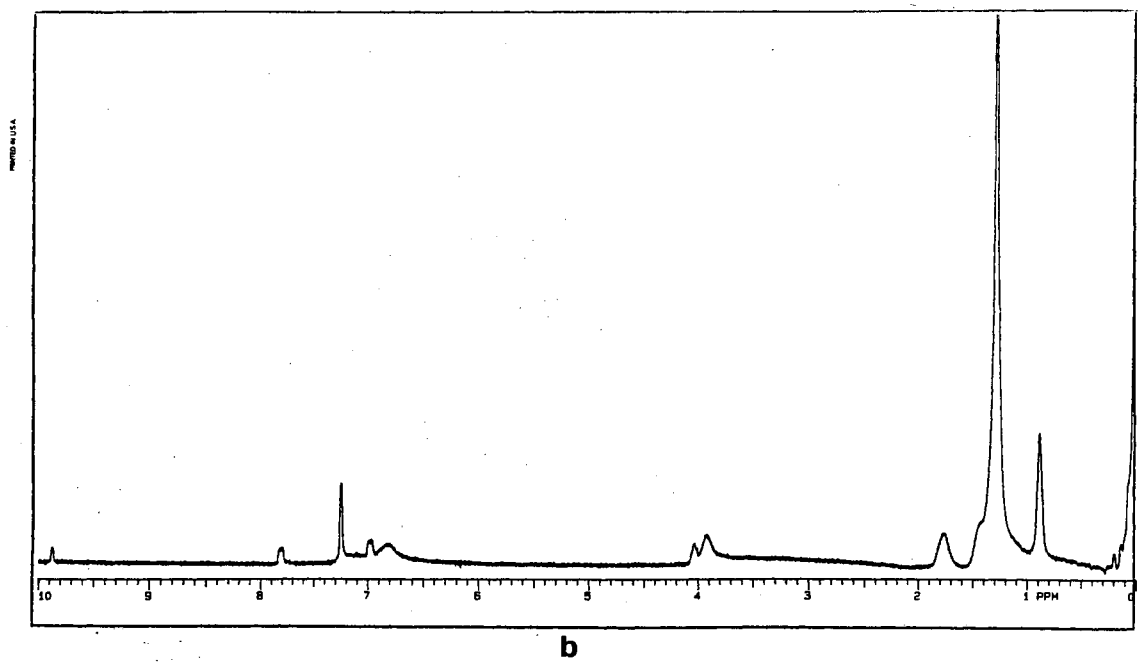

b

Figure 3. ^1H NMR spectra ($CDCl_3$, 20 °C). (a) hexamine **2**; (b) complex of $FeCl_3$ and **2**; (c) complex of $Cu(O_2CCH_3)_2$ and **2**; (d) complex of $Cu(O_3SCF_3)_2$ (1 : 1) and **2**; (e) complex of $Zn(O_3SCF_3)_2$ and **2**; (f) complex of $Mg(O_3SCF_3)_2$ and **2**; (g) complex of $CoCl_2$ and **2**; (h) solution of $Cu(O_3SCF_3)_2$ (1 : 1) and **2** in $CDCl_3$.

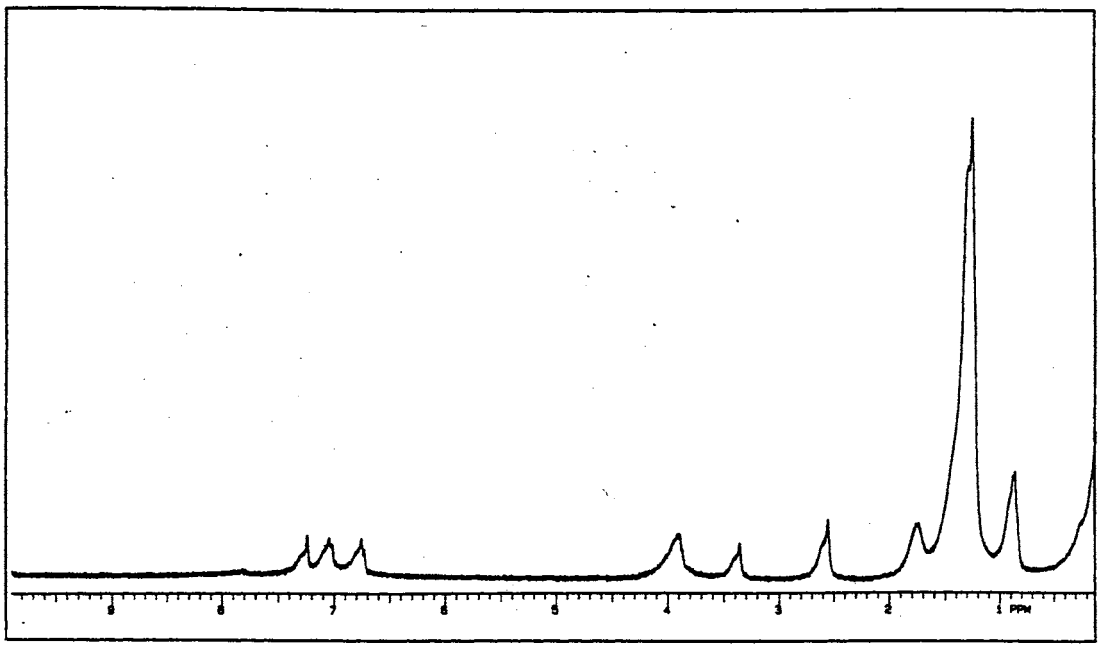

c

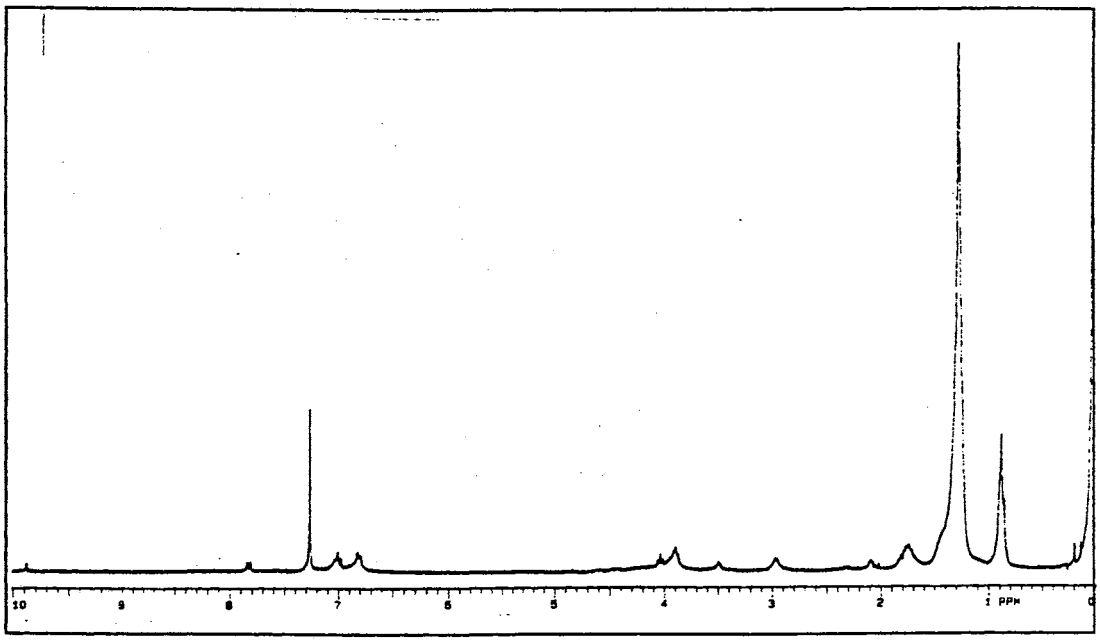

d

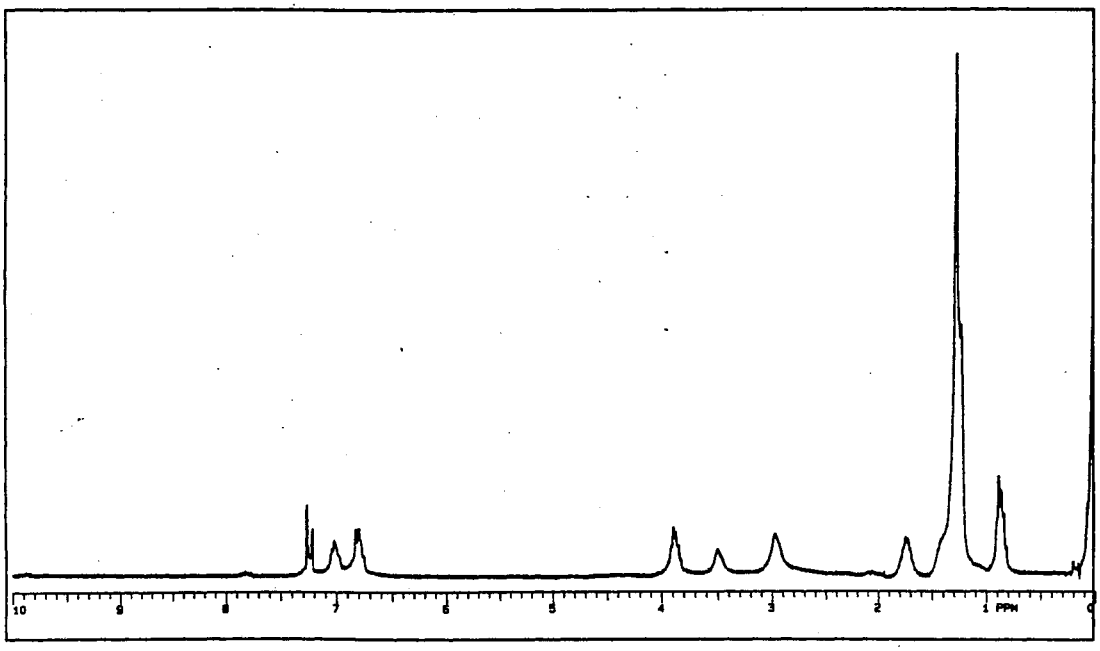

e

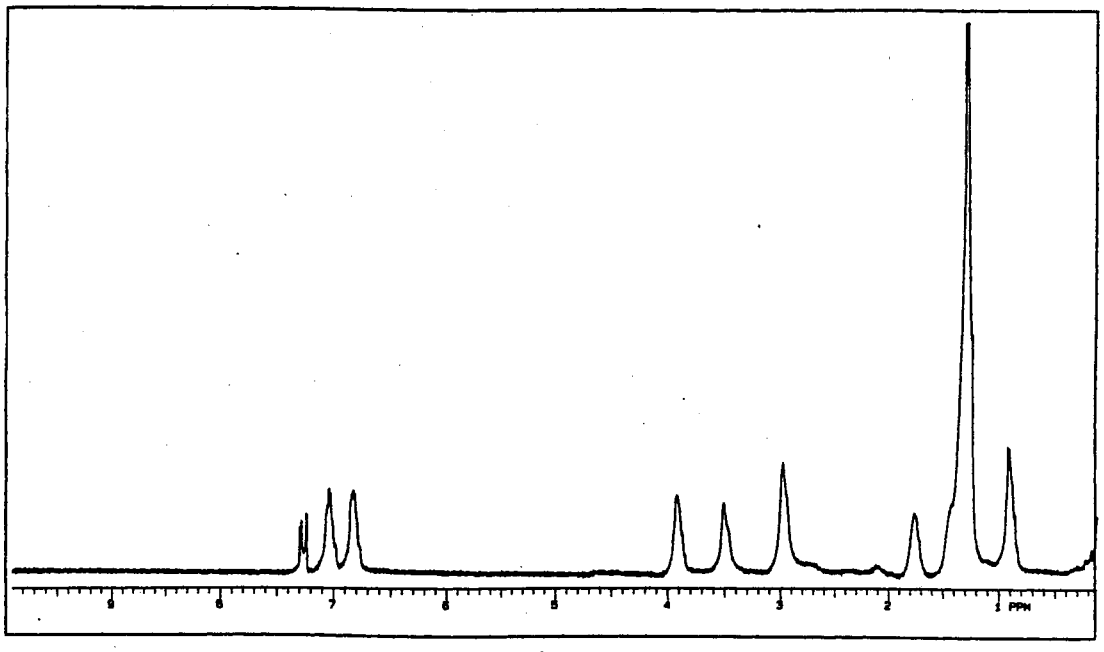

f

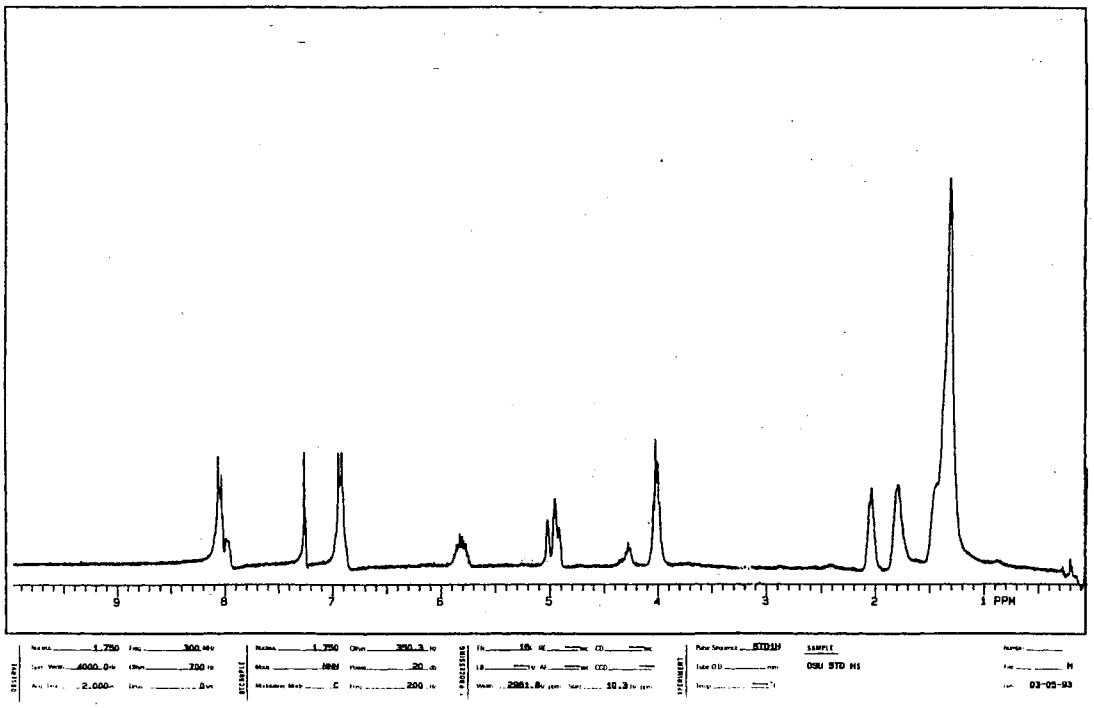

g

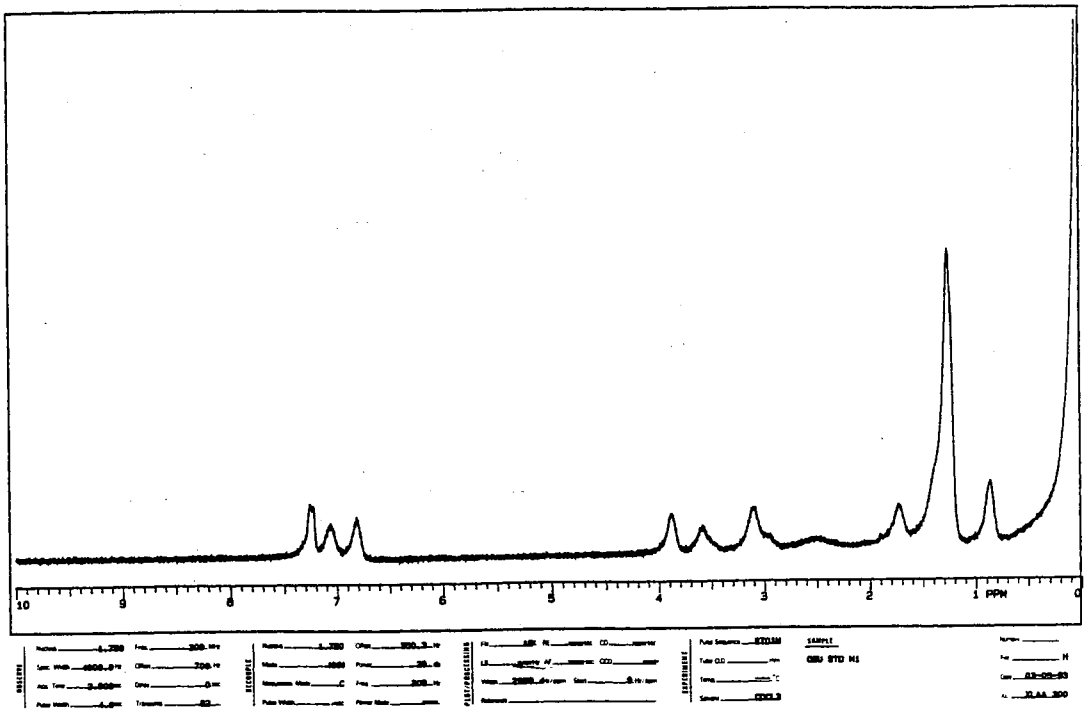

h

a

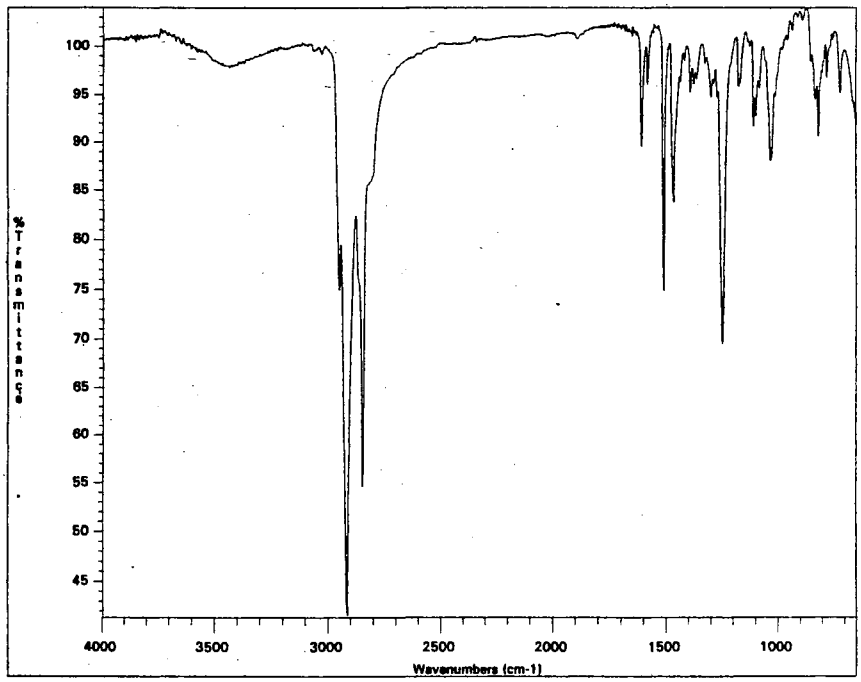

b

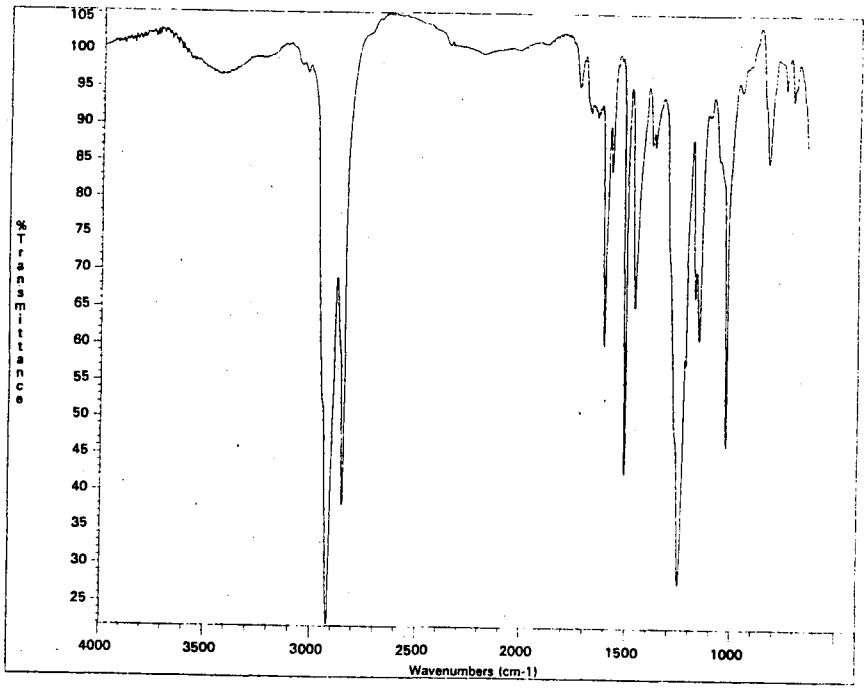

Figure 4. FT-IR spectra. (a) hexamine **2**; (b) **2** complex of $Cu(O_3SCF_3)_2$ (1 : 1); (c) magnified a and b; (d) **2** complex of $Cu(O_3SCF_3)_2$ (Cu : amine = 0.5 : 1).

c

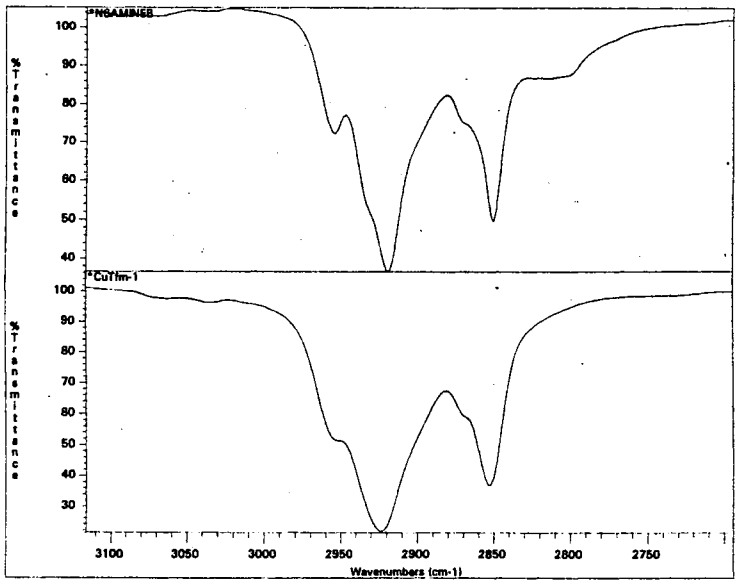
%Transmittance
Wavenumbers (cm-1)
3100
3050
3000
2950
2900
2850
2800
2750

d

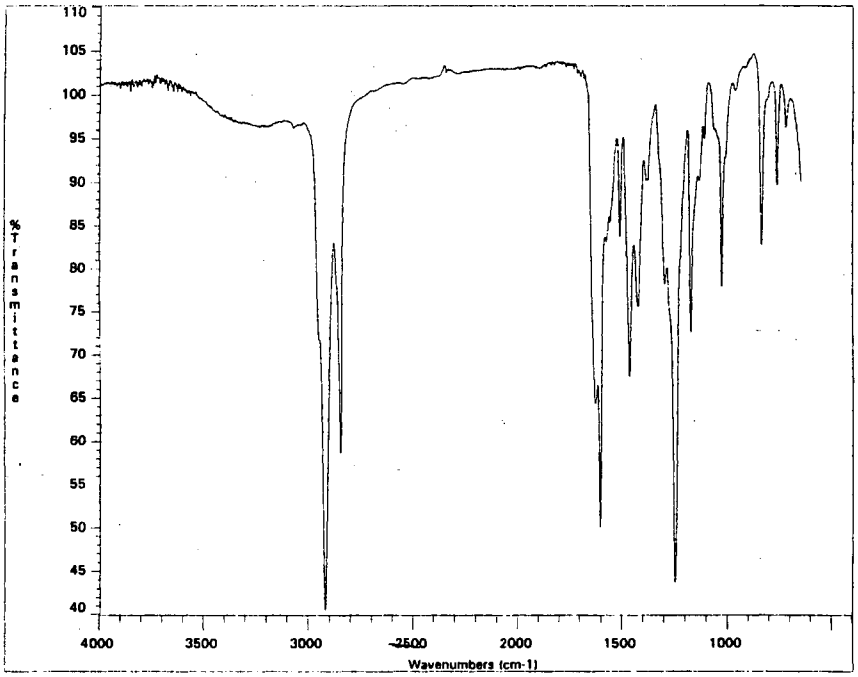
%Transmittance
Wavenumbers (cm-1)
4000
3500
3000
2500
2000
1500
1000

Table II. Phase Behavior of Transition Metal Complexes of Hexamine **2**.[a,b]

metal salt	color of complex	ratio of host/guest		phases transition °C (ΔH, cal/g)
none	white		(heat)	C 84 (17.7) I
			(cool)	C 57 (16.3) I
$Mg(O_3SCF_3)_2$	white	1/1	(heat)	C 47 (1.7) M 75 (1.0) I
			(cool)	C/M 67 (0.4) I
$FeCl_3$	green	1/1	(heat)	C_1 53 (0.3) C_2/M 99 (0.4) I
			(cool)	no peak
$CoCl_2 \cdot 6H_2O$	yellow	1/1	(heat)	C -3 (4.2) M 76 (3.9) I
			(cool)	C -25 (1.7) M 61 (3.4) I
$Cu(O_3SCF_3)_2$	green	1/1	(heat)	C/M 68 (1.9) I
			(cool)	no peak
$Cu(O_3SCF_3)_2$	green	2/1	(heat)	C/M 78 (7.8) I
			(cool)	$C_1$16 (0.3) C_2/M 37 (6.7) I
$Cu(O_2CCH_3)_2$	green	1/1	(heat)	C/M 80 (16.5) I
			(cool)	C 20 (6.0) M 29 (1.2) I
$Zn(O_3SCF_3)_2$	white	1/1	(heat)	C_1 40 (0.4) C_2/M 68 (0.3) I
			(cool)	C/M 62 (0.3) I
$Pd(O_2CCH_3)_2$	yellow	1/1	(heat)	C/M 80 (7.6) I
			(cool)	C_1 15 (0.6) C_2/M 39 (5.0) I
AgO_3SCF_3	white	1/1	(heat)	C/M 79 (5.4) I
			(cool)	C_1 20 (3.3) C_2/M 29 (0.5) I

[a] Abbreviations: C = crystalline; M = mesophase; C/M = crystalline or mesophase; I = isotropic. [b] based on DSC second heating and cooling at 20 °C/min.

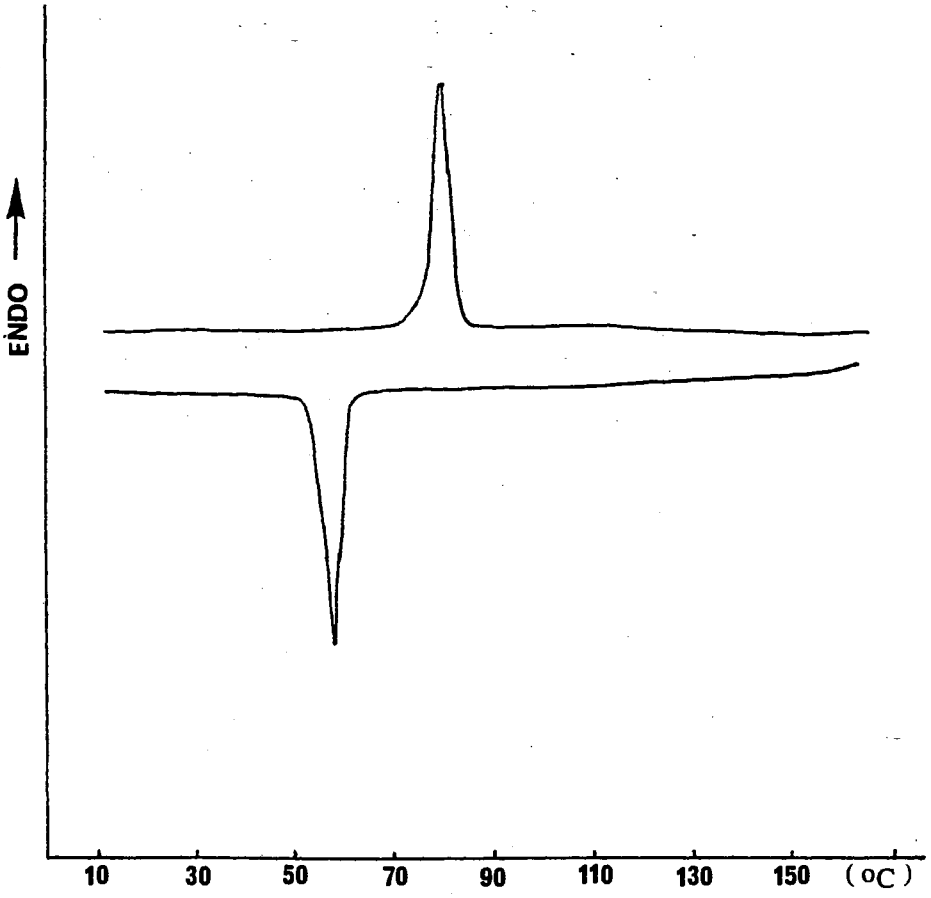

Figure 5. DSC thermogram (second run) of hexamine **2**.

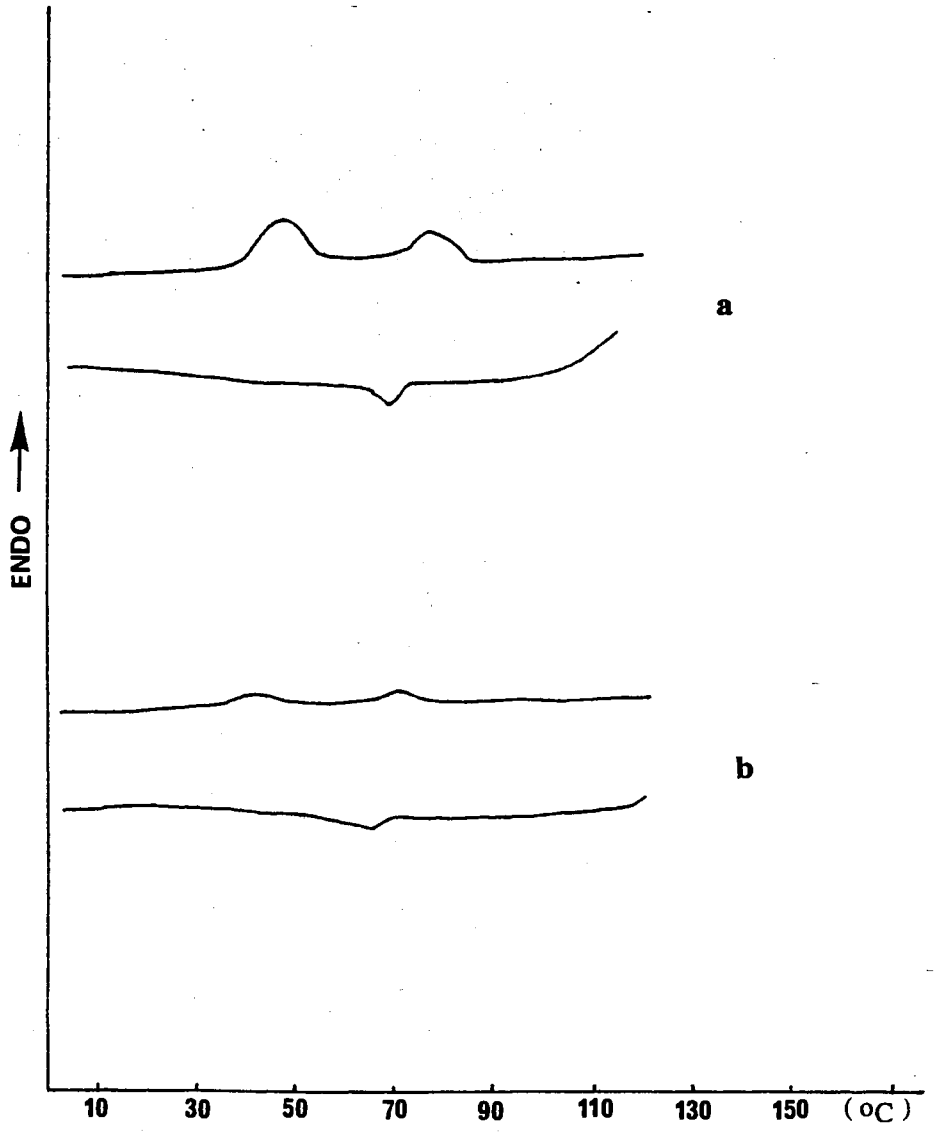

Figure 6. DSC thermograms (second run). (a) hexamine **2** complex of $Mg(O_3SCF_3)_2$; (b) hexamine **2** complex of $Zn(O_3SCF_3)_2$.

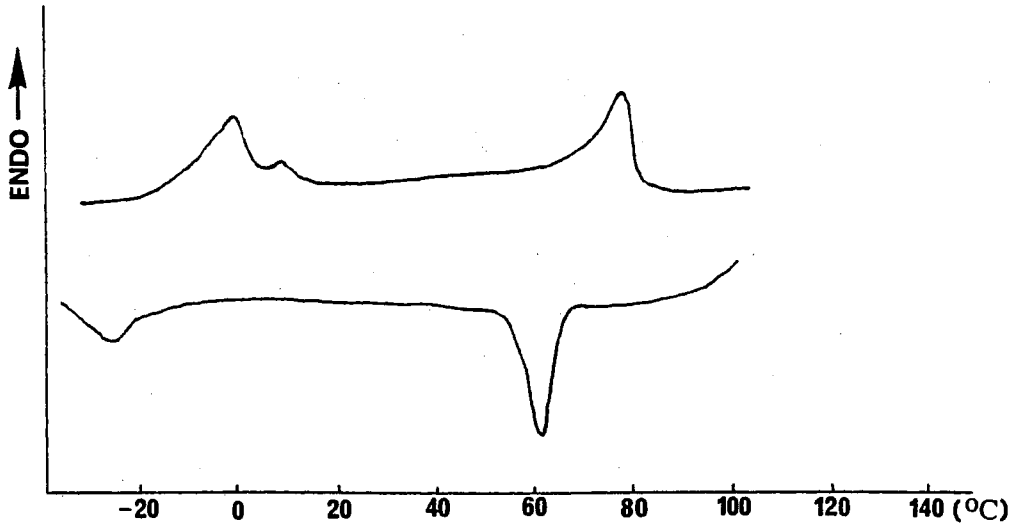

Figure 7. DSC thermograms (second run) of hexamine **2** complex of $CoCl_2$.

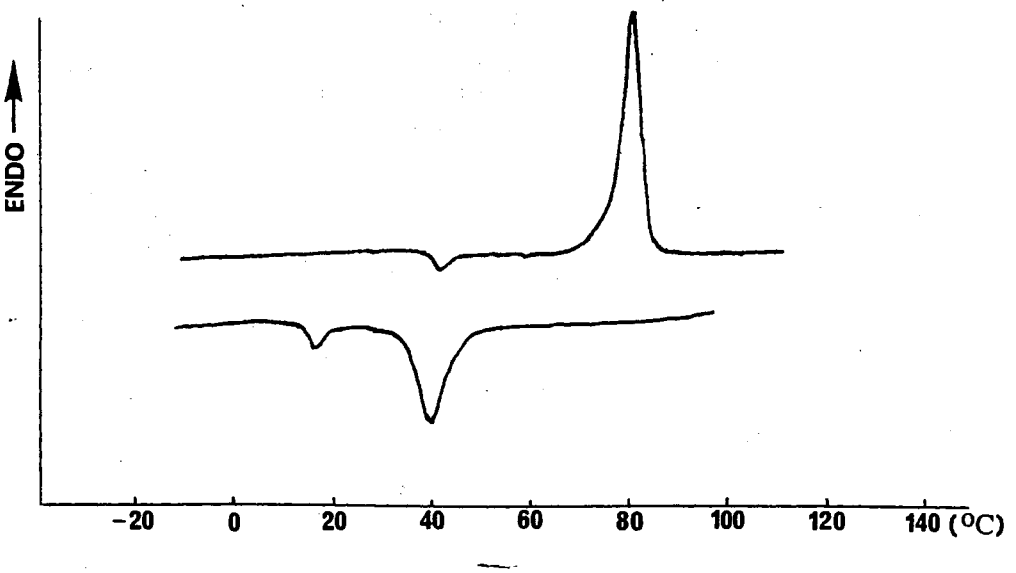

Figure 8. DSC thermograms (second run) of hexamine **2** complex of $Pd(O_2CCH_3)_2$.

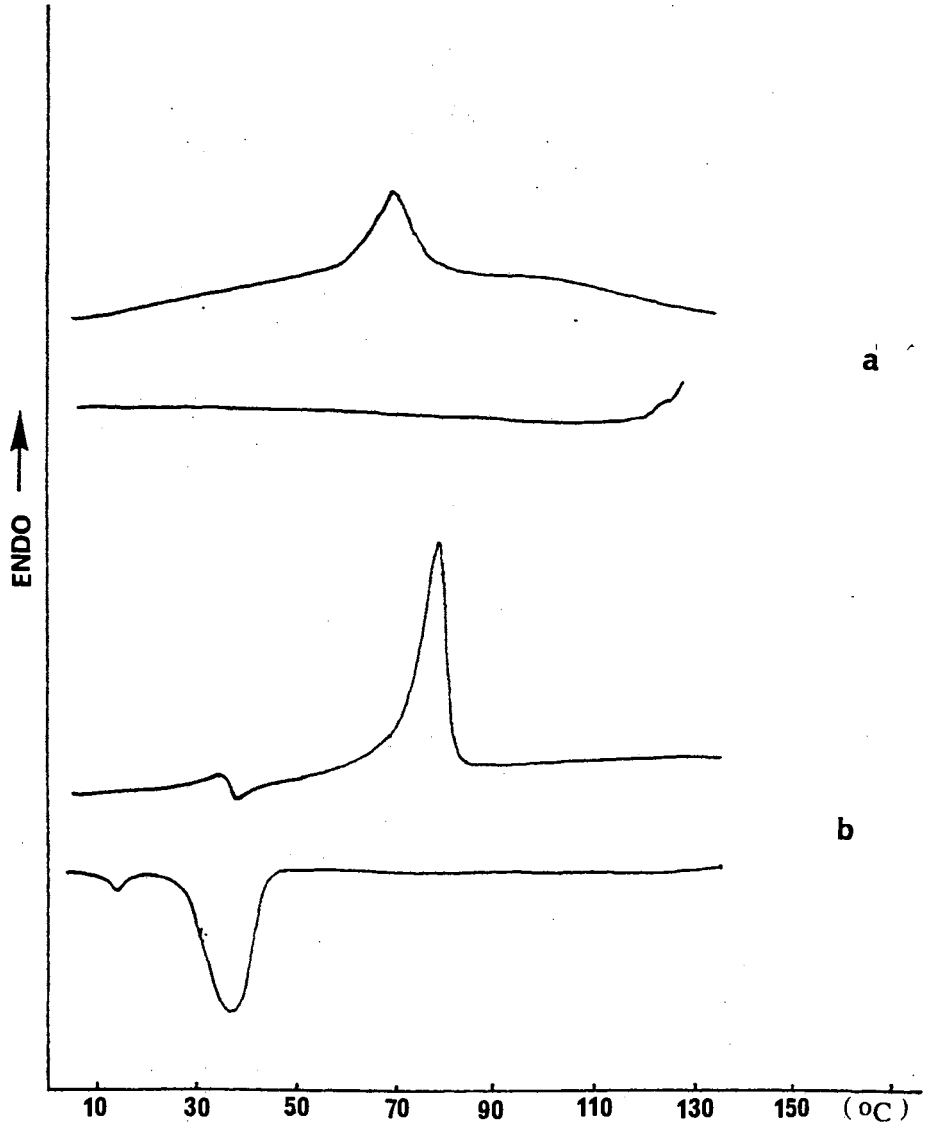

Figure 9. DSC thermograms (second run) of hexamine **2** complex of $Cu(O_3SCF_3)_2$. (a) Cu : amine = 1 : 1; (b) Cu : amine = 0.5 : 1.

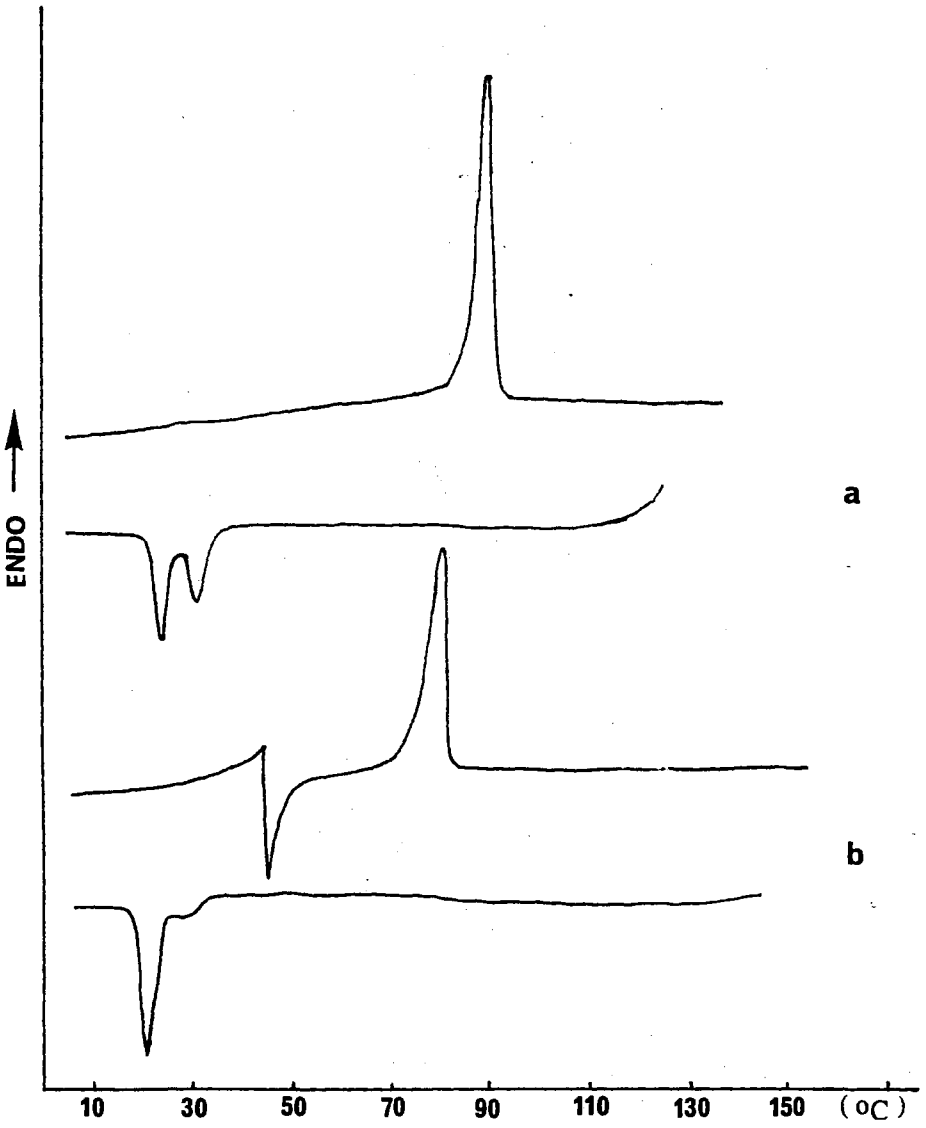

Figure 10. DSC thermograms of hexamine **2** complex of $Cu(O_2CCH_3)_2$.

(a) first run; (b) second run.

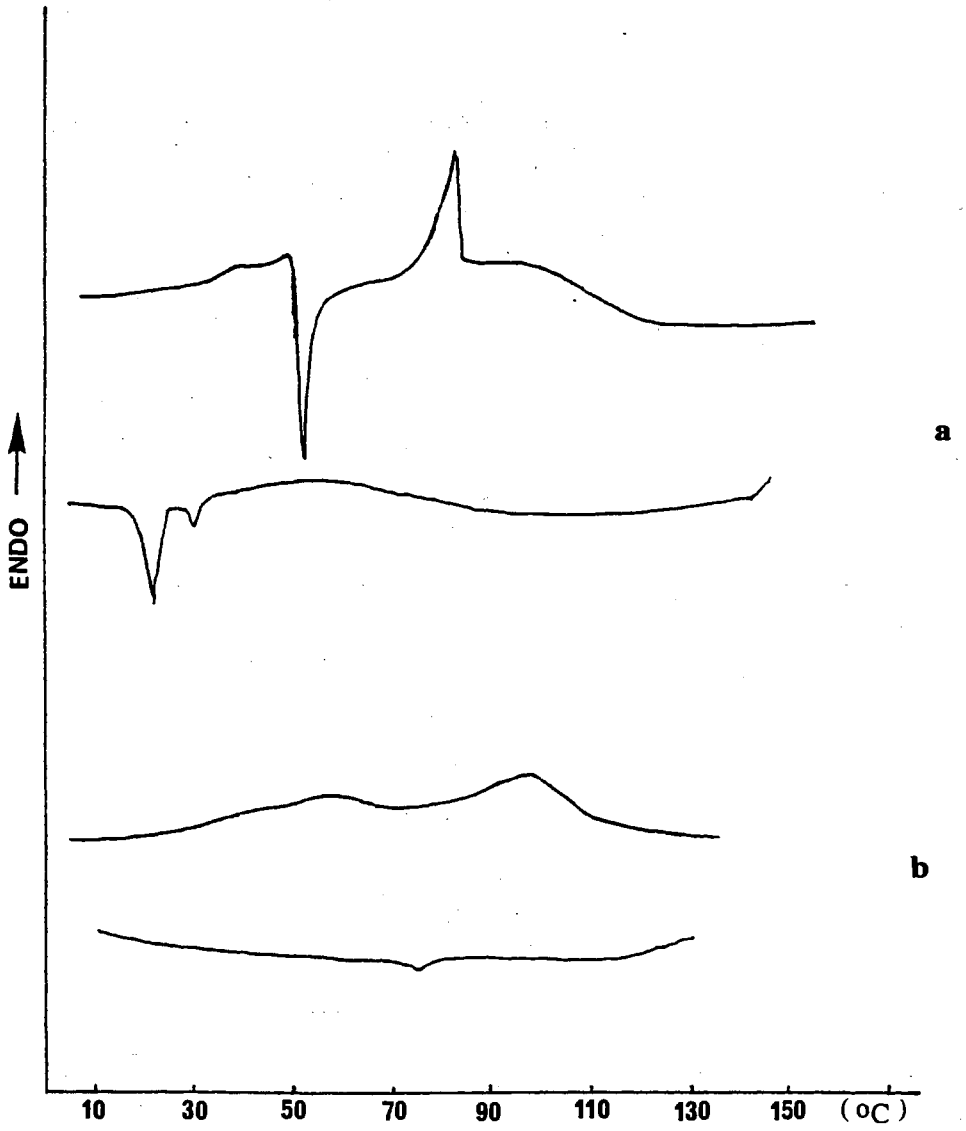

Figure 11. DSC thermograms (second run). (a) hexamine **2** complex of $Ag(O_3SCF_3)_2$; (b) hexamine **2** complex of $FeCl_3$.

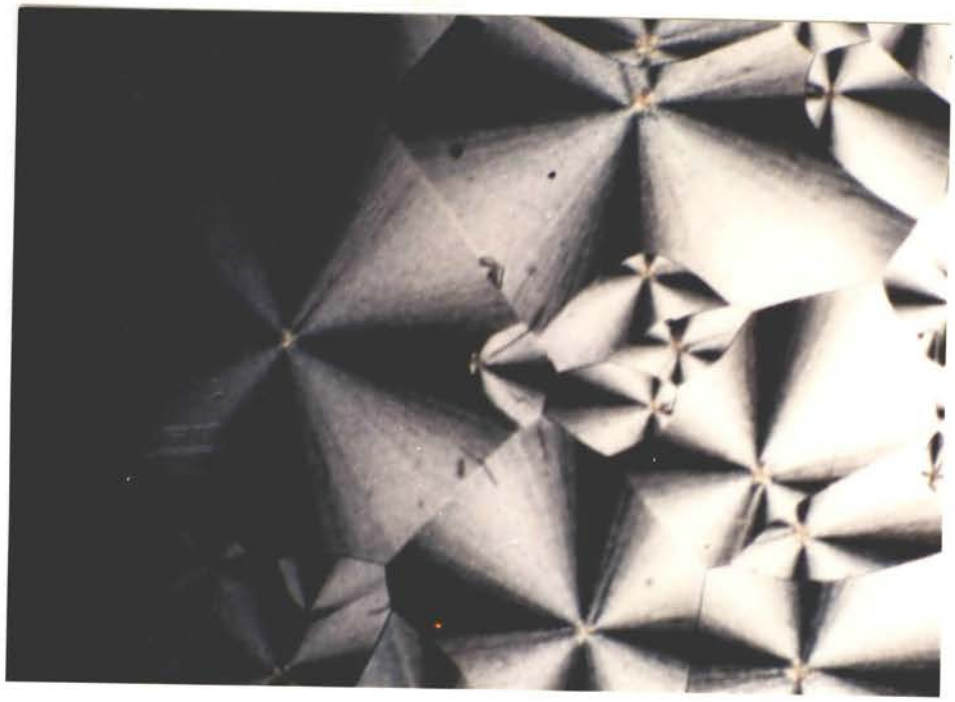

Figure 12. Polarizing micrograph of the texture of hexamine **2**, cooled from the 100 °C isotropic melt to 30 °C.

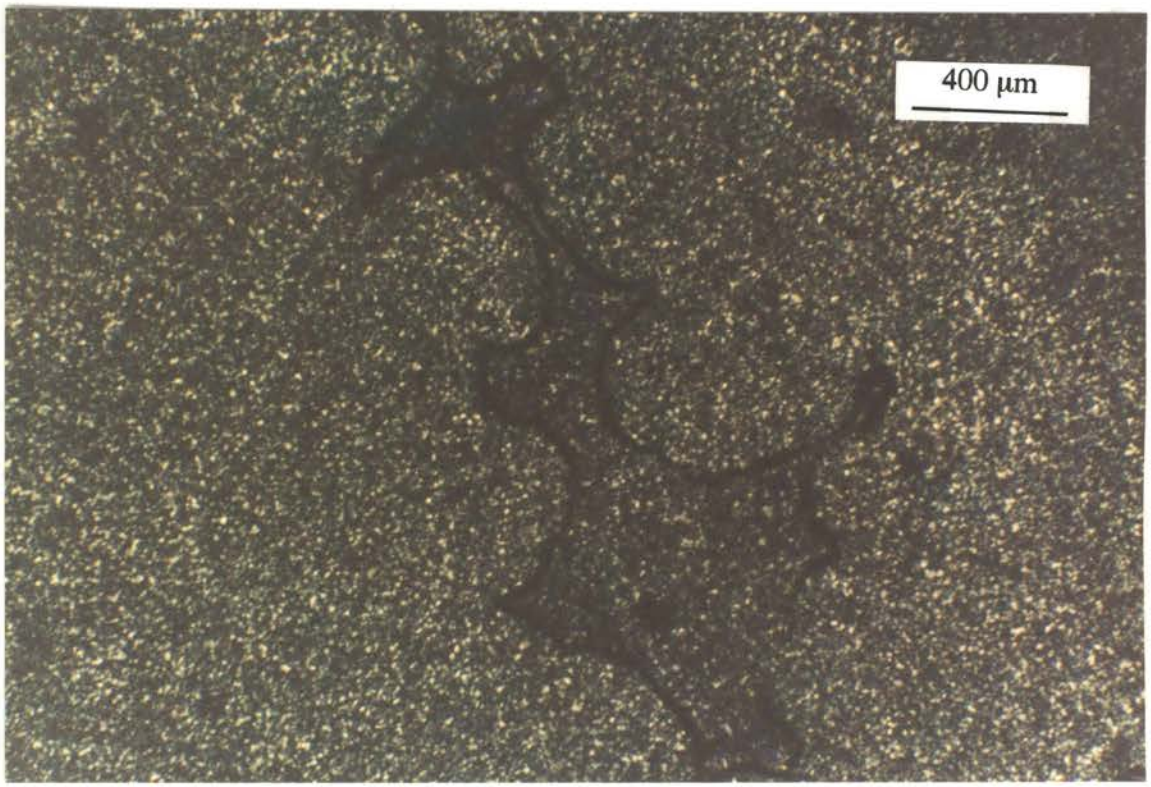

Figure 13. Polarizing micrograph of the hexamine **2** complex of $Mg(O_3SCF_3)_2$ heated from the isotropic melt to 70 °C.

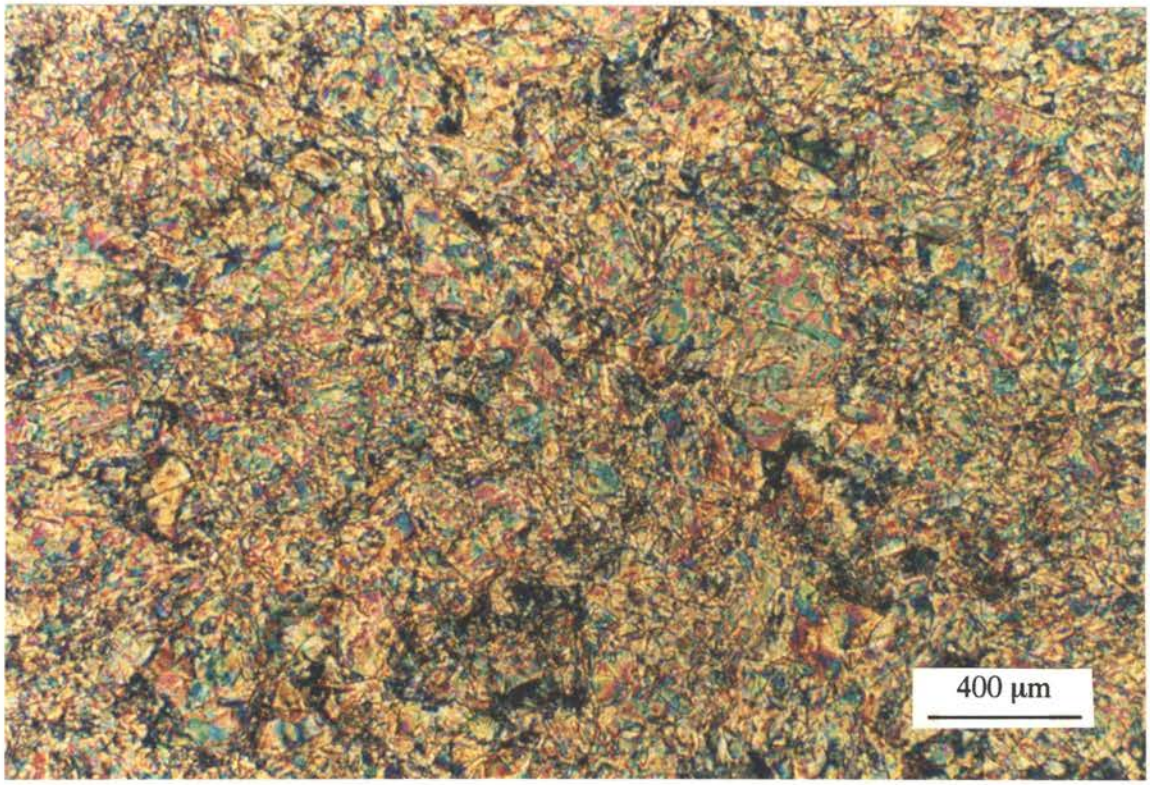

a

Figure 14. Polarizing micrographs of hexamine **2** complex of $CoCl_2$. (a) before heating at 20 °C; (b) cooling from the isotropic melt 100 °C to 80 °C; (c) cooling to 75 °C; (d) cooling to 60 °C; (e) cooling to 50 °C.

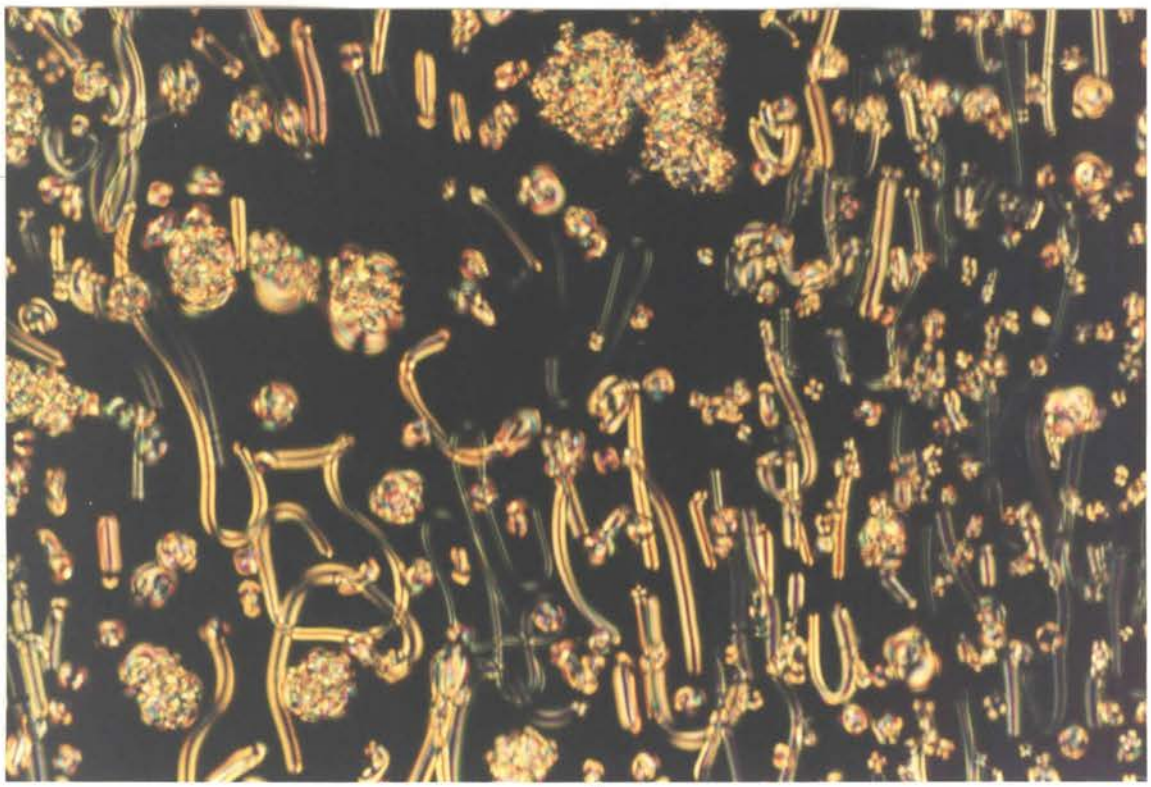

b

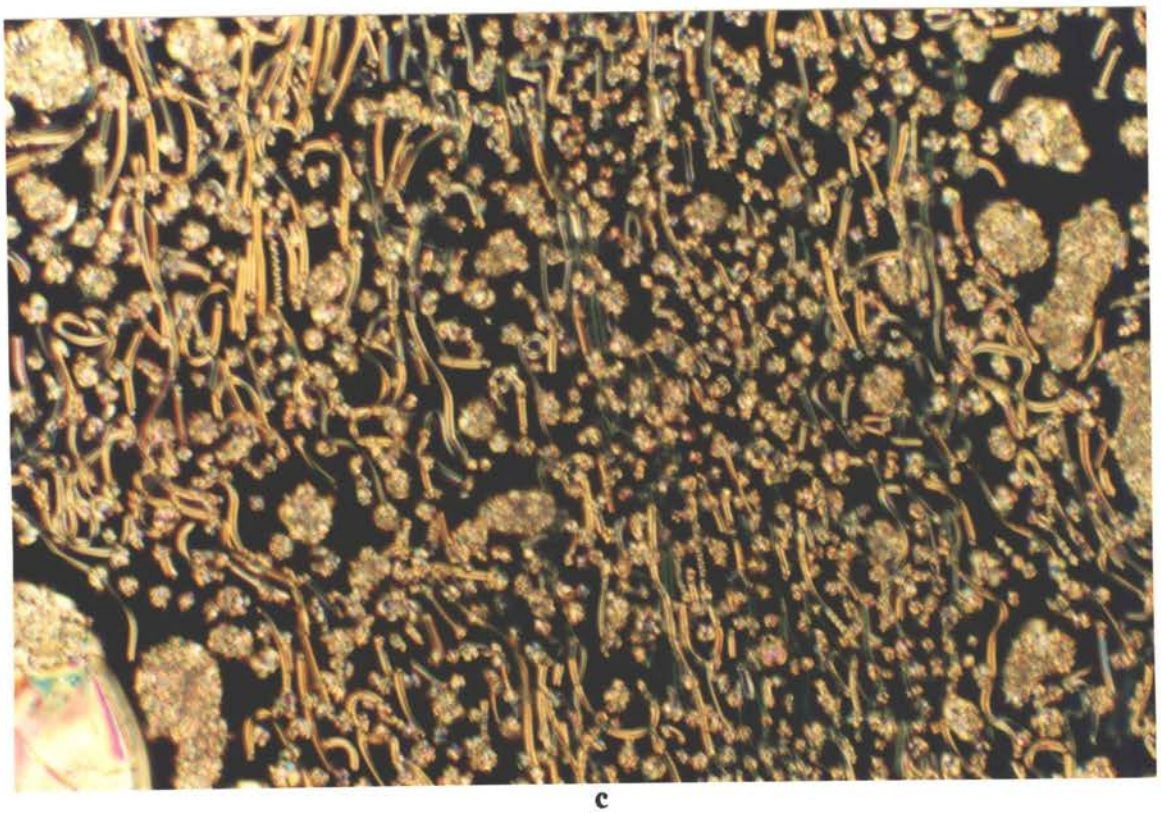

c

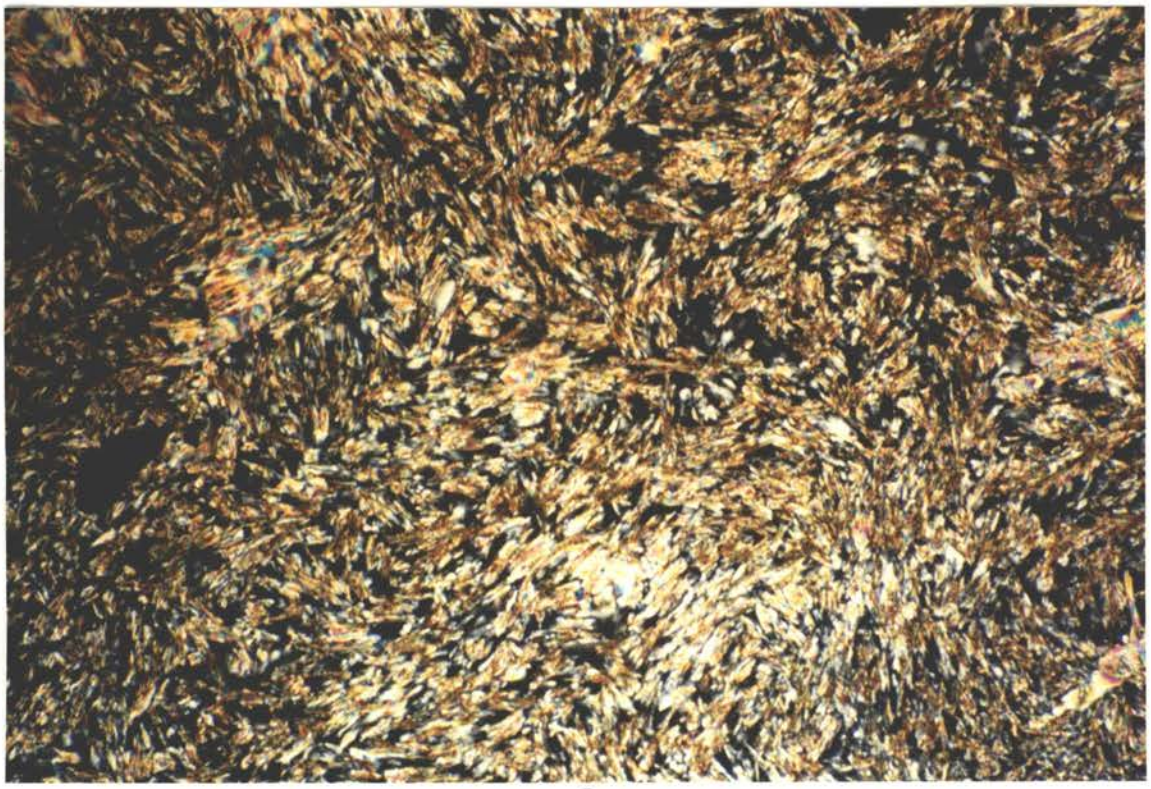

d

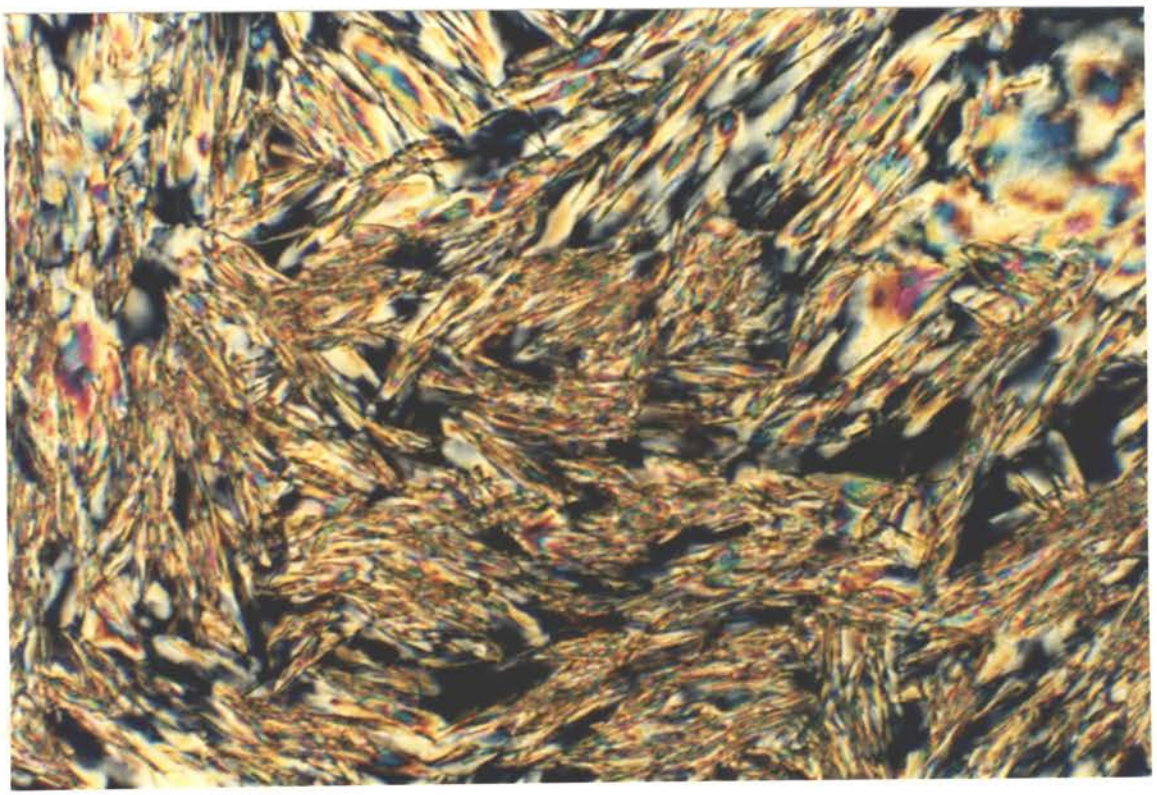

e

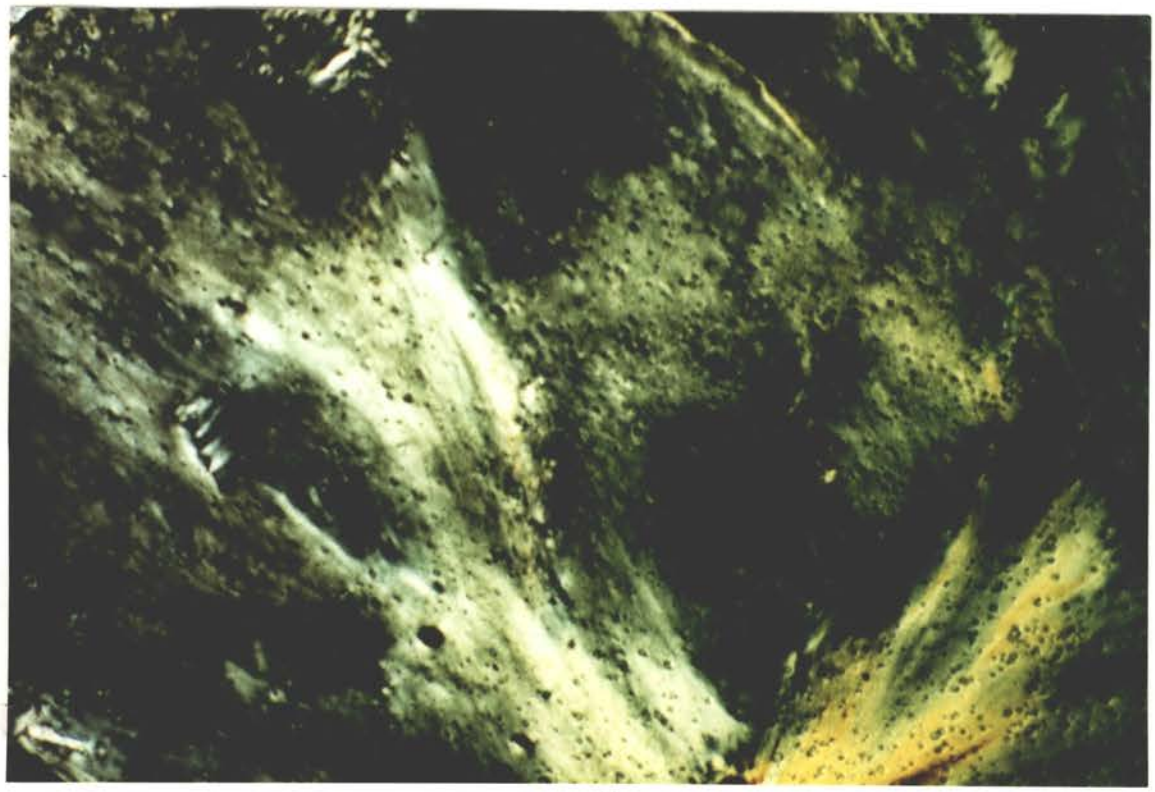

a

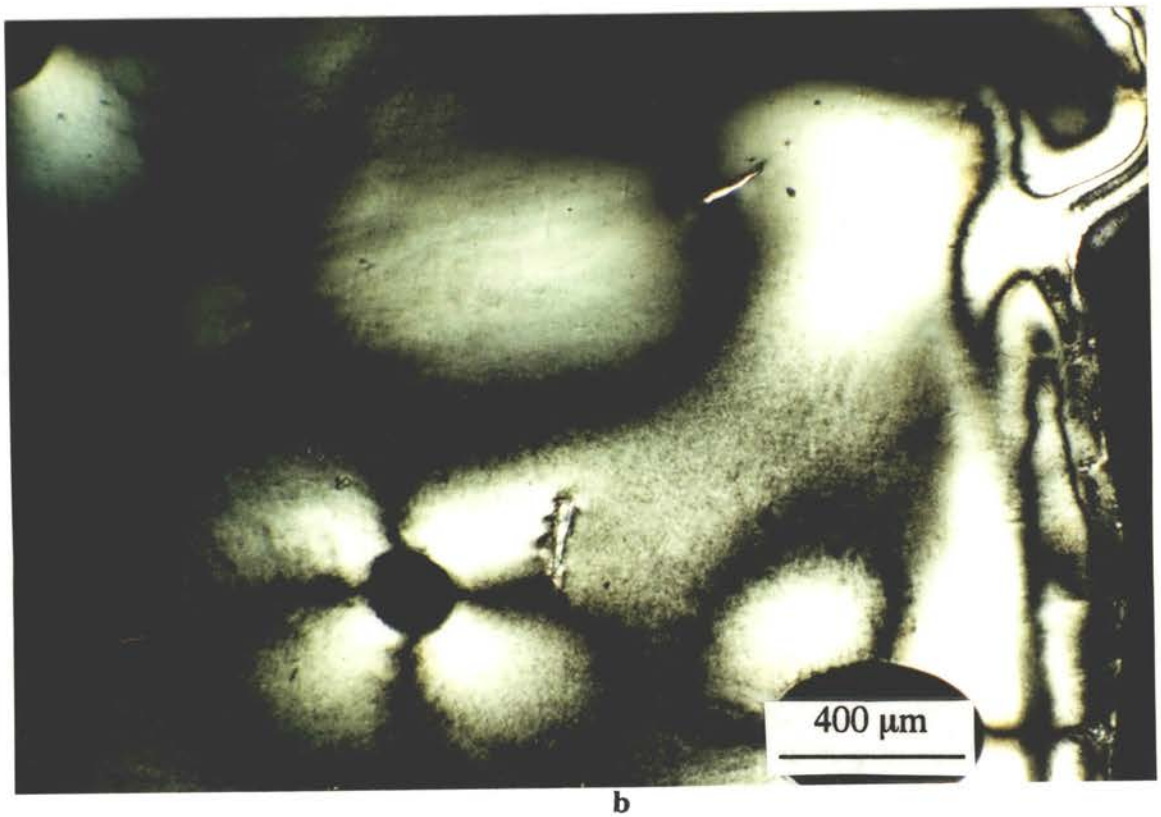

b

Figure 15. Polarizing micrographs of the hexamine **2** complex of $Cu(O_2CCH_3)_2$. (a) before heating, at 20 °C; (b) after cooling from the isotropic melt 100 °C to 20 °C.

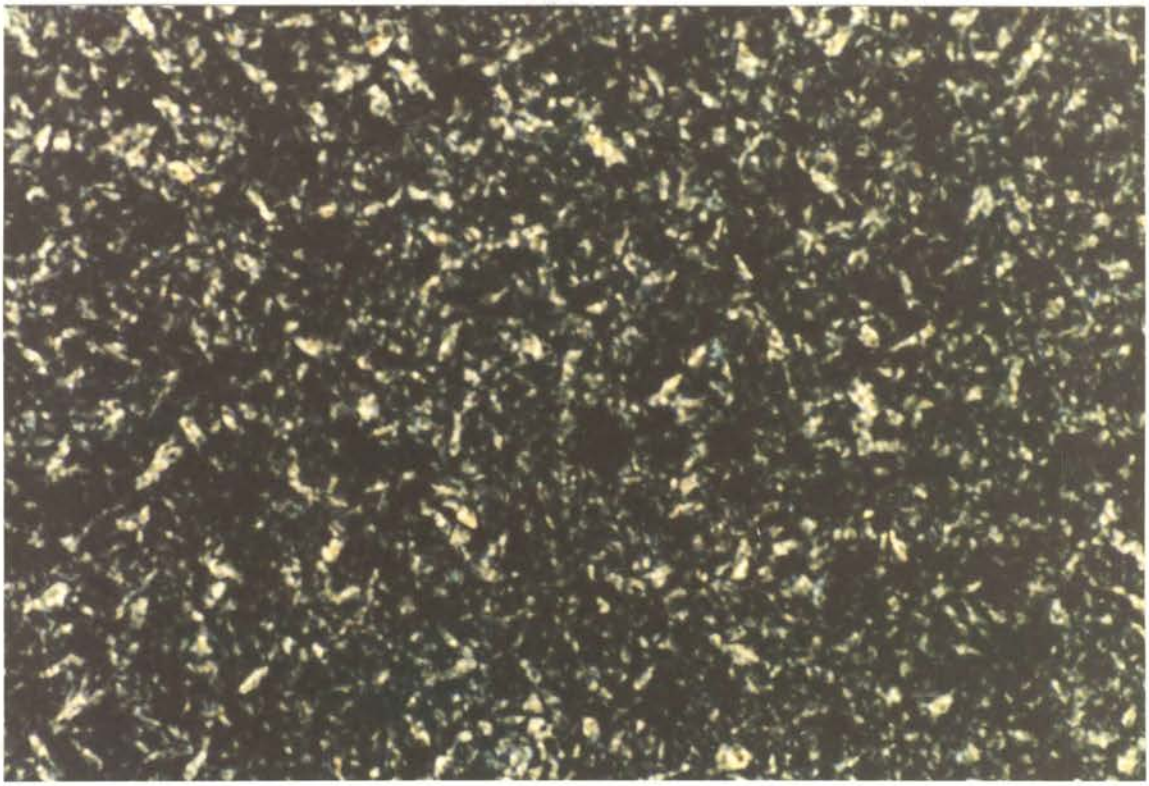

Figure 16. Polarizing micrograph of the hexamine **2** complex of $Zn(O_3SCF_3)_2$ heated to 65 °C.

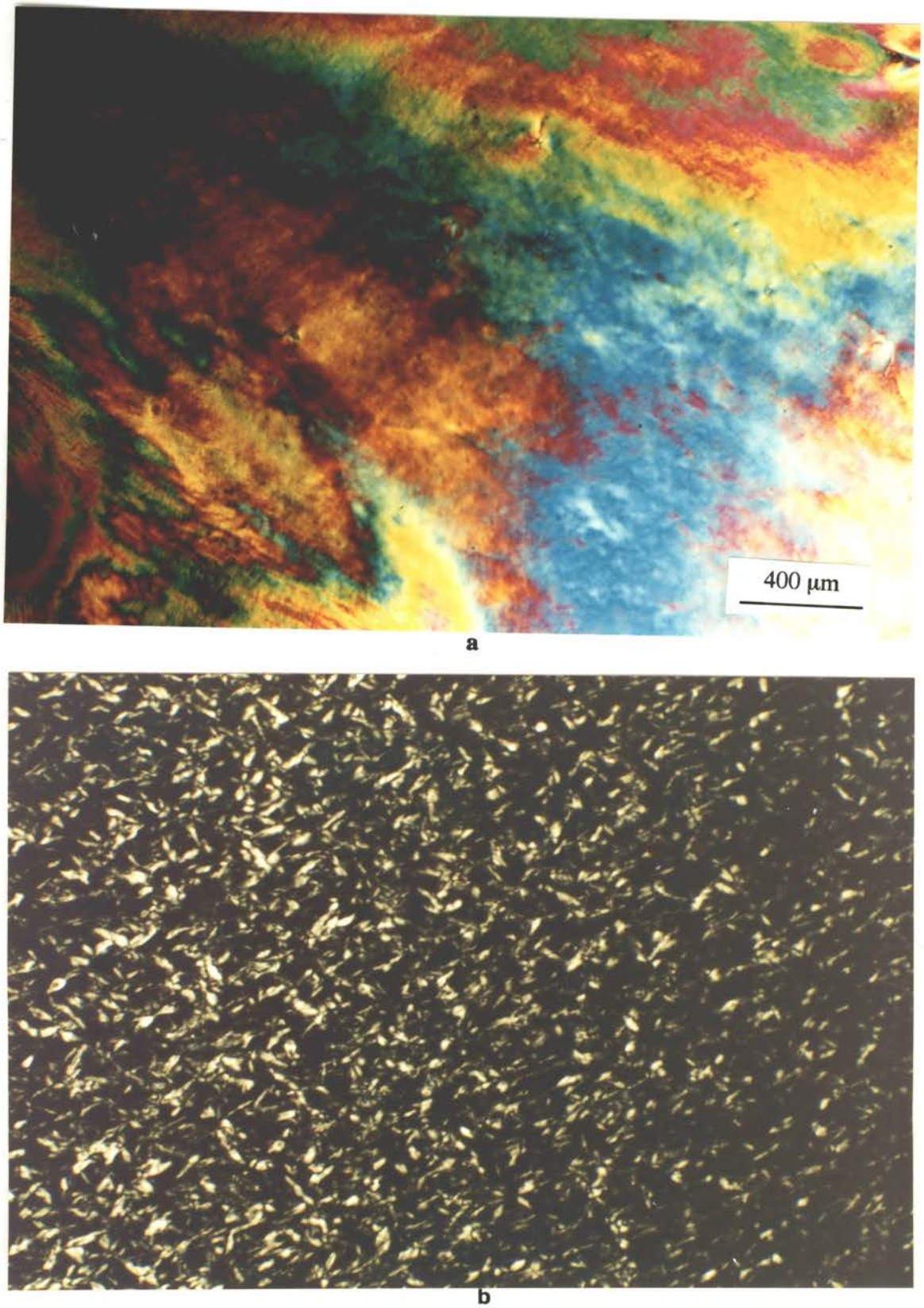

Figure 17. Polarizing micrographs of the hexamine **2** complex of $Pd(O_2CCH_3)_2$ (1:1). (a) before heating, at 20 °C; (b) heated to 70 °C.

$Mg(O_3SCF_3)_2$. At room temperature the complex is a white waxy solid. Unlike free hexamine **2**, which is a white crystal, the complex of $Mg(O_3SCF_3)_2$ can be pressed between two glass slides and shows green and yellow birefringence. The mesophase of the complex is quite clear in the second heating, as shown in Figure 13. The picture shows the liquid crystal was still flowing. The texture was similar to the mesophase texture reported by Lehn for hexamide **1**.[1]

$FeCl_3$. At room temperature the complex was a yellow waxy solid with a birefringent texture like that of Figure 15a but in yellow color. The texture obtained at 80 °C during the second heating looks like the mesophase texture of hexamide **1**.

$CoCl_2 \cdot 6H_2O$. The complex is a white paste-like solid and showed colorful birefringence at room temperature (Figure 14a). The rope-like texture of the mesophase is very interesting, which seems not have been reported before (Figure 14b,c). The liquid crystalline properties of this complex are very clear. The ^1H NMR spectrum of the complex shows larger chemical shifts because Co^{2+} is paramagnetic.

$Cu(O_2CCH_3)_2$. The complex is a green waxy solid before heating and shows green birefringence under the polarizing microscope (Figure 15a). Figure 15b shows a typical nematic schlieren texture for the hexamine **2** complex of copper acetate, which is similar to the nematic texture reported by Ringsdorf's group for the $Co(NO_3)_2$ complex of the macrocyclic compound analogous to **2** having C_{14} side chains.[13] The mesophase was not thermally stable, and it disappeared from the DSC thermogram after about five heating scans.

$Cu(O_3SCF_3)_2$. At room temperature the complex of 1:1 $Cu(O_3SCF_3)_2$/**2** was a dark green waxy solid, which could be pressed to flow between two glass slides and showed a green nematic texture like that of Figure 15b. After cooling from the isotropic melt the sample changed to an isotropic glass without birefringence, but the birefringence

appeared after about 24 h at room temperature. It seems that the complex needs longer time for organization to an ordered structure. The complex of 0.5 : 1 $Cu(O_3SCF_3)_2$/**2** at 25 °C was a light green solid, which could not be pressed to flow between two glass slides but showed a green birefringence. The texture obtained by cooling from the isotropic phase was like the mesophase texture of hexamide **1**.

$Zn(SO_3CF_3)_2$. The complex was a white gel-like solid, which showed green birefringence under the polarizing microscope with a texture like Figure 15a. The second heating led to a texture similar to that of hexamide **1** as shown in Figure 16.

$Pd(O_2CCH_3)_2$. The complex was a yellow waxy solid at 25 °C, which could be pressed to flow between two glass slides, and showed colorful birefringence under the polarizing microscope (Figure 17a). There is a mesophase during the first heating (Figure 17b). The second heating shows only an isotropic phase transition. The texture observed during the cooling was similar to the mesophase texture of hexamide **1**.

AgO_3SCF_3. At room temperature the complex was a red waxy solid, which showed a texture like that of Figure 15a but in a red color. In the DSC thermogram the complex showed a phase transition during cooling, but it could not be observed with the microscope. It might be decomposed after exposure to light.

One thing clear for all these complexes is that most virgin samples were not crystals but waxy solids with liquid crystalline properties, as shown by flow between two pressed glass slides and birefringence. After cooling from the isotropic melt usually a texture similar to that of hexamide **1** was observed, except for the $CoCl_2$ and $Cu(O_2CCH_3)_2$ complexes.

The DSC thermograms of complexes of $Cu(O_2CCH_3)_2$, $Pd(O_2CCH_3)_2$, $Cu(O_3SCF_3)_2$ (0.5:1) and AgO_3SCF_3 showed a crystallization exotherm in the second heating. It is an evidence of the slow organization processes of the complex molecules.

High viscosity made the phase transitions slow or incomplete. The complexes of $Mg(O_3SCF_3)_2$, $Zn(O_3SCF_3)_2$ and $FeCl_3$ showed similar DSC thermograms and textures. Some mesophases had deep colors and were not easy to observe by polarizing microscope. The identification of the mesophases of metal complexes is more difficult than of free organic liquid crystalline compounds because of the slow phase transitions.[16] Most textures of the complexes of hexamine **2** were not easy to identify. While it is hard to assign these mesopheses without X-ray evidence, most of these complexes probably have nematic phases, since the phase transitions between the mesophase and the isotropic phase showed only small enthalpy changes by DSC analysis. X-ray investigation will be most useful to characterize the mesophases.

Conclusions

Metal complexes of macrocyclic hexamine **2** with Cu^{2+}, Zn^{2+}, Mg^{2+}, Ag^{+}, Co^{2+}, and Fe^{3+} salts were prepared. The liquid crystalline properties of these complexes were examined by differential scanning calorimetry and polarizing microscopy. Unlike free hexamine **2**, which is a non-liquid crystalline compound, most of these complexes showed mesophases. The complexes of $CoCl_2$ and $Cu(OAc)_2$ showed the most interesting microscopic textures. The complexes were more easily decomposed thermally than free hexamine, and the phase behaviors were affected by thermal history. The high molecular weight and high viscosity lead to slow phase transitions, as indicated by the crystallization during the DSC second heating and different phase behavior of the virgin samples and the samples from the isotropic melt. While it is difficult to assign the mesophases, the low values of the enthalpies of the phase transitions between the liquid crystalline and isotropic phases suggest that the mesophases may be nematic.

References

(1) Lehn, J. M.; Malthete, J.; Levelut, A. M. *J. Chem. Soc., Chem. Commun.*, **1985**, 794.

(2) Lehn, J. M. *Angew. Chem. Int. Ed. Engl.* **1988**. *27*, 89.

(3) Malthete, J.; Poupinet, D.; Vilanove, R.; Lehn, J. M. *J. Chem. Soc., Chem. Commun.* **1989**, 1016.

(4) Mertesdorf, C.; Ringsdorf, H. *Liq. Cryst.* **1989**, *5*, 1757.

(5) Tatarsky, D.; Banerjee, K.; Ford, W. T. *Chem. Mater.* **1990**, 138.

(6) Idziak, S. H. J.; Maliszewskyj, N. C.; Heiney, P. A.; Maccauley, J. P.; Sprengeler, P. A.; Smith, A. B. III *J. Am. Chem. Soc.* **1991**, *113*, 7666.

(7) Idziak, S. H. J.; Maliszewskyj, N. C.; Vaughan, G. B. M.; Heiney, P. A.; Mertesdorf, C.; Ringsdorf, H.; McCauley, J. P.; Smith, A. B. III *J. Chem. Soc., Chem. Commun.* **1992**, 98.

(8) Lattermann, G. *Mol. Cryst. Liq. Cryst.* **1990**, *182B*, 299.

(9) Malthete, J.; Levelut, A. M.; Lehn, J. M. *J. Chem. Soc., Chem. Commun.* **1992**, 1434.

(10) Lattermann, G.; Schmidt, S.; Kleppinger, R.; Wendorff, J. H. *Adv. Mater.* **1992**, *4*, 30.

(11) Mertesdorf, C.; Ringsdorf, H. *Mol. Eng.* **1992**, (in press).

(12) Izatt, R. M.; Bruening, R. L.; Tarbet, B. J.; Griffin, L. D.; Bruening, M. L.; Kradowiak, K. E.; Bradshaw, J. S. *Pure Appl. Chem.* **1990**, *62*, 1115.

(13) Liebmann, A.; Mertesdorf, C.; Plesnivy, T.; Ringsdorf, H.; Wendorff, J. H. *Angew. Chem. Int. Ed. Engl.* **1991**, *30*, 1375.

(14) Fery-Forgues, S.; Bourson, J.; Dallery, L.; Valeur, B. *New J. Chem.* **1990**, *14*, 617.

(15) Tsukube, H.; Adachi, H.; Morosawa, S. *J. Polym. Sci.: Polym. Chem.* **1990**, *28*, 437.

(16) Giroud-Godquin, A-M., Maitlis, P. M. *Angew. Chem. Int. Ed. Engl.* **1991**, *30*, 375.

CHAPTER IV

EXTRACTION AND MEMBRANE TRANSPORT OF CATIONS BY AZACROWN[18]-N_6 DERIVATIVES

Introduction

In recent years research interest in azacrown[18]-N_6 derivatives has increased and different compounds have been synthesized.[1-11] The complexation properties of these new compounds are one of the major research objectives. What kind of metal ions will be complexed by these macrocyclic ligands? How are their binding properties different from oxygen-containing crown ethers? Some azacrown[18]-N_6 compounds have been studied by extraction and liquid membrane methods.[12-26] It was found that unlike crown ethers, which complex mainly with alkali or alkaline-earth metals, azacrown hexamines showed strong affinity for transition metal cations but not alkali or alkaline-earth metal cations. Azacrown hexamides complex with almost no metal ions.

In Chapter II we reported the synthesis and liquid crystalline properties of some azacrown[18]-N_6 derivatives. In this chapter we report the complexation of metal cations and organic cations by hexamides **1** and **2** and hexamine **3**. The complexing properties were studied by extraction and liquid membrane methods. For comparison a typical crown ether, i.e., dibenzo-18-crown-6 (DB-18-C-6) and the [14]-N_4 tetraamide **4** were also examined.

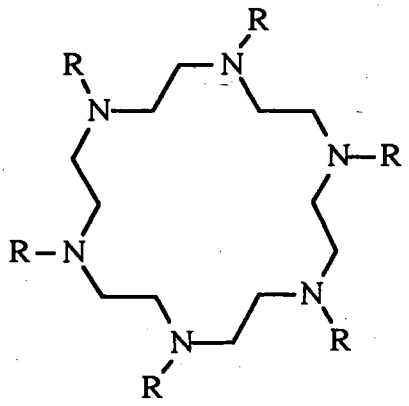

1: R = 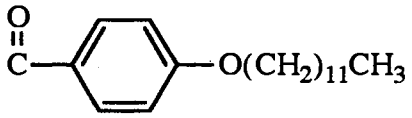

2: R = 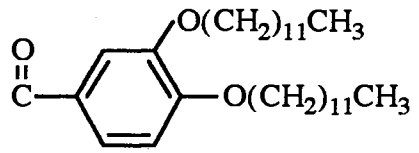

3: R = 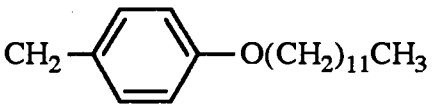

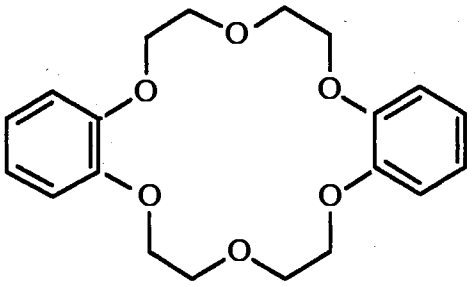

DB-18-C-6

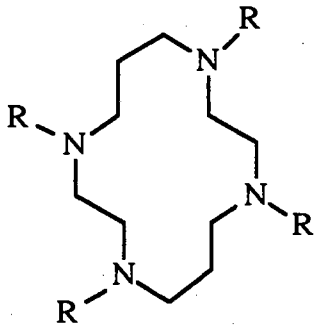

4: R = 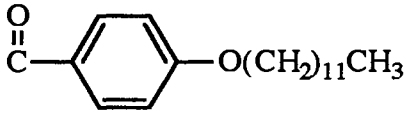

Experimental Section

Reagents. Reagent grade metal salts and dibenzo-18-crown-6 were obtained from Aldrich and used without further purification. Macrocycles **1**, **2**, **3**, and **4** were prepared as reported in Chapters II and III. Glycine ethyl ester hydrochloride (GlyOEt·HCl) and *L*-phenylalanine ethyl ester hydrochloride (PheOEt·HCl) were from Sigma. The aqueous

picric acid solution was made from Baker analyzed reagent (crystal with 12.2% water), and the concentration was determined with a standardized solution of sodium hydroxide (Chempure, Curtin Matheson Scientific). UV spectra were recorded on a Hewlett Packard 8452A Diode Array spectrophotometer with 1 cm quartz cells.

Extractions. The cation binding efficiencies of the macrocycles were evaluated by the distribution equilibrium of the picrate salts between an aqueous phase and chloroform that contained macrocycle. The deionized water was decarbonated by boiling and was saturated with chloroform in order to minimize the volume change on mixing. Chloroform was saturated with water before the experiment. The aqueous picric acid solution (0.1 mM) containing metal salt (10.0 mM) was made by dissolving metal salt (for example 58.4 mg of NaCl) into 100 mL of 0.1 mM picric acid solution. The pH of the picric acid-metal salt solution was adjusted with a pH meter from about 4.0 to 5.0 by adding a few drops of aqueous tetramethylammonium hydroxide (Aldrich).

To 5 mL of chloroform solution of the macrocycle (1.0 mM, for hexamine **3**, 190.5 mg/100 mL $CHCl_3$) was added 5 mL of an aqueous picric acid solution (0.1 mM) containing metal salt (10.0 mM). After efficient agitation by a Wrist-Action shaker for 20 min at 23.0 ± 1 °C, the concentration of picrate in the aqueous phase was determined spectrophotometrically. The picrate anion in water has its absorption maximum at 355 nm, and the extinction coefficient of aqueous picric acid was determined as $\varepsilon = 1.45 \times 10^4$ cm^{-1} M^{-1} at 355 nm. The extinction coefficient of picrate in chloroform varies with cation. The amount of picrate in chloroform was calculated from the difference of concentration of the aqueous phase before and after extraction. The amounts of picrate salts transferred to the chloroform phase in the absence of macrocycles were negligibly small. The extractability (f) was determined as follows:

$$f = 100 ([C_o] - [C]) / [C_o] = 100 (A_o - A) / A_o$$

where $[C_o]$ and [C] are the concentrations of picrate salts in the aqueous phase before and after extraction, respectively. The ratio of concentrations can be determined by the UV-visible absorption at 355 nm, and A_o and A are the absorbances of picrate salts in the aqueous phase before and after extraction. For example the absorbances of sodium picrate solution before and after extraction with hexamine **3** in chloroform were 1.43 and 1.08, so

$$f = 100\ (1.43 - 1.08) / 1.43 = 24.5\%$$

In another two measurements the f values were determined as 25.7% and 28.4%. Previous Tsukube investigations have found such data reproducible to 10-15%.[21,26]

Liquid Membrane Transport. The transport abilities of macrocycles for inorganic and organic cations were evaluated by a liquid membrane method. The experiments were performed at 23 ± 2 °C in a U-tube glass cell as shown in Figure 1. The internal diameter of the cell is 1.6 cm. The height of the aqueous layer is 2.4 cm and the height of the chloroform layer is 2.6 cm. Each interfacial area between two phases is about 2 cm^2, which was not affected by stirring. The macrocycle in chloroform (1.0 mM, 12 mL) was placed in the base of the U-tube, and aqueous phase I (source phase, 5 mL, the same aqueous solution containing 10.0 mM salt and 0.1 mM picric acid as in extraction experiments, pH 5.0) and aqueous phase II (receiving phase, 5 mL blank water, pH 7, 3 or 11) were placed in the arms of the U-tube. The membrane phase was stirred at constant speed of 500 rpm by a magnetic stirrer (VWR Scientific Co., model 400HPS). If the stirring speed was too high some liquid droplets of aqueous phase I would be mixed with organic phase and directly contacted with phase II. Magnetic stirring bars with a star head (Nalgene 6000) were used, and liquid motion was seen in both aqueous and organic phases. This same apparatus was used for all experiments. At the aqueous phase I-membrane interface, the macrocycle extracts metal picrate into the membrane. At the membrane-aqueous phase II interface, the metal picrate is released into aqueous phase II. Metal picrates are more soluble in chloroform than metal chlorides or nitrates. In a control

experiment without macrocycle in chloroform no picrate ion was detectable in aqueous phase II. The change in pH of aqueous phases I and II after the transport process was ≤0.2 units.

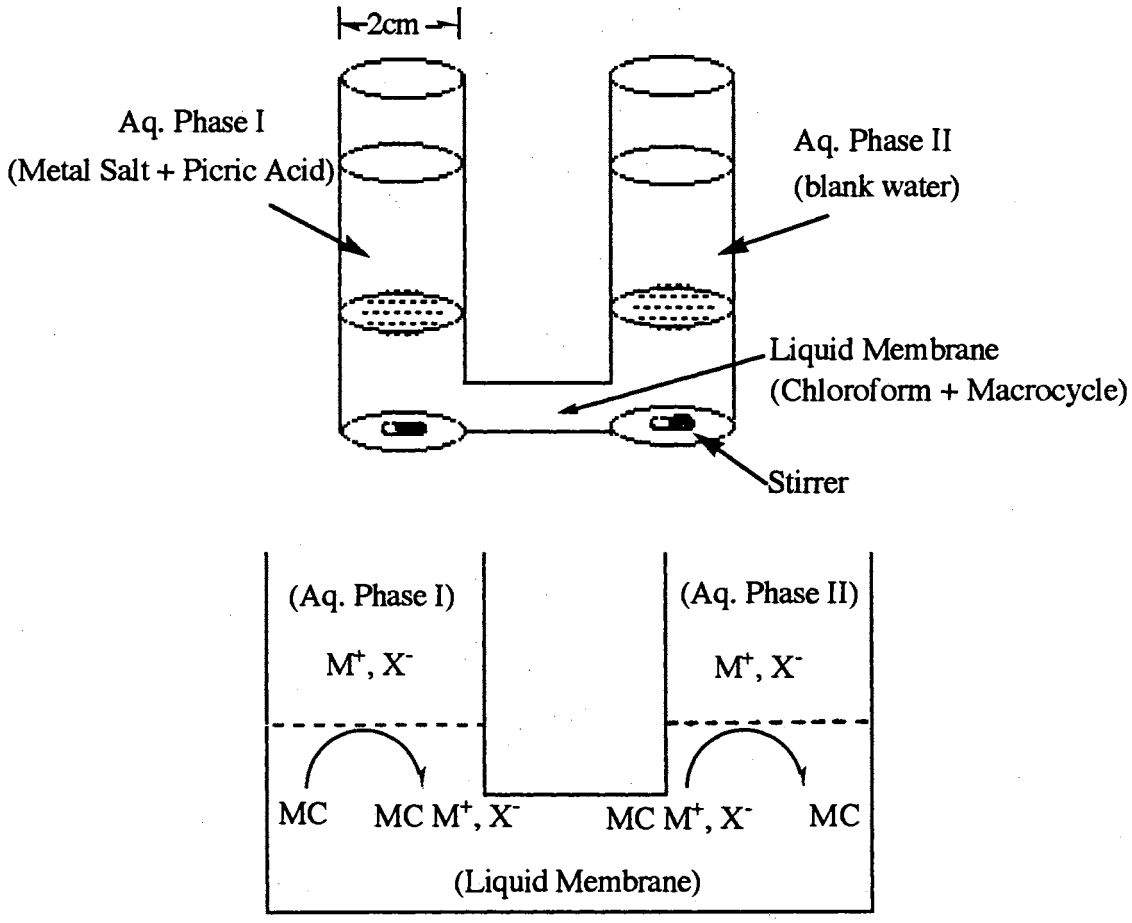

Figure 1. The U-tube and liquid membrane system for transport experiments. M^+: guest metal cation; X^-: co-transported anion; MC: macrocycle.

After stirring for one hour the transport was stopped and the UV absorbances of aqueous phases I and II (A_I and A_{II}) were measured. The distribution percentage of metal picrate in phase I; phase II and organic phase was calculated. The transport rates were expressed as the amount of picrate salts in the aqueous phase II after 1 h stirring. For example, in a potassium picrate/DB-18-C-6 experiment, after 1h the absorbance of aqueous phase I decreased from 1.45 (A_o) to 0.59 (A_I) and the absorbance of phase II increased from zero to 0.653 (A_{II}), so the concentration of picrate anion [Pic^-] in the aqueous phase II, which was also the concentration of K^+, can be calculated as

$$[Pic^-] = 0.653 / (1.45 \times 10^4\ cm^{-1}\ M^{-1} \times 1\ cm) = 0.0450\ mM$$

so the amount of transported $Pic^- K^+$ is:

$$0.0450\ mmol/L \times 5/1000\ L = 0.225 \times 10^{-3}\ mmol$$

and the distribution percentage of $Pic^- K^+$ is:

percentage of $Pic^- K^+$ in phase I = 0.59/1.45 = 40.7%

percentage of $Pic^- K^+$ in phase II = 0.65/1.45 = 45.0%

percentage of $Pic^- K^+$ in organic phase = 100% - 40.7% - 45.0% = 14.3%

In another two measurements the A_I were determined as 0.54 and 0.57; the A_{II} were determined as 0.564 and 0.610.

Results

Extraction Experiments. The reproducibility of the extraction and liquid membrane experiments in other laboratories usually was about 10-15%.[22,26,27] Because

the amounts of macrocycles available were small, most experiments were done only once so that a large number of metal ions could be tested.

To check the possible dissolution of macrocycle **3** in water, the chloroform solution of macrocycle **3** (1.0 mM) was extracted with an equal volume of water. The UV determination showed that there was no detectable **3** in the water phase. As examples the UV spectra of pH 5 and pH 7 water extracted with hexamine **3** are presented in Figure 2.

While hexamide **1** did not show interaction with picric acid, hexamine **3** was easily protonated by picric acid as indicated by UV analysis. Figure 3 shows the spectral changes of macrocycles **1** and **3** after extraction with picric acid. The spectral change (Figure 3e) shows that picric acid was extracted by hexamine **3**. As shown in Figure 3c, no spectral change was observed for hexamide **1**, because without complexing the metal picrate does not dissolve in chloroform. No macrocycle was extracted into water at pH 5 or pH 7 in control experiments.

Since in the water-chloroform extraction system the complexing by hexamine **3** was affected by the pH of the aqueous phase, control experiments were done and the results are reported in Table I.

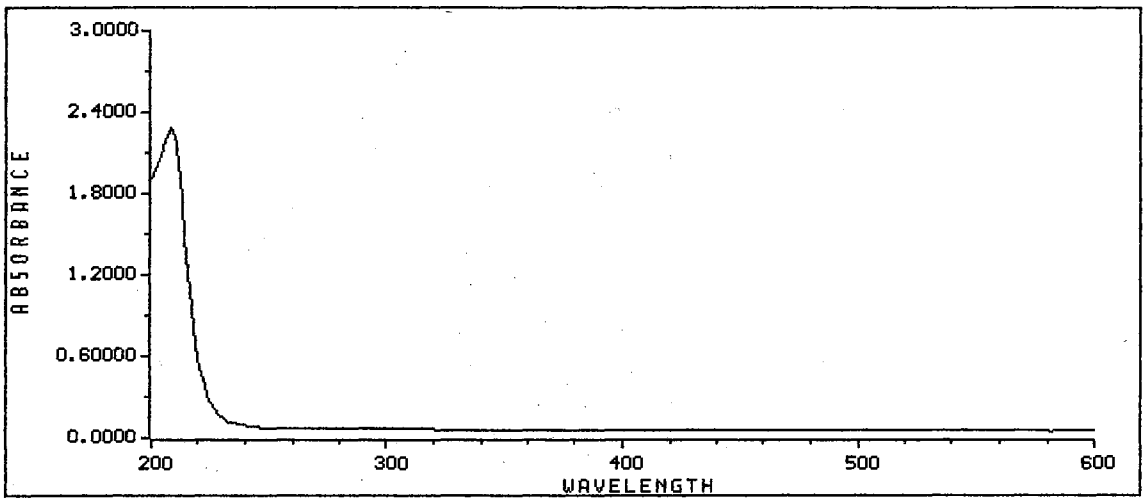

a

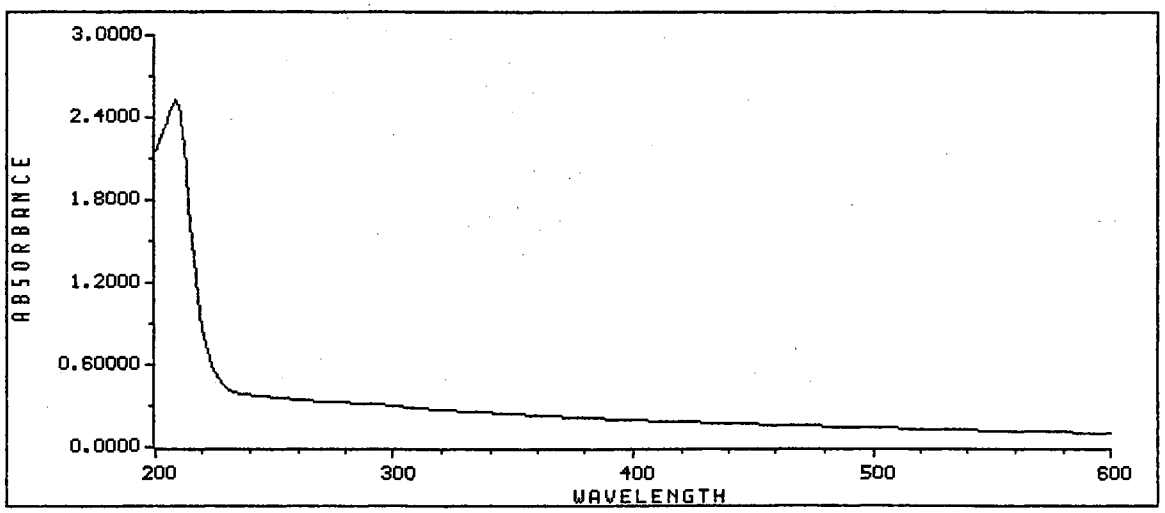

b

Figure 2. UV spectra. (a) water (pH 7) after extraction with hexamine **3**; (b) water (pH 5) after extraction with hexamine **3**.

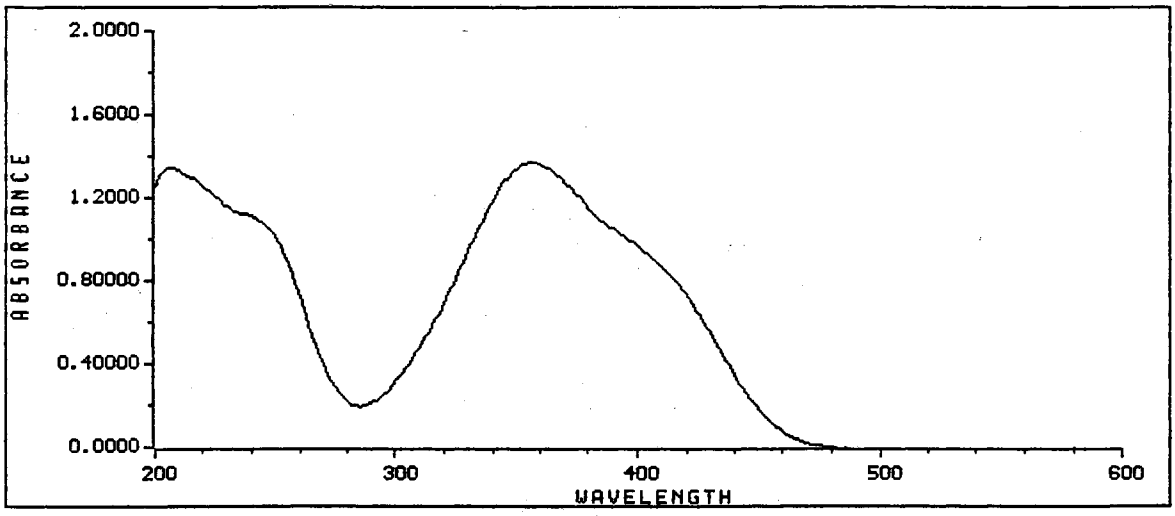

a

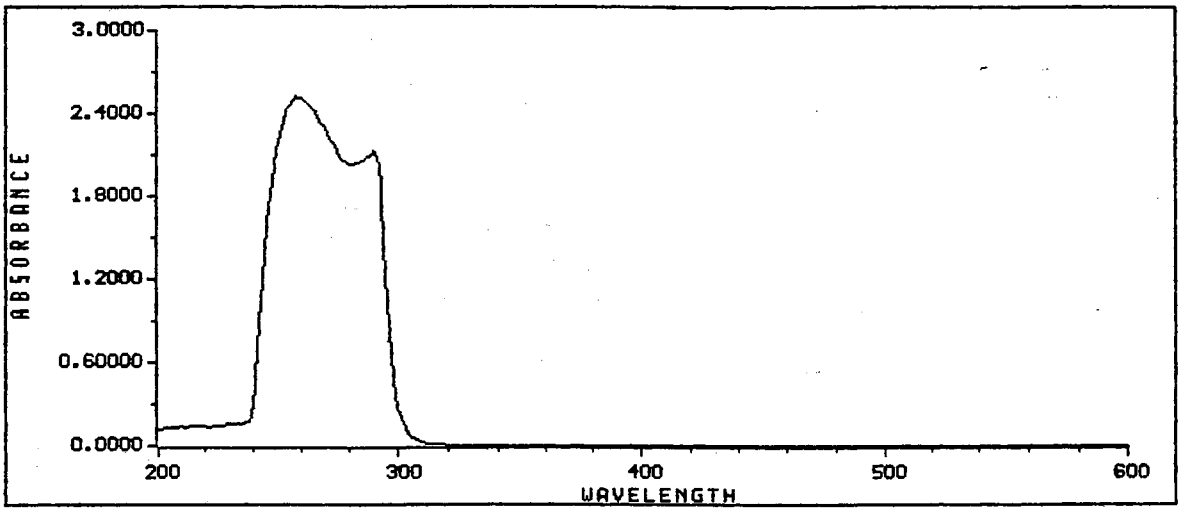

b

Figure 3. UV spectral changes of macrocycles (1.0 mM, $CHCl_3$) before and after extraction with picric acid. (a) picric acid (0.1 mM, H_2O, pH 4.2); (b) hexamide **1**, before extraction; (c) hexamide **1**, after extraction; (d) hexamine **3**, before extraction; (e) hexamine **3**, after extraction.

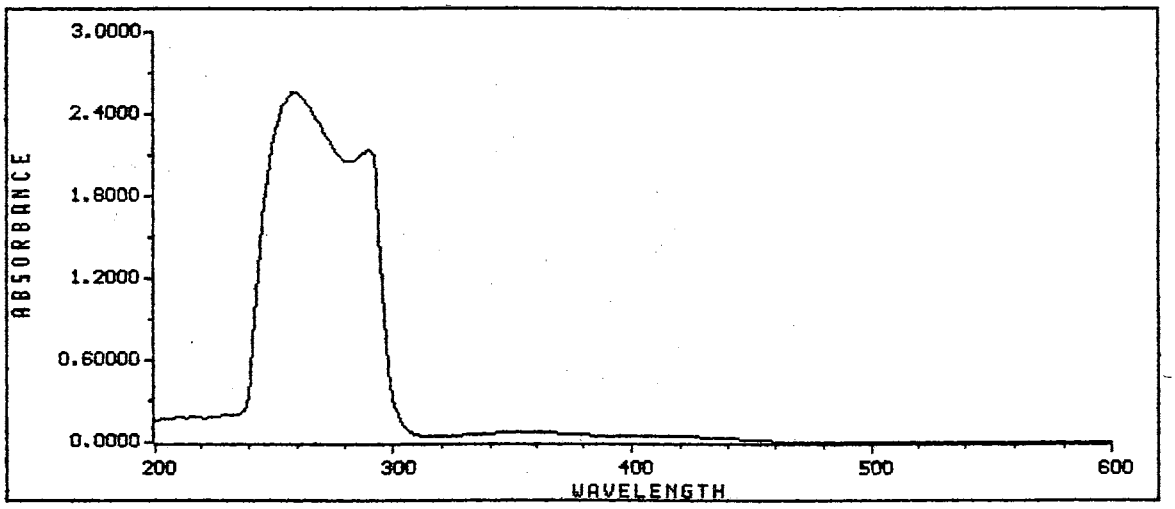
3.0000
2.4000
1.8000
1.2000
0.60000
0.0000
ABSORBANCE
200
300
400
500
600
WAVELENGTH

c

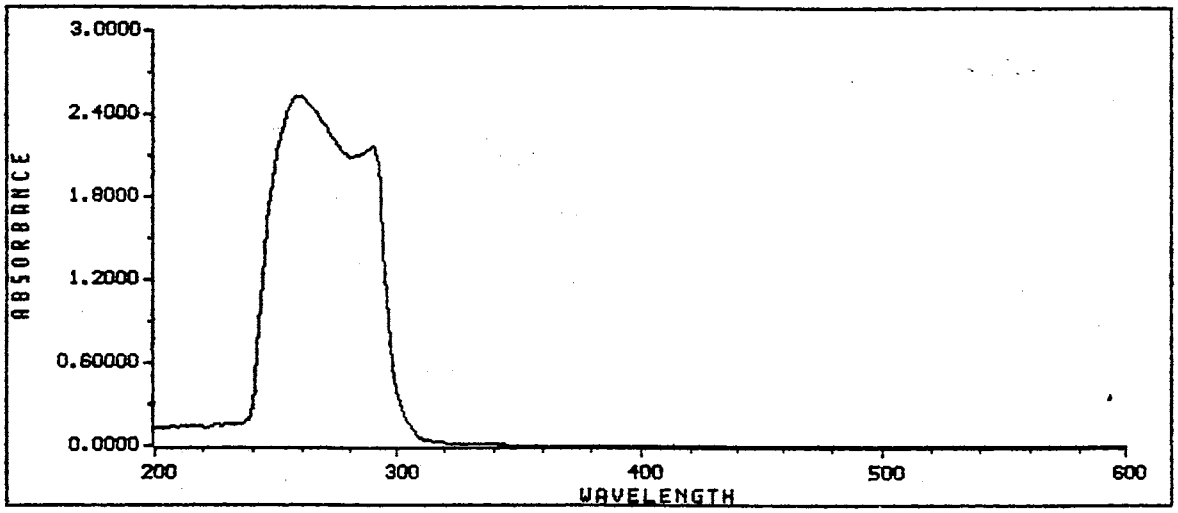
3.0000
2.4000
1.8000
1.2000
0.60000
0.0000
ABSORBANCE
200
300
400
500
600
WAVELENGTH

d

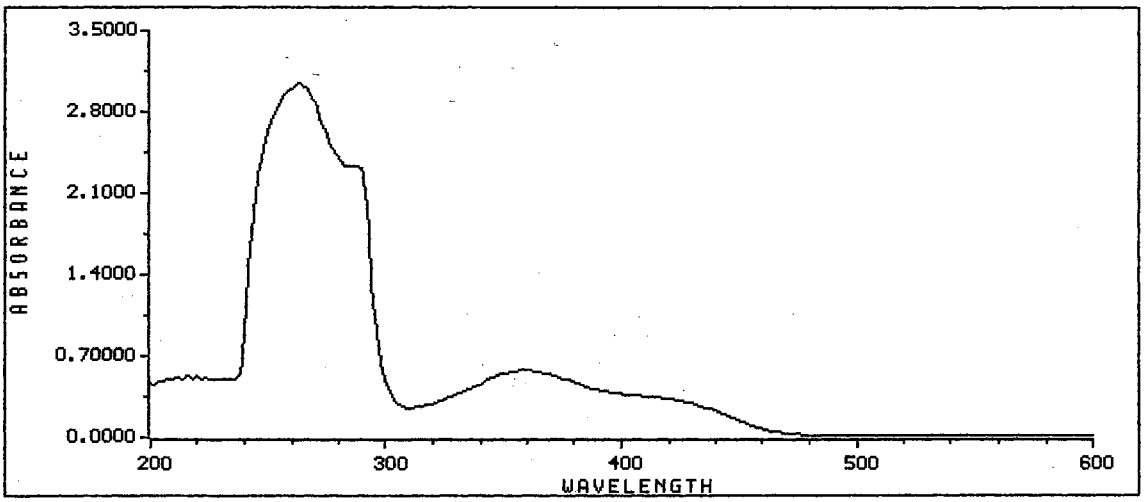

e

Table I. Absorbance of Picric Acid after Extraction with Hexamine **3** in $CHCl_3$[a]

UV absorbance (at 355 nm)	pH of aqueous phase 4.2	5.0	6.0	7.0	8.0	9.0	10.0
A (aqueous)	0.60	0.93	1.02	1.03	1.06	1.15	1.32
A (organic)	0.56	0.37	0.37	0.36	0.33	0.18	0.05
extractability (f), % [b]	58	35	28	28	25	19	7

[a] Extraction conditions: 5 mL of 1.0 mM hexamine **3** in chloroform, and 5 mL of 0.1 mM aqueous picric acid; pH was adjusted with $^{-}(CH_3)_4NOH$ before extraction. [b] ± 15% estimated error.

It is clear that the extraction of picric acid by hexamine **3** decreases with the increase of pH. For determination of the extractability of the metal cations the extraction experiment should be done with the aqueous phase of controlled and lower pH value, since some metal cations, such as Cu^{2+} and Pb^{2+}, may be precipitated from solution if pH is higher than 6. So pH 5 was used for all other extraction experiments. The calculated extractabilities of metal picrates by macrocycles are reported in Table II.

Liquid Membrane Experiments. The transport process was followed by monitoring the increase in picrate concentration in aqueous phase II spectrophotometrically at 355 nm. A typical liquid membrane experiment is presented in Figure 4. The transport rates of metal cations and amino acid ester cations obtained from liquid membrane experiments at pH 7 in aqueous phase II are reported in Table III. The transport rate was affected by the pH of the aqueous phase II (receiving phase) as reported in Table IV.

Table II. Extractability (f, %) of Metal and Organic Picrates by Macrocycles[a]

salt	cation radius[b] (Å)	hexamide 1	hexamide 2	hexamine 3	DB-18-C-6
blank(H^+)		6	9	35	5
LiCl	0.76	6	7	29	5
NaCl	1.02	7	4	26	6
KCl	1.38	4	6	21	29
$CaCl_2$	1.00	4	9	28	5
$CoCl_2$	0.75	9	6	68	8
$NiCl_2$	0.69	5	6	55	4
$CuCl_2$	0.77	8	17	99	12
$ZnCl_2$	0.74	4	6	77	5
$AgNO_3$	1.15	9	11	99	10
$CdCl_2$	0.95	5	4	57	5
$HgCl_2$	1.19	10	18	88	12
$Pb(OAc)_2$	1.19	9	10	99	11
GlyOEt		6	16	97	28
PheOEt		69	67	99	76

[a] Extraction conditions: macrocycle solution in chloroform, 5 mL (1.0 mM); aqueous solution, 5 mL (pH 5, 0.1 mM picric acid; 10.0 mM metal salt), error limits of f values are estimated to be ± 15%. [b] Ref. 13.

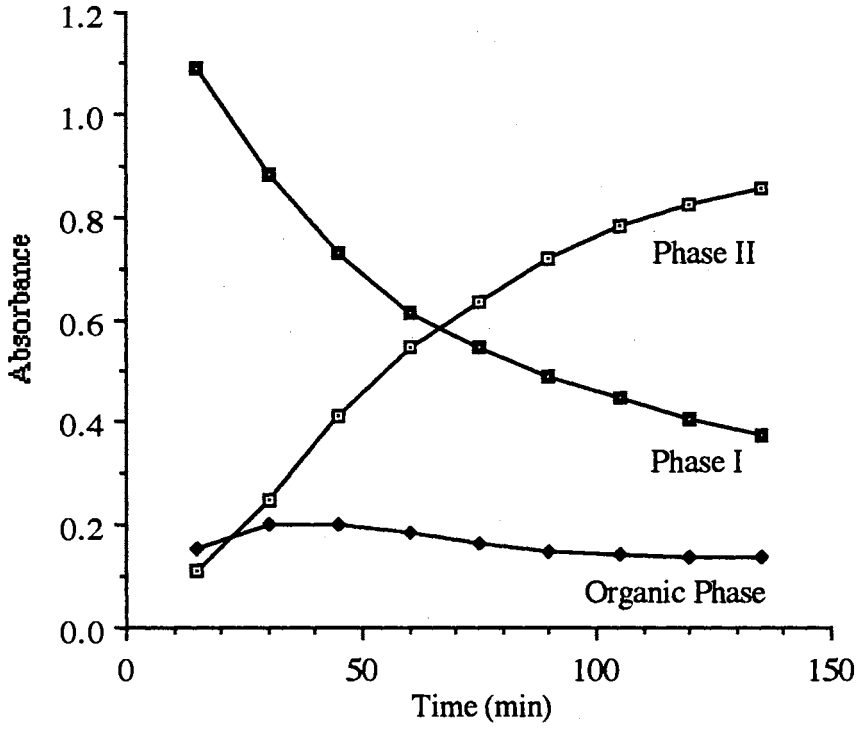

Figure 4. UV absorbance-time plot of the DB-18-C-6 / KCl liquid membrane system. Aq. phase I: 5 mL (picric acid 0.1 mM, KCl 10.0 mM, water, pH 5). Liquid Membrane: 12 mL (DB-18-C-6 1.0 mM, chloroform); Aq. phase II: 5 mL, (water, pH 7).

Table III. Transport Rates of Picrate Salts through Liquid Membranes[a]

macrocycle	metal salt	A_I	A_{II}	distribution of Pic^- (%)			transport rate[b]
				I	II	$CHCl_3$	x10^6(mmol in 1h)
Hexamide **1**							
	$HgCl_2$	1.25	0.079	86.2	5.4	8.4	27
	$CuCl_2$	1.36	0.036	93.8	2.4	3.8	12
Hexamide **2**							
	$AgNO_3$	1.25	0.083	86.2	5.7	8.1	29
	$HgCl_2$	1.24	0.060	85.5	4.1	10.4	21
	$CuCl_2$	1.27	0.038	87.6	2.6	9.8	13
	$NiCl_2$	1.37	0.031	94.4	2.1	3.5	11
Hexamine **3**							
	none	1.02	0.013	70.3	0.9	28.8	4
	$HgCl_2$	0.19	0.024	13.1	1.7	85.2	8
	$NiCl_2$	0.91	0.023	62.8	1.6	35.6	8
	KCl	1.30	0.020	89.7	1.4	8.9	7
	$CoCl_2$	0.48	0.013	33.1	0.9	66.0	4
	$CuCl_2$	0.23	0.005	15.9	0.3	83.8	2
	$Pb(OAc)_2$	0.32	0.003	22.1	0.2	77.7	1
	GlyOEt·HCl	0.31	0.002	21.4	0.1	78.5	1
DB-18-C-6							
	KCl	0.57	0.609	39.3	42.0	18.7	225
	$HgCl_2$	1.31	0.038	90.3	2.6	7.1	13
	$NiCl_2$	1.39	0.020	95.9	1.4	2.7	7
	$CuCl_2$	1.34	0.012	92.4	0.8	6.8	4

[a] Aq. phase I pH = 5; aq. phase II pH = 7. Refer to experimental section for details.

[b] Error limits of transport rate are estimated to be ± 15%.

Table IV. Transport Rates of Picrate Salts through a Liquid Membrane to pH 3 and pH 11 Aqueous Phase II[a]

macrocycle (phase II pH)	metal salt	A_I	A_{II}	distribution of Pic^- (%) phase I	phase II	phase $CHCl_3$	transport rate[b] x10^6(mmol in 1h)
Hexamine **3**							
(pH 3)	none	0.98	0.002	67.6	0.1	32.3	1
(pH 11)	none	1.06	0.005	73.1	0.3	26.6	2
(pH 3)	$HgCl_2$	0.11	0.002	7.6	0.1	92.3	1
(pH 11)	$HgCl_2$	0.17	0.005	11.7	0.3	88.0	2
(pH 3)	$CoCl_2$	0.18	0.010	12.4	0.7	86.9	3
(pH 11)	$CoCl_2$	0.44	0.132	30.3	9.1	60.6	46
(pH 11)	$CuCl_2$	0.65	0.431	44.8	29.7	25.5	149
(pH 11)	$AgNO_3$	1.00	0.006	69.0	0.4	30.6	2
(pH 11)	$Pb(OAc)_2$	0.93	0.238	64.1	16.4	19.5	82
(pH 11)	$NiCl_2$	1.30	0.036	89.7	2.5	7.8	12
(pH 11)	$ZnCl_2$	1.25	0.063	86.2	4.3	9.5	22
(pH 11)	KCl	1.21	0.003	83.4	0.2	16.4	1
(pH 11)	GlyOEt·HCl	0.67	0.390	46.2	26.9	26.9	135
DB-18-C-6							
(pH 11)	GlyOEt·HCl	0.69	0.347	47.6	23.9	28.5	120
(pH 11)	$CuCl_2$	1.30	0.068	89.7	4.7	5.6	23

Table IV. (continued)

macrocycle (phase II pH)	metal salt	A_I	A_{II}	distribution of Pic^- (%) phase I	phase II	$CHCl_3$	transport rate[b] $x10^6$(mmol in 1h)
Hexamide **1**							
(pH 11)	$CuCl_2$	1.36	0.041	93.8	2.8	3.4	14
(pH 11)	$AgNO_3$	1.11	0.096	76.6	6.6	16.8	33
Hexamide **2**							
(pH 11)	$CuCl_2$	1.16	0.127	80.0	8.8	11.2	44
(pH 11)	$AgNO_3$	0.93	0.258	64.1	17.8	18.1	89
Hexamide **4**							
(pH 11)	$CuCl_2$	1.13	0.149	77.9	10.3	11.8	51

[a] Aq. phase I pH = 5; aq. phase II pH = 3 or 11. Refer to experimental section for details.

[b] Error limits of transport rate are estimated to be ± 15%.

Discussion

As expected, the binding of metal ions by hexamides **1** and **2** in extraction experiments was very weak. But hexamide **2** showed a little stronger binding than hexamide **1** to Cu^{2+}, Hg^{2+}, Ag^+ and GlyOEt cations. This may be attributed to the additional binding site on the second side chain in the benzene ring. Hexamine **3** showed a strong affinity for transition metal cations but not alkali or alkaline-earth metal cations. This selectivity is only partly based on the size of its molecular cavity. The ionic radii of soft metal cations such as Ag^+, Pb^{2+}, Hg^{2+} (about 1.2 Å) are similar to a rigid [18]-C-6

macrocycle cavity radius (about 1.34 - 1.43 Å).[13] The cavity radius of a flexible macrocycle may be less than that of a rigid one, and this may be the reason for complexation of Cu^{2+}, Zn^{2+}, Co^{2+} and Ni^{2+}, which have small ionic radii. The selective binding more depends on the nature of donor sites. Unlike oxygen donor sites, nitrogen donor sites tend to form stable complexes with soft, polarizable metal cations but less stable complexes with hard, non-polarizable alkali or alkaline metal cations. Hexamine **3** also showed strong binding to organic amino acid cations.

From the data in Table III and Table IV, we can get some information about the relationship between extractability and rate of cation transport through liquid membranes. High extractability or high concentration of the complex of picrate ion in the chloroform phase confirmed by the high UV absorbance of the organic phase, was not proportional to high transport rate. For example, the extractabilities of Hg^{2+}, Cu^{2+}, Pb^{2+}, and Ag^{+} were very high, but transport rates were very low. The reason is that the transport rate also depends on the dissociation of complex and diffusion into the receiving phase. Similar results have been reported by Lamb, and it was found for maximum cation transport, there was an optimum range of values of the cation-macrocycle complex stability constant.[27]

When pH in the aqueous phase II changed from 7 to 3, there was a slight increase in the concentration of picrate ion because of binding of H^{+}. Because of the high concentration of metal salt, the extractibility was less sensitive to the change of pH. There was not much change in transport rate with an acidic receiving phase. When the pH in the aqueous phase II changed from 7 to 11, there was a rate increase for all cations, except for Hg^{2+} and Ag^{+}. This may be explained as the increase of dissociation of complex and release of picrate in the presence of OH^{-} anion. It is not clear why there was no rate increase for Hg^{2+} and Ag^{+}.

Among the metal ions with small ionic radii hexamine **3** showed highest efficiency for Cu^{2+} in transport experiments. This may be attributed to the loose binding between

nitrogen and guest cation, which more easily decomplex in the release process. Both hexamide **1** and **2** showed low complexing for most metal cations. However in liquid membrane experiments with an aqueous phase II of pH 11, the transport rates of Cu^{2+} and Ag^{+} were reasonably high using hexamide **2**. In general, macrocyclic amides show weak binding for metal cations. But for liquid membrane transport weak binding may be good for the dissociation of complexes and the release of metal cations. As far as we know this is the first observation of a macrocyclic hexamide with good transport ability for metal cations in a liquid membrane system. The transport ability of hexamide **2** may be attributed to the second alkoxyl side chain on the benzene ring. It has been reported that when a donor was added to the sidearm of the macrocycle the transport rate increased nearly fivefold.[28] Since hexamide **2** exhibits clear liquid crystalline properties, the combination of ordered molecular architecture with its transport ability for cations will made this kind of macrocyclic ligands interesting for ion transport through thin films of pure material.

Tsukube has examined the extraction and transport of amino acid ester salts by hexamide **5**, hexamine **6**, and DB-18-C-6.[21] For comparison his results are presented in Table V.

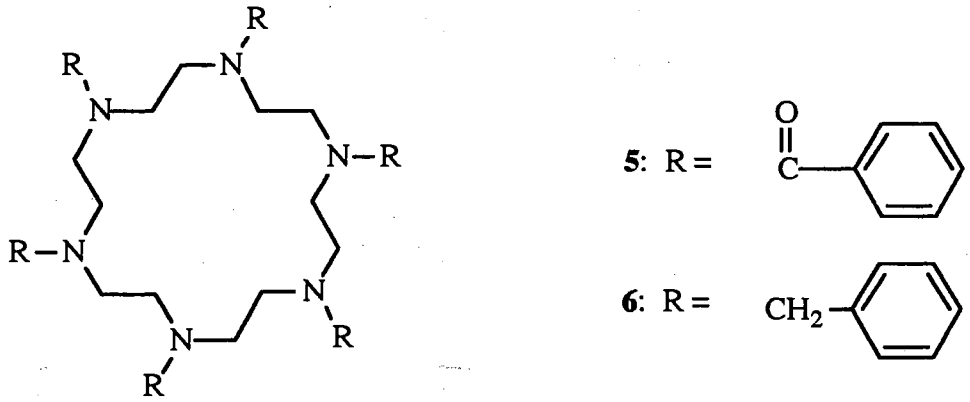

Table V. Results of Extraction and Liquid Membrane Transport by **5** and **6**

macrocycle	extraction (percentage)[a]		transport rate ($x10^{-3}$ mmol/h)[b]		
	PheOEt	GlyOEt	KCl	PheOEt	GlyOEt
5	9.0	< 2.0	< 0.1	0	0
6	16.0	< 2.0	< 0.1	9.5	1.7
DB-18-C-6			5.7	0	0

[a] Extraction conditions: amino acid ester-HCl, 0.01 mmol in 2 mL H_2O, macrocycle, 0.02 mmol in 2 mL $CHCl_3$.

[b] Transport conditions: Aq. phase I, amino acid ester.HCl, in 5 mL H_2O. Organic phase, macrocycle, 0.0372 mmol in 12 mL $CHCl_3$. Aq. phase II, H_2O, 5 mL. In a U-tube apparatus similar to that of Figure 1.

While the experimental conditions used by the Tsukube group are different from our conditions, the results are similar. In both cases only DB-18-C-6 showed a high transport rate for K^+, and the hexamine showed higher binding ability than the hexamide did. One important difference is that hexamine **3** showed strong complexing with the organic cation of GlyOEt, and the transport rate was high using a basic receiving phase.

Izatt reported the complexing of metal cations with the silica gel-bound hexamine **8** and the log K values are cited in Table VI.[24]

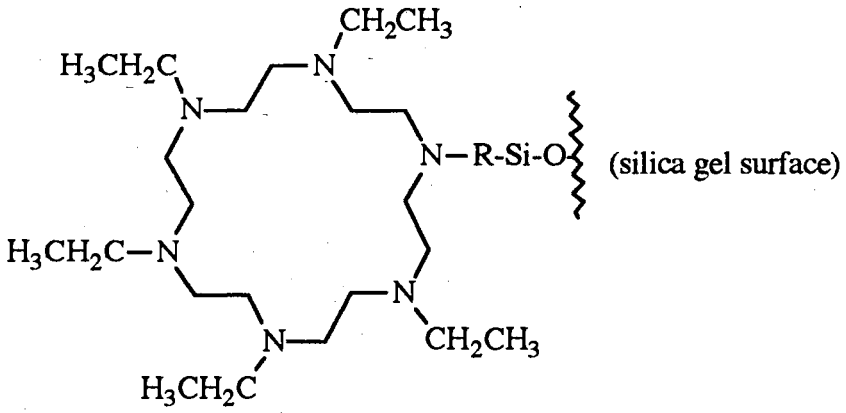

7

Table VI. log K Values of Silica Gel-bound Hexamine **7** with Metal Cations[24] and Comparison with Hexamine **3**

cation	Hg^{2+}	Cu^{2+}	Pb^{2+}	Zn^{2+}	Ni^{2+}	Ag^{+}	K^{+}
hexamine **7**							
log K[a]	28.8	16.3	14.0	10.0	9.8	9.3	< 2.0
hexamine **3**							
Extract.(%)	88.4	98.6	98.6	77.1	54.9	98.6	21.4
Transp. rate[b]	3.5	148.5	83.0	20.5	14.0	3.5	3.5

[a] $K = [M^{n+}L]/[M^{n+}][L]$. [b] 10^{-6} mmol/h

Comparison of the data of Table II and Table VI suggested that while both macrocyclic amines showed strong binding for heavy metals, hexamine **3** showed stronger binding for Ag^+. The difference may due to the cation-ligating oxygen donor side chains, which may help to complex the metal cation bound in the parent macrocycle.

Conclusion

Azacrown[18]-N_6 hexamides **1** and **2** and hexamine **3** were evaluated for their cation-binding abilities by liquid-liquid extraction and liquid membrane methods. Hexamine **2** exhibited strong binding to Ag^+, Pb^{2+}, Cu^{2+}, Hg^{2+}, and some organic cations of amino acid esters. The binding of hexamides **1** and **2** was weak to both metal and organic cations. The transport rates of cations through a liquid membrane were not proportional to their extraction efficiencies and were affected by the pH values in the receiving aqueous phase. Hexamine **3** showed a high transport rate for Cu^{2+}, and hexamide **2** showed a high transport rate for Ag^+ to a basic receiving aqueous phase.

References

(1) Lehn, J. M.; Malthete, J.; Levelut, A. M. *J. Chem. Soc., Chem. Commun.*, **1985**, 794.

(2) Lehn, J. M. *Angew. Chem. Int. Ed. Engl.* **1988**. *27*, 89.

(3) Malthete, J.; Poupinet, D.; Vilanove, R.; Lehn, J. M. *J. Chem. Soc., Chem. Commun.* **1989**, 1016.

(4) Mertesdorf, C.; Ringsdorf, H. *Liq. Cryst.* **1989**, *5*, 1757.

(5) Tatarsky, D.; Banerjee, K.; Ford, W. T. *Chem. Mater.* **1990**, *2*, 138.

(6) Idziak, S. H. J.; Maliszewskyj, N. C.; Heiney, P. A.; McCauley, J. P.; Sprengeler, P. A.; Smith, A. B. III *J. Am. Chem. Soc.* **1991**, *113*, 7666.

(7) Idziak, S. H. J.; Maliszewskyj, N. C.; Vaughan, G. B. M.; Heiney, P. A.; Mertesdorf, C.; Ringsdorf, H.; McCauley, J. P.; Smith, A. B. III. *J. Chem. Soc., Chem. Commun.* **1992**, 98.

(8) Lattermann, G. *Mol. Cryst. Liq. Cryst.* **1990**, *182B*, 299.

(9) Malthete, J.; Levelut, A. M.; Lehn, J. M. *J. Chem. Soc., Chem. Commun.* **1992**, 1434.

(10) Lattermann, G.; Schmidt, S.; Kleppinger, R.; Wendorff, J. H. *Adv. Mater.* **1992**, *4*, 30.

(11) Mertesdorf, C.; Ringsdorf, H. *Mol. Eng.* **1992**, (in press).

(12) Cox, B. G.; Schneider, H. *Coordination and Transport Properties of Macrocyclic Compounds in Solution* ; Elsevier: Amsterdam, 1992

(13) Izatt, R.; Bradshaw, J. S.; Nielsen, S. A.; Lamb, J. D.; Christensen, J. J. *Chem. Rev.* **1985**, *85*, 271.

(14) Kodama, M.; Kimura, E.; Yamaguchi, S. *J. Chem. Soc. Dalton Trans.* **1980**, 2536.

(15) Bencini, A.; Bianchi, A.; Micheloni, M.; Paoletti, P.; Garcia-Espana, E; Nino, M. A. *J. Chem. Soc. Dalton Trans.* **1991**, 1171.

(16) Martin, L. Y.; Sperati, C. R.; Busch, D. H. *J. Am. Chem. Soc.* **1977**, *99*, 2968.

(17) Nagai, R.; Kodama, M. *Inorg. Chem.* **1984**, *23*, 4184.

(18) Kato, M.; Ito, T. *Inorg. Chem.* **1985**, *24*, 504.

(19) Kato, M.; Ito, T. *Inorg. Chem.* **1985**, *24*, 509.

(20) Tsukube, H. *J. Chem. Soc., Chem. Commun.* **1983**, 970.

(21) Tsukube, H.; Takagi, K.; Higashiyama, T.; Iwachido, T.; Hayama, N. *J. Chem. Soc. Perkin Trans. II* **1985**, 1541.

(22) Tsukube, H. *J. Coord. Chem.* **1987**, *16*, 101.

(23) Liebmann, A.; Mertesdorf, C.; Plesnivy, T.; Ringsdorf, H.; Wendorff, J. H. *Angew. Chem. Int. Ed. Engl.* **1991**, *30*, 1375.

(24) Izatt, R. M.; Bruening, R. L.; Tarbet, B. J.; Griffin, L. D.; Bruening, M. L.; Kradowiak, K. E.; Bradshaw, J. S. *Pure Appl. Chem.* **1990**, *62*, 1115.

(25) Cordier, D.; Hosseini, M. W. *New J. Chem.* **1990**, *14*, 611.

(26) Tsukube, H. *J. Chem. Soc., Perkin Trans I*, **1985**, 615.

(27) Lamb, J. D., Christensen, J. J., Oscarson, J. L., Nielsen, B. L., Asay, B. W., Izatt, R. M. *J. Am. Chem. Soc.* **1980**, *102*, 6820.

(28) Hernandez, J. C.; Trafton, J. E.; Gokel, G. W. *Tetrahedron Letters*, **1991**, *32*, 6269.

APPENDIX

SELECTED NMR AND MASS SPECTRA

Spectrum 1. ^{1}H NMR spectrum of 1,4,7,10,13,16-Hexa-(3,4-bisdodecyloxybenzoyl)-1,4,7,10,13,16-hexaazacyclooctadecane

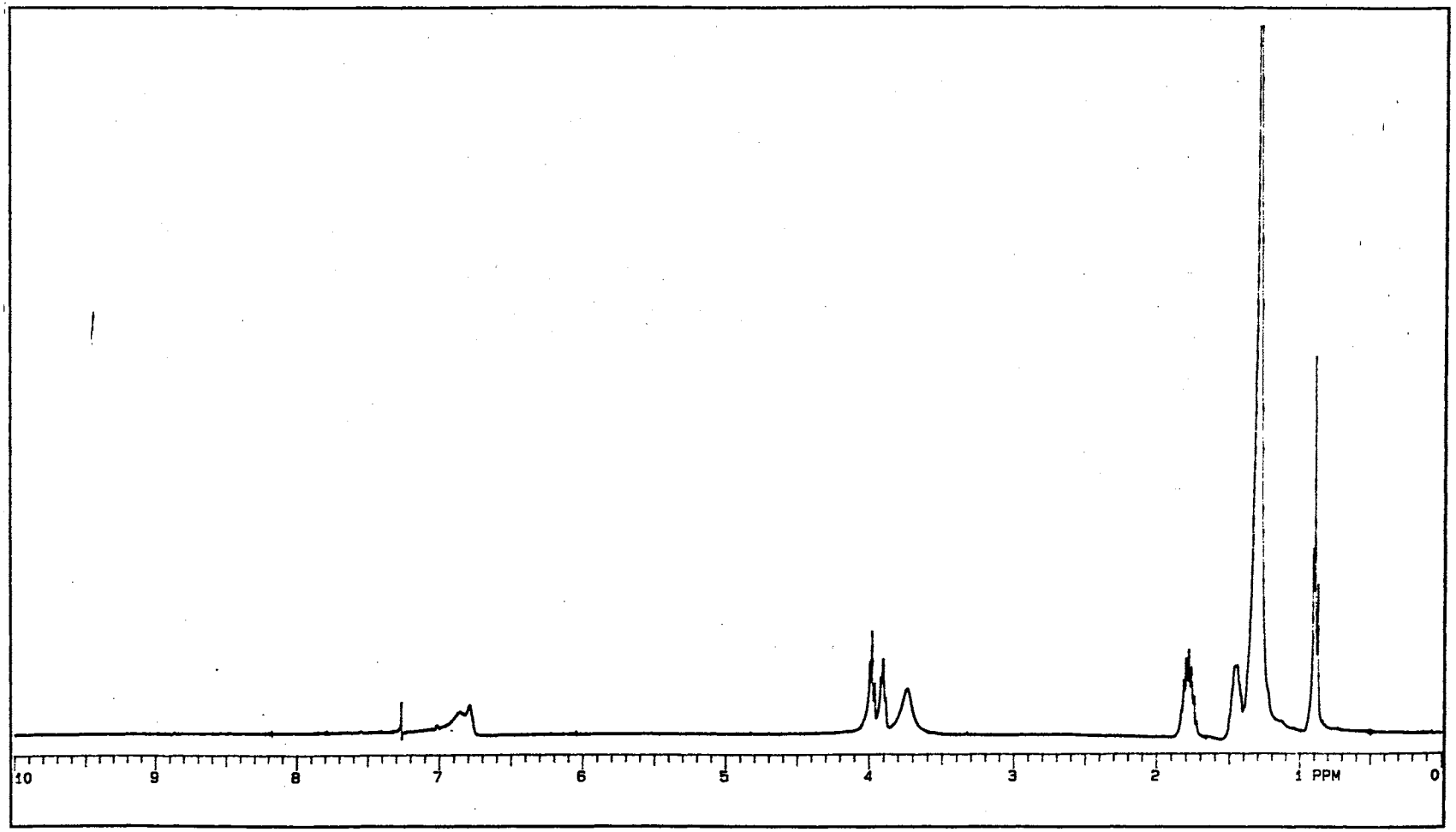

Spectrum 2. ^{13}C NMR spectrum of 1,4,7,10,13,16-Hexa-(3,4-bisdodecyloxybenzoyl)-1,4,7,10,13,16-hexaazacyclooctadecane

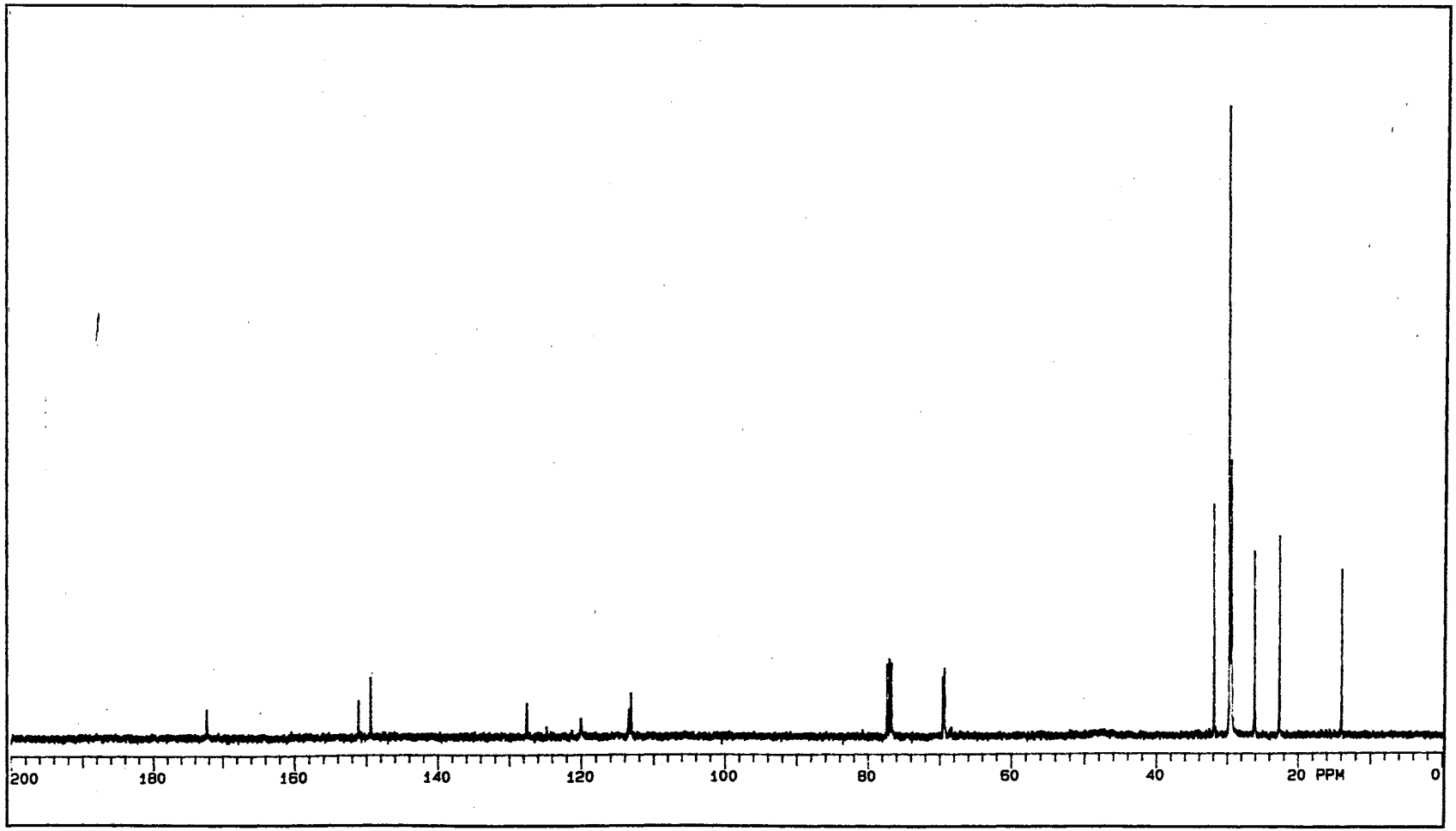

Spectrum 3. Mass spectrum of 1,4,7,10,13,16-Hexa-(3,4-bisdodecyloxybenzoyl)-1,4,7,10,13,16-hexaazacyclooctadecane

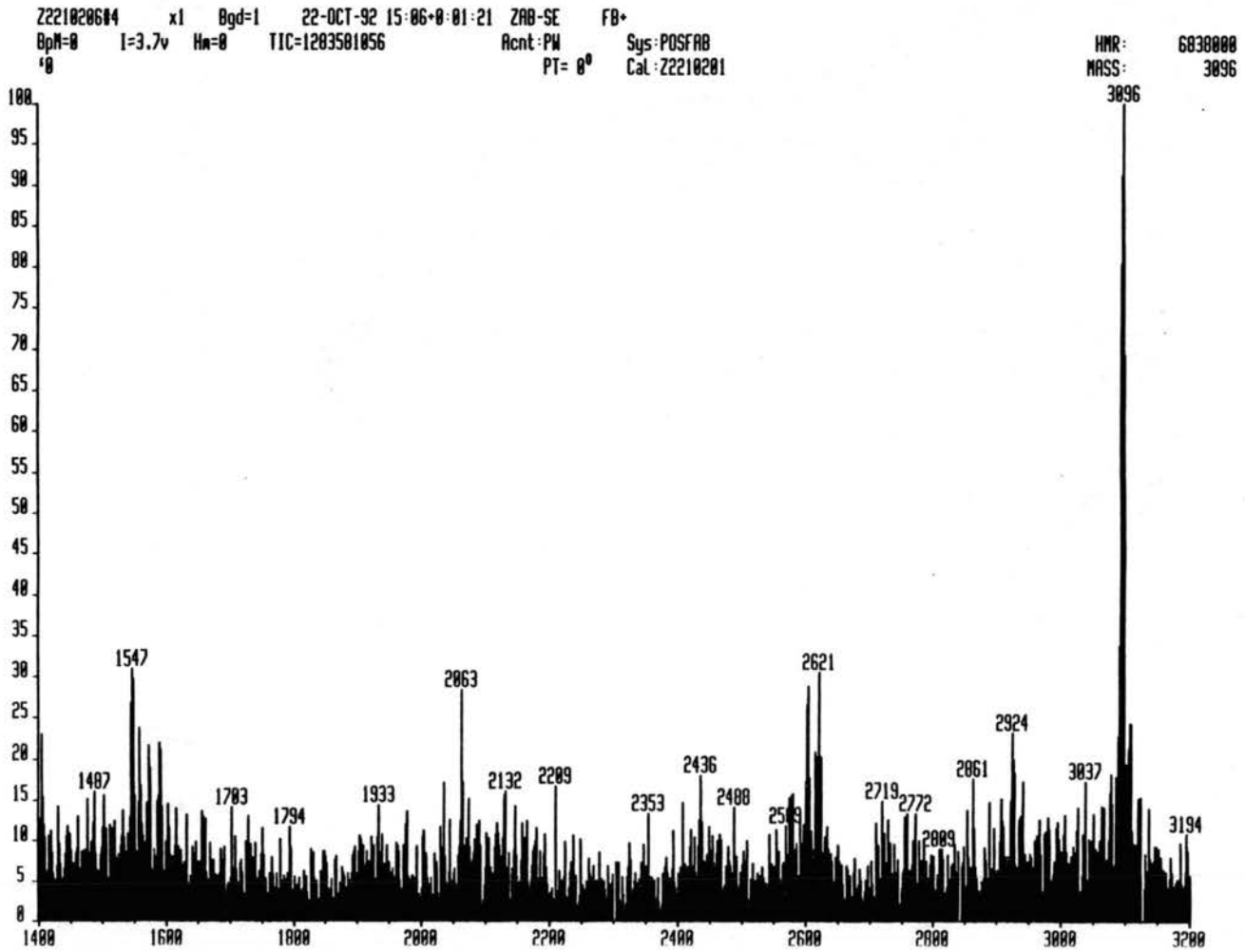

Spectrum 4. ^{1}H NMR spectrum of 1-[4-(10-Undecylenyloxy)benzoyl]-1,4,7,10,13,16-hexaazacyclooctadecane

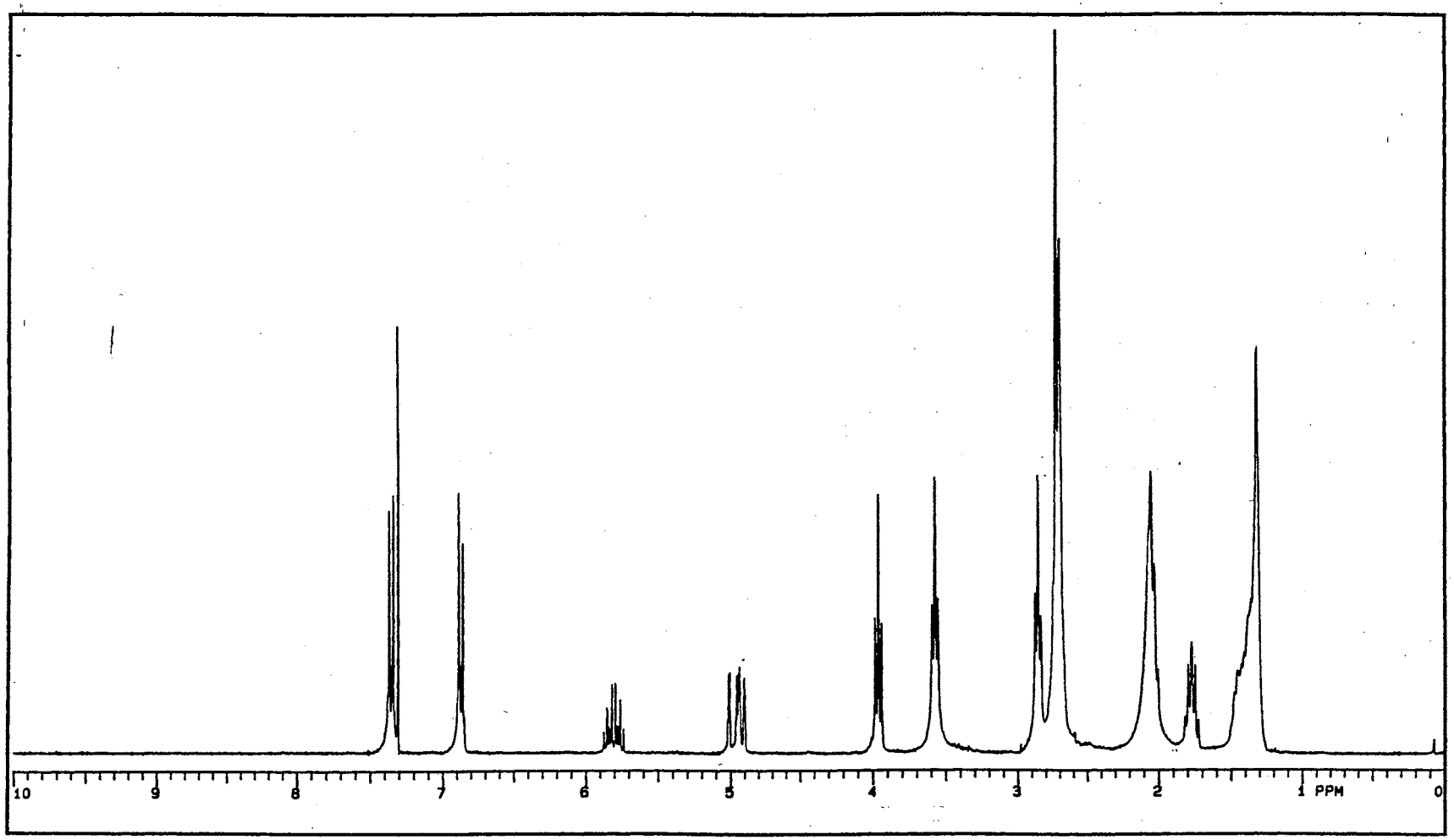

Spectrum 5. ^{13}C NMR spectrum of 1-[4-(10-Undecylenyloxy)benzoyl]-1,4,7,10,13,16-hexaazacyclooctadecane

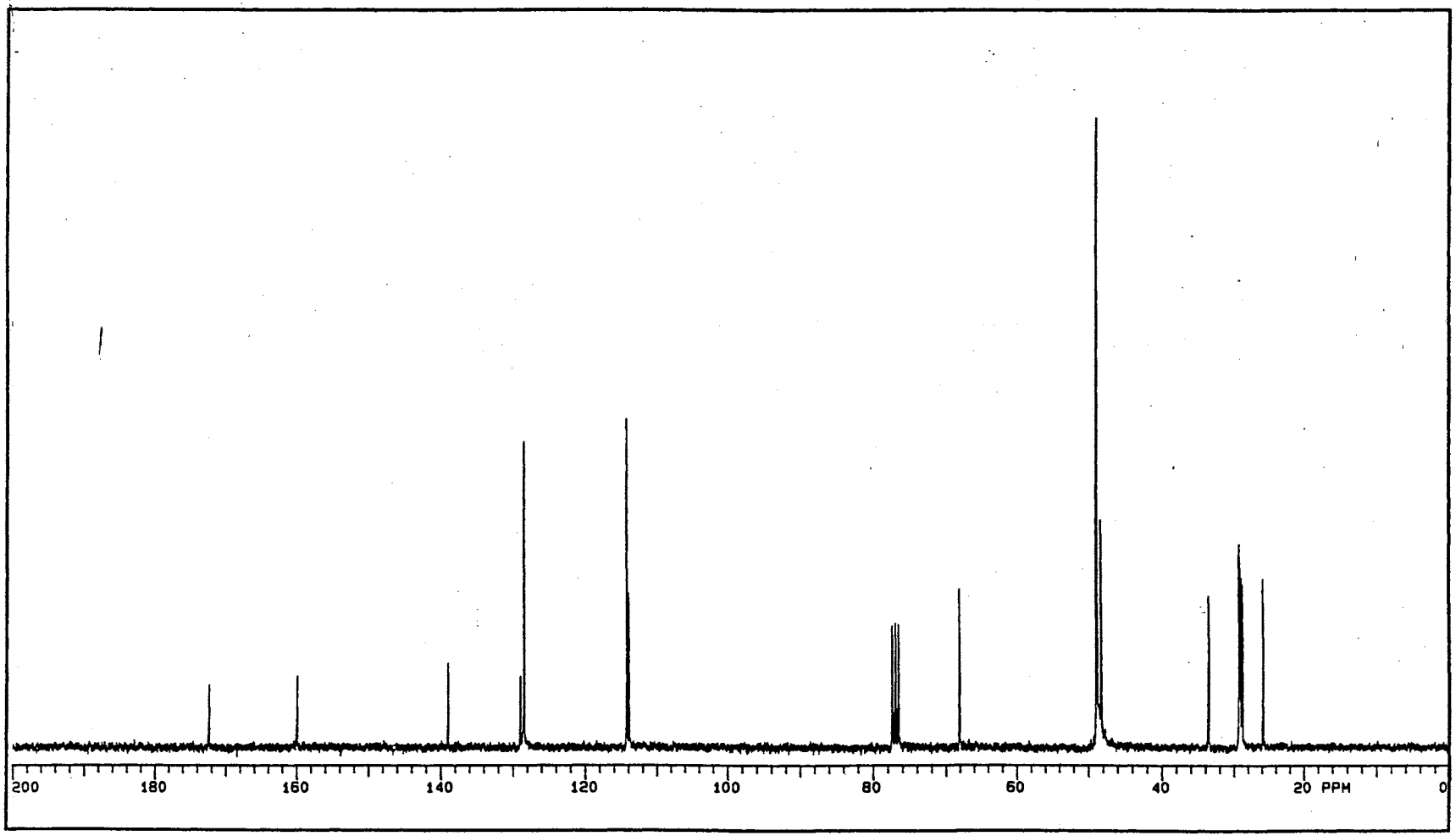

Spectrum 6. ^{1}H NMR spectrum of 4,7,10,13,16-Penta-(4-dodecyloxybenzoyl)-1-[4-(10-undecylenyloxybenzoyl)]-1,4,7,10,13,16-hexaazacyclooctadecane

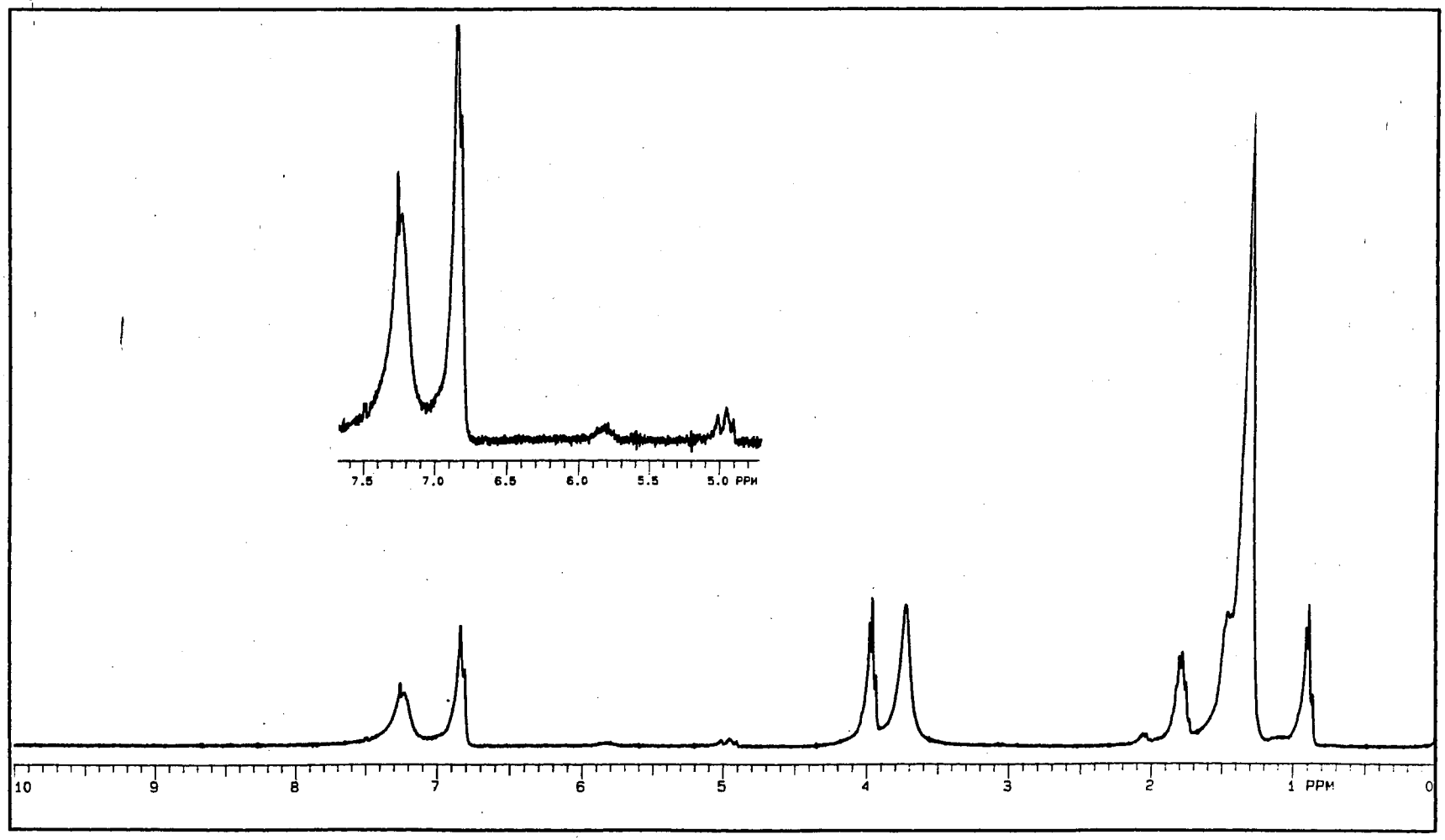

Spectrum 7. ^{13}C NMR spectrum of 4,7,10,13,16-Penta-(4-dodecyloxybenzoyl)-1-[4-(10-undecylenyloxybenzoyl)]-1,4,7,10,13,16-hexaazacyclooctadecane

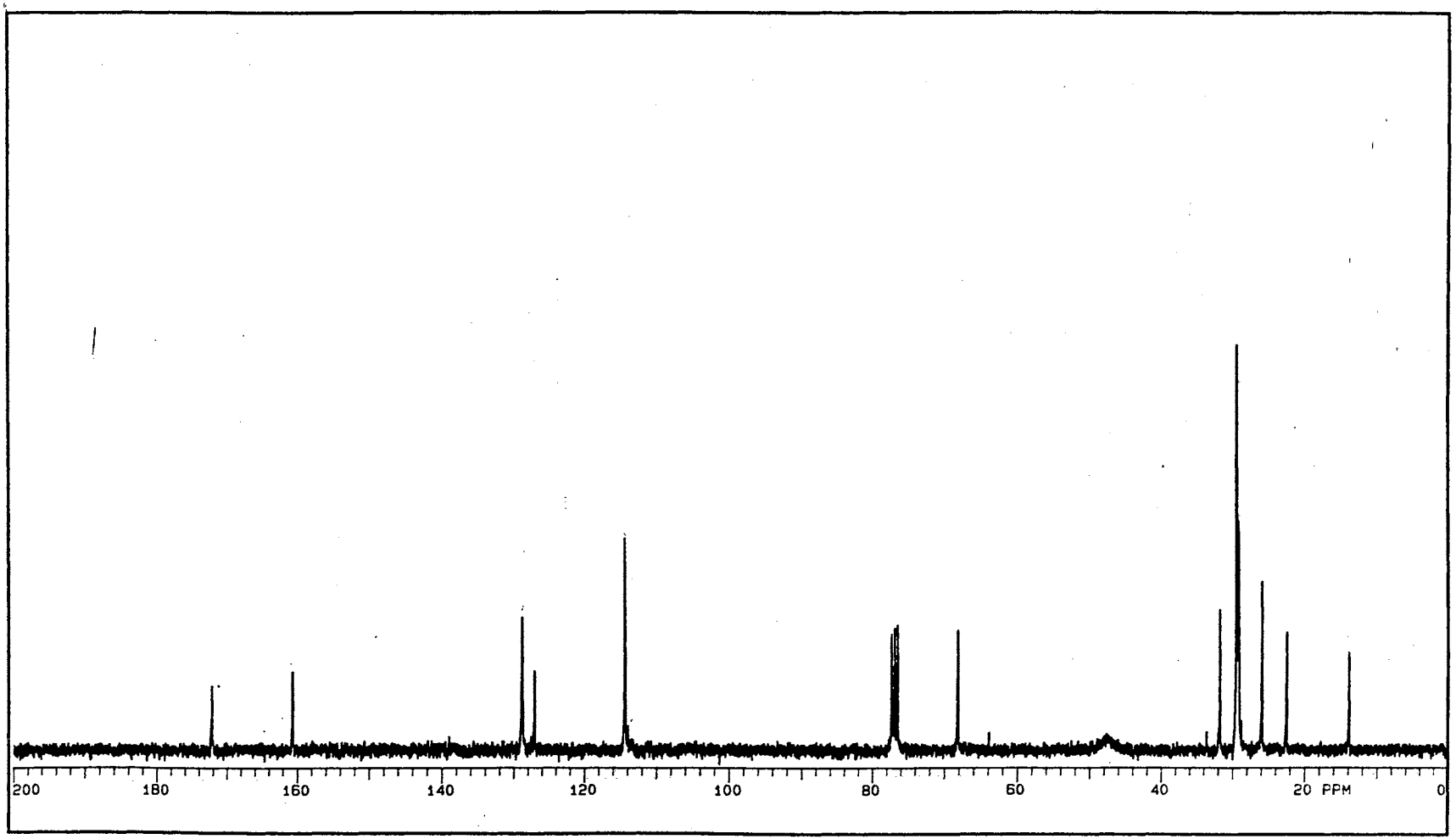

VITA

Mingyang Zhao

Candidate for the Degree of

Doctor of Philosophy

Thesis: AZACROWN[18]-N_6 DERIVATIVES: SYNTHESIS, LIQUID CRYSTALLINE PROPERTIES, AND COMPLEXATION

Major Field: Chemistry

Biographical:

Personal Data: Born in Beijing, China, January 10, 1950, the son of Di Zhao and Shuqin Zhao.

Education: Graduated from Qinghua University, Beijing, China, in October, 1978; received Master of Engineering in Polymer Materials from Beijing Research Institute of Chemical Industry, P. R. China, in October, 1984; completed requirements for the Degree of Doctor of Philosophy in Chemistry at Oklahoma State University in May, 1993.

Professional Experience: Technician, Beijing 3rd Chemical Factory, 1978 to 1980; Research engineer, Polymer Department, Beijing Research Institute of Chemical Industry, 1984 to 1986; Teaching and Research Assistant, Department of Chemistry, Oklahoma State University, 1987 to 1993.